VTRC
Virginia Transportation Research Council

We Bring Innovation to Transportation

Behavior of the Expanded Polystyrene Elastic Inclusion at Integral Abutments

https://vtrc.virginia.gov/media/vtrc/vtrc-pdf/vtrc-pdf/25-R24.pdf

BURAK F. TANYU, Ph.D., Professor

F. EROL GULER Ph.D., Adjunct Professor

YASIN KARAKUS, Graduate Research Assistant

George Mason University

EDWARD J. HOPPE, Ph.D., P.E.
Associate Principal Research Scientist

Final Report VTRC 25-R24

VIRGINIA TRANSPORTATION RESEARCH COUNCIL
530 Edgemont Road, Charlottesville, VA 22903-2454
vtrc.virginia.gov

Standard Title Page - Report on Federally Funded Project

1. Report No.: FHWA/VTRC 25-R24	2. Government Accession No.:	3. Recipient's Catalog No.:
4. Title and Subtitle: Behavior of the Expanded Polystyrene Elastic Inclusion at Integral Abutments		5. Report Date: June 2025
		6. Performing Organization Code:
7. Author(s): Burak F. Tanyu, F. Erol Guler, Yasin Karakus, and Edward Hoppe		8. Performing Organization Report No.: VTRC 25-R24
9. Performing Organization and Address: Virginia Transportation Research Council 530 Edgemont Road Charlottesville, VA 22903		10. Work Unit No. (TRAIS):
		11. Contract or Grant No.: 120040
12. Sponsoring Agencies' Name and Address: Virginia Department of Transportation 1401 E. Broad Street Richmond, VA 23219 Federal Highway Administration 400 North 8th Street, Room 750 Richmond, VA 23219-4825		13. Type of Report and Period Covered: Final
		14. Sponsoring Agency Code:
15. Supplementary Notes: This is an SPR-B report		

16. Abstract:

This report presents the findings of a laboratory study conducted by the Sustainable Geotransportation/Geoenvironmental Infrastructure (SGI) Research Group at George Mason University. The research focused on investigating the ability of standard (S) and elasticized (E) expanded polystyrene (EPS) to provide elastic inclusion in integral abutments. EPS materials in this study were selected based on input from the Technical Review Panel of this research. The laboratory tests were divided into the following three tasks.

Task 1 focused on quantifying the behavior of EPS when the material is loaded under uniform uniaxial compression (not cyclic loading) at a 10% per minute strain rate per the current ASTM D1621 (2016) standard. The findings showed that the behavior of E-EPS differs when loaded in the elasticized versus non-elasticized directions. The direction of loading did not affect the behavior of S-EPS. Specimen shape did not significantly influence stress-strain behavior, but specimen size affected the stress-strain behavior of both EPS types. In all testing conditions, both EPS types exhibited elastic behavior only when the applied load induced no more than 2 to 3% strain on EPS.

Task 2 focused on developing a specific testing protocol to evaluate the cyclic behavior of EPS that simulates the thermally induced movement of the bridge. In these tests, the findings showed that the elastic range of both EPS types may be increased as long as EPS is confined and imposed to a constant minimum 3% strain. Under these conditions, both EPS types stayed elastic as long as the cyclic-induced strains stayed within the 4.6% range (e.g., EPS is strained to 7.6%). The results also showed that if the immediately expected behavior of the bridge after installation becomes in the direction of expansion, the minimum constant strain imposed on EPS has to be increased from 3 to 7.6%. The constant strain condition is envisioned to be achieved in the field by controlling the compaction efforts of the aggregate surrounding EPS at the time of installation (not investigated as part of this research).

Task 3 focused on evaluating EPS behavior under cyclic traffic loading without a concrete approach slab. The magnitude of traffic-induced stresses on EPS was calculated as 1.6 psi using the KENPAVE software model and based on 18 inches of pavement layers (imposing a constant 2 psi stress) on top of EPS. However, for conservatism, laboratory tests were conducted with a 5 psi vertical stress (traffic-induced stress plus overburden). Due to test setup limitations, traffic loading tests in the laboratory were conducted without confinement pressure. Based on the traffic loading test results, S-EPS and E-EPS experienced approximately 0.9% strain.

Based on the overall findings, researchers suggest a new equation (with a step-by-step decision tree) to calculate the required thickness of both types of EPS. The results indicate that both EPS types appear to satisfy Virginia Department of Transportation's (VDOT) Kp limiting value for abutment design. This study also proposes recommendations for revising the current VDOT SP404-000130-00 Special Provision for Elastic Inclusion.

Supplemental files can be found at https://library.vdot.virginia.gov/vtrc/supplements.

17 Key Words: Integral abutment, elastic inclusion, EPS, passive pressure.	18. Distribution Statement: No restrictions. This document is available to the public through NTIS, Springfield, VA 22161.

19. Security Classif. (of this report): Unclassified	20. Security Classif. (of this page): Unclassified	21. No. of Pages: 67	22. Price:

Form DOT F 1700.7 (8-72) Reproduction of completed page authorized

FINAL REPORT

BEHAVIOR OF THE EXPANDED POLYSTYRENE ELASTIC INCLUSION AT INTEGRAL ABUTMENTS

Burak F. Tanyu, Ph.D.
Professor

F. Erol Guler Ph.D.
Adjunct Professor

Yasin Karakus
Graduate Research Assistant

Sid and Reva Dewberry
Department of Civil, Environmental, and Infrastructure Engineering
Sustainable Geotransportation/Geoenvironmental Infrastructure (SGI) Research Group
George Mason University

Edward J. Hoppe, Ph.D., P.E.
Associate Principal Research Scientist
Virginia Transportation Research Council

In Cooperation with the U.S. Department of Transportation
Federal Highway Administration

Virginia Transportation Research Council
(A partnership of the Virginia Department of Transportation
and the University of Virginia since 1948)

Charlottesville, Virginia

June 2025

VTRC 25-R24

DISCLAIMER

The contents of this report reflect the views of the author(s), who is responsible for the facts and the accuracy of the data presented herein. The contents do not necessarily reflect the official views or policies of the Virginia Department of Transportation, the Commonwealth Transportation Board, or the Federal Highway Administration. This report does not constitute a standard, specification, or regulation. Any inclusion of manufacturer names, trade names, or trademarks is for identification purposes only and is not to be considered an endorsement.

ABSTRACT

This report presents the findings of a laboratory study conducted by the Sustainable Geotransportation/Geoenvironmental Infrastructure (SGI) Research Group at George Mason University. The research focused on investigating the ability of standard (S) and elasticized (E) expanded polystyrene (EPS) to provide elastic inclusion in integral abutments. EPS materials used in this study were selected based on the input from the Technical Review Panel of this research. The laboratory tests were divided into the following three tasks.

Task 1 focused on quantifying the behavior of EPS when the material is loaded under uniform uniaxial compression (not cyclic loading) at a 10% per minute strain rate per the current ASTM D1621 (2016) standard. The findings showed that the behavior of E-EPS differs when loaded in the elasticized versus non-elasticized directions. The direction of loading did not affect the behavior of S-EPS. Specimen shape did not significantly influence stress-strain behavior, but specimen size affected the stress-strain behavior of both EPS types. In all testing conditions, both EPS types exhibited elastic behavior only when the applied load induced no more than 2 to 3% strain on EPS.

Task 2 focused on developing a specific testing protocol to evaluate the cyclic behavior of EPS that simulates the thermally induced movement of the bridge. In these tests, findings showed that the elastic range of both EPS types may be increased as long as EPS is confined and imposed to a constant 3% strain. Under these conditions, both EPS types stayed elastic as long as the cyclic-induced strains stayed within the 4.6% range (e.g., EPS is strained to 7.6%). The results also showed that if the immediately expected behavior of the bridge after installation becomes in the direction of expansion, the minimum constant strain imposed on EPS has to be increased from 3 to 7.6%. The constant strain condition is envisioned to be achieved in the field by controlling the compaction efforts of the aggregate surrounding EPS at the time of installation (not investigated as part of this research).

Task 3 focused on evaluating EPS behavior under cyclic traffic loading without a concrete approach slab. The magnitude of traffic-induced stresses on EPS was calculated as 1.6 psi using the KENPAVE software model and based on 18 inches of pavement layers (imposing a constant 2 psi stress) on top of EPS. However, for conservatism, laboratory tests were conducted with a 5 psi vertical stress (traffic-induced stress plus overburden). Due to test setup limitations, traffic loading tests in the laboratory were conducted without confinement pressure. Based on the traffic loading test results, S-EPS and E-EPS experienced approximately 0.9% strain.

Based on the overall findings, researchers suggest a new equation (with a step-by-step decision tree) to calculate the required thickness of both types of EPS. The results indicate that both EPS types appear to satisfy the Virginia Department of Transportation's (VDOT) Kp limiting value for abutment design. This study also proposes recommendations for revising the current VDOT Special Provision for Elastic Inclusion.

Supplemental materials can be found at https://library.vdot.virginia.gov/vtrc/supplements.

FINAL REPORT

BEHAVIOR OF THE EXPANDED POLYSTYRENE ELASTIC INCLUSION AT INTEGRAL ABUTMENTS

Burak F. Tanyu, Ph.D.
Professor

F. Erol Guler Ph.D.
Adjunct Professor

Yasin Karakus
Graduate Research Assistant

Sid and Reva Dewberry
Department of Civil, Environmental, and Infrastructure Engineering
Sustainable Geotransportation/Geoenvironmental Infrastructure (SGI) Research Group
George Mason University

Edward J. Hoppe, Ph.D., P.E.,
Associate Principal Research Scientist
Virginia Transportation Research Council

INTRODUCTION

Two types of expanded polystyrene (EPS) material are available commercially: standard (S-EPS) and elasticized (E-EPS). It should be noted that although S-EPS is widely available in the market, to the best of the authors' knowledge, only one manufacturer currently produces E-EPS in the United States. Although both EPS types may appear similar, their production processes differ. S-EPS is produced from cured polystyrene resins that expand using hot steam to form beads (Kannan et al., 2007; Ramli Sulong et al., 2019). The process starts with molding beads to form blocks of the desired size. E-EPS is produced from processed S-EPS. According to the method described in the expired patent by Horvath and VonWagoner (1992), E-EPS is created from the S-EPS block initially compressed uniaxially until the block reaches one-third of its initial thickness. Subsequently, the applied load is released to create an EPS that rebounds to 85% of its original thickness. EPS produced by this mechanical process is referred to as E-EPS. EPS material is used in various applications by the U.S. Department of Transportation (DOT) across the United States. Table 1 outlines these applications. The table is compiled based on examining DOT specifications within the United States. It should be noted that the underlying source and reasons for the values in Table 1 have not been cited in the reviewed specifications.

Table 1. Summary of DOT Specifications for Using EPS Material

State	Applications Listed for EPS	Min. Density (pcf)	Min. Compr. Resistance (psi)	Max. Water Absorption (%)	References
Arizona	Vertical Restrainer for Concrete Structures	-	16–40 (at 5% strain)	-	AZDOT (2021)
California	Pre-Molded Expansion Joint Filler	-	16–40 (at 5% strain)	-	Caltrans (2018)
Florida	Joint Material	0.8	-	2.6	FDOT (2022)
Hawaii	Joint Material	-	16–40 (at 5% strain)	-	HIDOT (2013)
Indiana	Joint Material—Preformed Expansion Joint Filler	-	40 (at 10% strain)	1	INDOT (2022)
Iowa	Filling Material	1.8	10.9 (at 1% strain)	-	IADOT (2017)
Kansas	Bearings and Pads for Structures	1.35	7.3 (at 1% strain)	-	KDOT (2015)
Minnesota	Expansion Joint Sealer Material	-	30 (at 5% strain)	-	MnDOT (2020) Vol II
Mississippi	Joint Material	0.8	-	2.6	MDOT (2017)
Missouri	Bedding Material for Prestressed Panels	-	60 (at 10% strain)	2	MODOT (2021)
Missouri	Material for Corrugation Areas of Stay-in-Place Forms	-	10 (at 10% strain)	2	MODOT (2021)
New Hampshire	Strips for Precast Deck Panels	-	55 (at 10% strain)	-	NHDOT (2016)
New York	Protective Cover for Pipes	2	30 (at 10% strain)	-	NYDOT (2019)
New York	Elastic Inclusion*	-	5 (at 10% strain)	3	NYDOT (2019)
Pennsylvania	Geofoam Lightweight Fill	1.35	19.6 (at 10% strain)	3	PennDOT (2018)
Pennsylvania	Geofoam Lightweight Fill	2.4	40 (at 10% strain)	2	PennDOT (2018)
Tennessee	Internal Form of Structure (Joint)	0.9	10 (at 10% strain)	3	TNDOT (2021)
Texas	Geofoam Fill	1.8	29 (at 10% strain)	2	TXDOT (2004)
Virginia	Elastic Inclusion*	-	5 (at 10% strain)	3	VDOT (2020a) Special Provision 404-000130-00
Washington	Joint Sealing Material	1.5	-	-	WSDOT (2022)

EPS = expanded polystyrene.
*EPS type for these states is specifically defined as elasticized EPS.

Table 1 reveals that EPS applications are present in only one-third of all DOTs. These specifications commonly emphasize using EPS as the joint seal and filling material for constructing lightweight fill embankments. The key property in Table 1 for identifying EPS is the minimum compressive resistance value. This value is obtained through unconfined compressive laboratory testing following ASTM protocol D1621 (2016). In addition, some states also consider other properties (i.e., density, elasticity modulus, elastic limit) to specify EPS. The EPS types defined by these additional properties are categorized in ASTM C578 (2022) and ASTM D6817 (2021).

As Table 1 shows, only two state DOTs, namely New York and Virginia, employ E-EPS for elastic inclusion at integral abutments. The specified EPS for both states is defined as E-EPS. The purpose of elastic inclusion is to accommodate cyclic movements in the bridge superstructure due to daily and seasonal temperature variations. E-EPS is expected to exhibit elastic behavior under cyclic loading along with reducing thermally induced stresses that are transferred from the bridge abutment to the adjoining backfill. Consequently, the lateral earth pressure value used in abutment design is decreased.

Virginia is one of the leading states constructing integral abutment bridges in the United States. Some of the oldest integral bridges constructed in Virginia date back to the 1980s. VDOT constructs two types of integral abutment bridges, referred to as full- and semi-integral. In the full-integral abutment, the superstructure and abutment are monolithic. In the semi-integral abutment, a bearing is between the footing and the integral backwall, allowing lateral movement of the superstructure. Unlike traditional bridges with joints, full- and semi-integral abutment bridges constructed in Virginia utilize an elastic inclusion between the back of the abutment and the adjoining granular backfill material. Since the early 2000s, VDOT has been using E-EPS to create this elastic zone. Although E-EPS shows promise as an elastic inclusion material, field observations reported by VDOT indicate some discrepancies in the behavior of different constructed bridges. Considering the complexity of the EPS material properties and the limited availability of E-EPS producers, VDOT has requested thorough research to understand the behavior of the EPS elastic inclusion used in these applications.

One of the complexities associated with EPS is that the material may exhibit a negative Poisson's ratio (Atmatzidis et al., 2001; Elragi et al., 2000). Materials with a negative Poisson's ratio, unlike conventional materials, do not expand laterally when subjected to a vertical compressive load. Instead, materials with a negative Poisson's ratio exhibit an inward-collapsing behavior by shortening both in the vertical and lateral axes. This phenomenon is referred to as auxetic behavior. Figure 1 shows the differences between conventional and auxetic behaviors. Depending on the range of stresses, EPS may behave similarly to conventional or auxetic materials.

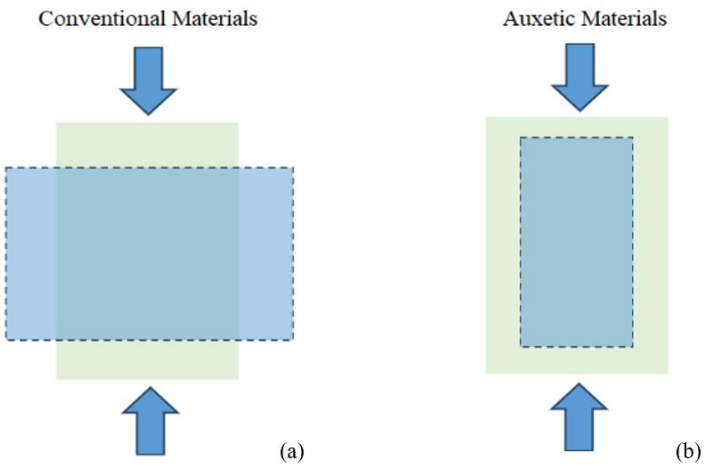

Figure 1. Differences Between Material Behaviors: (a) Conventional; (b) Auxetic

Summary of Relevant Literature

Some of the problems associated with EPS have already been identified in the literature. Plastic deformations in EPS may occur when bridge movements exceed the elastic range, causing backfill slippage from top to bottom (Al-qarawi et al., 2020). Consequently, this undesired backfill movement may lead to differential settlement and contribute to a bump at the end of the bridge (Liu et al., 2021). In addition, EPS has benefits in terms of lateral earth pressure. It can decrease lateral earth pressure on the abutment and maximum settlement compared with cases without EPS (Alqarawi et al., 2016; Liu et al., 2021).

Because of the limited availability of E-EPS, most of the literature focuses on the evaluation of S-EPS. Studies have shown that the stress-strain behavior of S-EPS is influenced by parameters such as density, specimen size, specimen shape, aspect ratio of EPS, and strain rate of loading. Based on the findings of previous literature with monotonic loading on S-EPS, the initial elastic modulus increases with the increase in density (Abdelrahman et al., 2008; Beinbrech and Hohwiller, 2000; Duškov, 1997; Elragi, 2000; Horvath, 1995; Preber et al., 1994; Negussey, 2008). It is also indicated that as the density increases, the compressive resistance of S-EPS increases. Concerning E-EPS, the only study available in the literature was conducted by Beinbrech and Hohwiller (2000). In their study, E-EPSs with densities between 0.7 and 1.35 pcf are subjected to monotonic loading. Results showed that an increase in the density of E-EPS led to an increase in compressive resistance. When S-EPS is tested under cyclic loading, the increase in density results in reduced permanent deformations (Beju and Mandal, 2016; Ossa and Romo, 2009; Ossa and Romo, 2011; Malai et al., 2017; Padade and Mandal, 2012; Trandafir et al., 2010; Siabil et al., 2020). No studies were available in the literature in which E-EPS was tested under cyclic loadings.

Elragi (2000) conducted compression tests on S-EPS (densities between 0.94 and 1.81 pcf) specimens of different sizes (2 inches versus 24 cubic inches specimens) and found that larger specimens had a higher elastic modulus than smaller ones. Atmatzidis et al. (2001) demonstrated that the elastic modulus of S-EPS increased based not only on different densities (between 0.6 to 2.2 pcf) but also on different specimen sizes (2 cubic inches versus 3 different

cylindrical specimens with Diameter (D) = Height (H) = 2, 4, and 6 inches). Srirajan et al. (2001) reported no significant difference in compressive resistance (at 5% strain) between large and small S-EPS (2 versus 6 cubic inches) specimens (density between 0.94 and 1.25 pcf). Despite valuable studies in the literature, the effect of specimen size on the behavior of S-EPS has yet to be investigated using cylindrical specimens (all previous studies focused on testing cube specimens of S-EPS). In addition, no study has examined the influence of specimen size on the stress-strain behavior of E-EPS.

Hazarika (2006) explored the effect of specimen shape on the stress-strain behavior of S-EPS using cubic and cylindrical specimens. According to Hazarika, cylindrical S-EPS specimens (with densities of 1.0 and 1.25 pcf) (H = 4 inches, D = 2 inches) exhibit lower compressive resistance compared with cubic specimens (2 and 4 cubic inches). In addition, Ahmed Awol (2012) found that larger cylindrical S-EPS specimens (H = D = 2 inches) displayed a higher initial elastic modulus than smaller cylindrical specimens (H = 1 inch, D = 2 inches). However, the existing literature lacks investigation into the specimen shape effect on E-EPS.

Atmatzidis et al. (2001) explored the aspect ratio of S-EPS, revealing that cylindrical specimens with higher ratios (D/H = 0.5, 1.0, and 2.0) exhibit greater elastic modulus. Hazarika (2006) studied the effect on S-EPS using cubic and rectangular prism specimens, finding that specimens with a 1:1 ratio (2 cubic inches) show higher compressive resistance. The literature lacks investigation into the influence of aspect ratio on E-EPS.

In the literature, most EPS compression tests were conducted with a 10% per minute strain rate based on ASTM D1621 (2016). However, strain rate is a substantial parameter affecting EPS stress-strain behavior. Previous studies have shown that as strain rate increases, compressive resistance decreases for S-EPS (Athanasopoulos et al., 1999; Duškov, 1997; Khalaj et al., 2020; Ossa and Romo, 2009; Ouellet et al., 2006). Conversely, the strain rate effect on E-EPS is not investigated. It should be noted that the 10% per minute strain rate is significantly higher than the strain rate applied to EPS due to thermally induced annual bridge movements.

Previous literature studies also focused on the contributions of EPS to integral abutments. A study conducted by Horvath (2000) centered on modeling E-EPS (density = 0.75 pcf) in Finite Element analysis. Findings indicated that using E-EPS may reduce lateral earth pressures on integral abutments. Alqarawi et al. (2016) modeled cyclic behavior in Finite Element analysis of S-EPS (density = 1.25 pcf) under temperature-induced bridge movements, demonstrating the benefits of S-EPS in mitigating the bump at the end of the bridge problem in integral abutments. To investigate the elastic inclusion performance of a combined system of S-EPS (density = 1.0 pcf) and geogrids, Liu et al. (2021) conducted laboratory experiments. The results indicated that the combined use of geogrids and EPS offer a potential solution to mitigate the backfill settlement problem. Despite these valuable studies, there has been a lack of research investigating the performance differences between S-EPS and E-EPS as materials considered for elastic inclusion.

A limited number of studies have investigated the behavior of S-EPS under traffic loads. Beinbrech and Hillman (1997) conducted full-scale experiments on pavement sections (8 inches concrete, 8 inches gravel, 5.5 inches cement-bound sand, 40 inches S-EPS, 4 inches sand on a

soft layer) using S-EPS (density = 1.25 and 1.9 pcf) and subjected EPS to traffic loading (11.2 klbf load with one-million-wheel passes). Test results showed no permanent deformation in S-EPS exposed to traffic loads. Dave and Dasaka (2018) conducted a laboratory study in which S-EPS was used behind the retaining wall, and Haversine traffic load was applied to the backfill to investigate the effect of cyclic horizontal loads on the behavior of EPS inclusion. The variation in earth pressures acting on the retaining wall was measured after applying traffic loads up to 10,000 cycles. The results showed that the earth pressures acting on the retaining wall decreased with an increase in the number of traffic loading cycles due to the presence of S-EPS. In addition, Dave and Dasaka (2018) noted that installing S-EPS as a compressible inclusion is an effective solution for reducing earth pressures on the upper part of the retaining wall subjected to traffic loads. Neither Beinbrech and Hohwiller (2000) nor Dave and Dasaka (2018) studies have investigated the traffic load application related to S-EPS being used as part of an elastic inclusion in integral abutments. No study could be found that specifically investigated the behavior of E-EPS under repeated traffic loads.

Overall, based on the literature review and the examination of DOT specifications, researchers observed the following:

- Long-term cyclic properties of E-EPS have not been sufficiently evaluated in the available literature.
- Comparison of data from literature is difficult because the density of S-EPS material strongly influences its behavior.
- Monotonic stress-strain behavior of S-EPS determined from laboratory tests is also influenced by specimen size, shape, aspect ratio, and strain rate.
- Cyclic behavior of S-EPS is influenced by the same parameters for monotonic loading.
- When evaluating the thermally induced cyclic behavior simulating bridge movement, very slow strain application must be considered. Therefore, adequate cyclic laboratory testing requires the test to be conducted at a very slow strain rate. Previous literature is limited in simulating this field condition.
- When evaluating cyclic traffic loading, there is insufficient research characterizing the EPS behavior when used as an elastic inclusion.
- Currently, VDOT (2020a) characterizes the required E-EPS to be used as an elastic inclusion in Special Provision 404-000130-00. This document lacks information regarding E-EPS density, testing direction, cyclic behavior evaluation (for thermally induced and traffic-induced), and target compaction-induced strains. In addition, compressive resistance of E-EPS is defined based only on a 10% strain.

Summary of the Current VDOT Design Practice

VDOT has developed special provisions and drawing details to facilitate the use of E-EPS in constructing elastic inclusions at integral abutments. These documents are presented in the supplemental materials. Chapter 17 of VDOT's (2023) *Manual of the Structure and Bridge Division* provides an equation to calculate the required thickness of the E-EPS material as:

$$EPS_t = 10 \times (0.01 \times h + 0.67 \times \Delta L) \qquad \text{Equation 1}$$

Where—

EPS_t = required EPS thickness in inches.
h = height of integral backwall and abutment in inches.
ΔL = total thermally induced longitudinal range of movement at the abutment in inches.

The number "10" in Equation 1 represents the intended elastic range of E-EPS. Thus, VDOT assumes that E-EPS behaves elastically with up to 10% strains. The "0.01h" component of Equation 1 denotes the initial compaction-induced displacement on E-EPS during backfill compaction (Hoppe and Eichental, 2012). The actual thermally induced movement acting on E-EPS is assumed to be 0.67 of the calculated displacement, based on field observations. The theoretical maximum thermally induced bridge movements (ΔL) are calculated by the following equation:

$$\Delta L = \alpha \times \Delta T \times L_0 \qquad \text{Equation 2}$$

Where—

α = thermal expansion coefficient (0.0000065/°F and 0.000006/°F for steel and concrete bridges, respectively).
ΔT = difference between the maximum ambient temperature and construction temperature.
L_0 = length of bridge from the neutral displacement point to the abutment.

VDOT is currently using ΔT as 120°F for the design of steel beam composite bridges, and ΔT as 80°F for design of concrete beam composite bridges (Hoppe and Eichental, 2012). Maximum allowable thermally induced superstructure displacements are restricted to 1.5 inches for full-integral abutments and 2.25 inches for semi-integral abutments in the current VDOT design practice (in addition to the maximum allowable integral bridge span lengths).

It is important to note that Equation 1 is used to calculate E-EPS thickness when the integral bridge has an approach slab (see Item B in the supplemental materials for drawing details). For bridges without approach slabs, current VDOT practice mandates a consistent 10-inch E-EPS thickness (irrespective of bridge length) in the upper 3 feet of the backwall (from the approach seat). The E-EPS layer thickness below the 3-foot depth is then adjusted to align with the value calculated from Equation 1.

The lateral earth pressure coefficient (Kp) used in integral abutment design is outlined in the VDOT (2023) *Manual of the Structure and Bridge Division*, Chapter 17. Presently, VDOT's designated Kp values for abutment design are 4 with E-EPS installation and 12 without EPS. This study aims to validate these design assumptions.

Based on communications with VDOT bridge engineers, it is understood that significant cost savings can be realized when the abutment design is based on a Kp value of 4 compared with a Kp value of 12. However, there is no practical advantage to developing lateral conditions resulting in Kp values smaller than 4 because they cannot be translated into a more economical structural section design due to default geometric constraints.

PURPOSE AND SCOPE

The primary purpose of this study was to evaluate the elastic range of both standard and elasticized EPS under cyclic loading, which may be relevant to bridge motions resulting from thermal expansion and contraction. The intention is to use the findings to assist VDOT (2020a) in modifying Special Provision 404-000130-00. The scope of this study is limited to laboratory tests designed to replicate the actual integral bridge in-service conditions. In addition to the EPS material characterization, tests simulating the long-term performance under cyclic thermally induced loading were conducted. Cyclic loads due to vehicle traffic were simulated in addition.

METHODS

Laboratory investigations conducted in this study were divided into three tasks:

Task 1—Characterization of Materials

Characterize the stress-strain behavior of S-EPS and E-EPS (created from the same S-EPS) to identify similarities and differences. Determine the elastic range of both materials through monotonic uniaxial compression tests, investigating the effects of specimen size, shape, aspect ratio, loading direction, and strain rates.

Task 2—Cyclic Load Testing Simulating Movement of Bridge Superstructure

Develop a specific cyclic testing protocol to evaluate the behavior of EPS related to thermally induced bridge movement. The intended outcome is to ascertain the range at which EPS remains elastic under these conditions. Results will be used to revise the EPS thickness equation in Chapter 17 of the VDOT (2023) *Manual of The Structure and Bridge Division*.

Task 3—Cyclic Load Testing Simulating Traffic Loading

Evaluate the elastic behavior of EPS when cyclic traffic loads are applied at the ground level and propagate to the top of EPS as reduced cyclic stresses. Conditions simulating no approach slab and a thin asphalt layer were selected.

Overview

Three different laboratory testing conditions were used in this study. For task 1, strain-controlled monotonic loading tests were conducted. In task 2, strain-controlled quasi-static simulated cyclic loading and unloading tests simulating thermal expansion of the bridge deck were performed. Task 3 involved stress-controlled cyclic loading tests where the applied load was imposed every second based on Haversine to simulate traffic loading. The following sections elaborate on the methods used for each testing task.

Methods Implemented to Address Task 1: Characterization of Materials

Although the primary focus of this study is to evaluate EPS, some tests in this research also involve evaluating EPS in a combined setup with aggregate and geotextile. Therefore, in Task 1 of this study, the research focused on characterizing all materials used, including aggregate, geotextile, and EPS. The following describes the details of the methods used to characterize these materials.

Characterization of Aggregate

The aggregate used in this study was obtained from one of VDOT's bridge construction sites (at Route 682) visited as part of this study. Figure 2 illustrates the EPS installation and the temporary stockpile of the aggregate at this site. Aggregate specimens were characterized by grain-size distribution. Wet sieve analyses with No. 200 sieve were also conducted. The selected sieve openings correspond with Virginia Testing Method (VTM) 25 and Table II-9 of VDOT's (2020b) *Road and Bridge Specifications* for backfill soil.

Figure 2. (a) Stockpile of Backfill Aggregate; (b) Installation of Expanded Polystyrene at the Bridge Construction Site over Route 682

The aggregate was also characterized for compaction following VTM 1 procedures to determine the maximum dry density and optimum moisture content. Specimens were compacted at six different moisture levels. After determining the optimum water content and maximum dry density, necessary corrections were applied per VTM 1.

Characterization of Geotextile

VDOT currently uses a nonwoven separation geotextile to protect EPS from aggregate abrasion. As Figure 2 shows, the geotextile wraps around the EPS during construction, and aggregate is placed adjacent to it.

VDOT shipped the geotextile used in this study to George Mason University (GMU), which is identified as Propex Geotextile 1001. The properties of this geotextile, as provided by the manufacturer, are summarized in Table 2. The reported properties meet VDOT (2020a) requirements listed in Special Provision 404-000130-00 for the geotextile protection fabric.

Table 2. Properties of Propex Geotextile 101 (Provided by the Manufacturer)

Features	ASTM Test Method	Properties
Grab Strength (lb)	D-4632	250
Puncture Strength (lb)	D-4833	112
Tear Strength (lb)	D-4533	90
Permittivity (sec-1)	D-4491	0.5
Apparent Opening Size	D-4751	Opening of U.S. 100 Sieve

Characterization of EPS Material

Two types of EPS were investigated in this study: standard and elasticized. Both materials are produced by Cellofoam North America Inc. (https://www.cellofoam.com/), as it is currently the only vendor in the U.S. market manufacturing elasticized EPS.

EPS for this research was procured through Universal Foam Products (UFP) (https://univfoam.com/), which communicated with Cellofoam on behalf of the research team for material production. Both E-EPS and S-EPS specimens, obtained from UFP, were precut into 2-inch by 2-inch cubes and 12-inch high, 6-inch diameter cylinders for this study. Both EPS specimens were precut in two different directions. This approach was used to assess the effects of load application relative to the EPS orientation.

During communications with UFP to procure EPS, UFP notified GMU and VDOT that Cellofoam manufactures E-EPS from S-EPS with a 0.9 pcf density. This material is classified as EPS15 per ASTM D6817 (2021) and Type I EPS per ASTM C578 (2022). Therefore, for this research, S-EPS with 0.9 pcf density was selected, and Cellofoam was requested to manufacture E-EPS from this material. The density of the manufactured E-EPS reported by Cellofoam is 1.0 pcf. This change in density is expected due to the elasticization procedure, which leads to a reduction in the total volume of EPS. UFP notified the GMU team that Cellofoam used Nexkemia M464-D beads for S-EPS and Styropek BF395M beads for E-EPS. UFP interpreted the sizes of these beads to be very close to each other. Therefore, for practical purposes, it was assumed that both materials were produced from similar materials but underwent different production procedures.

As part of Task 1, both types of EPS were characterized based on the ASTM D1621 (2016) testing procedure. This ASTM test method was chosen because communications with vendors and distributors showed that almost everyone is using this test method to report the properties of the manufactured EPS available in the market. ASTM D1621 (2016) is based on EPS specimens loaded under monotonic unconfined compression (UC) at a rate of 10% per minute. The ASTM procedure allows the specimens to be of cubic or cylindrical shapes, even though the most common size used by the vendors is the cubic shape.

To investigate the effects of specimen shape on test results, researchers tested EPS specimens in both cube and cylindrical shapes. In addition to the 2- inch cube specimens, cylindrical EPS specimens were prepared with dimensions of 2 inches height and 2 inches diameter, 2 inches height and 6 inches diameter, 6 inches height and 6 inches diameter, 12 inches height and 6 inches diameter, and 12 inches height and 4 inches diameter. These dimensions resulted in aspect ratios of height to diameter as 1:1, 1:3, 1:1, 2:1, and 3:1, respectively. Figure 3 shows photos of the tested specimens. An SGI coffee mug was used for scale. To investigate the effects of strain rates during testing, UC tests were conducted at 50%, 10%, 5%, 1%, 0.5%, and 0.1% per minute strain rates.

Figure 3. Cubic and Cylindrical Specimens Used in Monotonic and Cyclic Loadings

The UC tests were conducted using SGI Research Group's Geocomp LoadTrack II machine. The LoadTrack II machine has a load capacity of up to 10,000 lbf and a displacement rate between 10^{-6} and 1.0 inch per minute. Figure 4 shows examples of the specimen configurations tested in UC tests.

ASTM D1621 (2016) defines material characterization based on compressive resistance. Figure 5, created (not actual test results), illustrates how ASTM D1621 (2016) defines these parameters. Compressive resistance is determined as the applied stress on EPS during the test corresponding to a 10% strain. The tangent elastic modulus (E_{tan}) is determined from the slope of the red dashed line shown in Figure 5. ASTM D1621 (2016) does not provide a direct definition for the range of strain conditions under which the material is elastic; however, E_{tan} is defined as the modulus of elasticity during compression. Therefore, it is implied that the range that is used to calculate E_{tan} is the range for the elastic behavior. In the example in Figure 5, the elastic range can be defined as 3% strain.

Figure 4. Example Setups Used to Conduct Unconfined Compressive Tests with Expanded Polystyrene

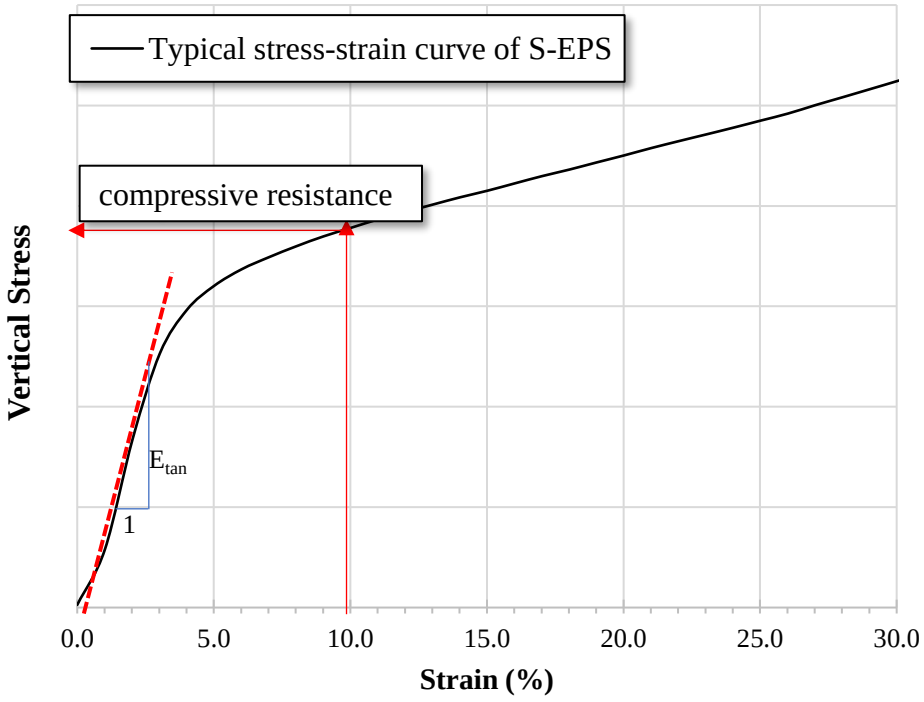

Figure 5. Description of Compressive Resistance and Initial Tangent Modulus of Expanded Polystyrene Based on Monotonic Unconfined Compressive Test. S-EPS = standard expanded polystyrene.

Methods Implemented to Address Task 2: Cyclic Load Testing Simulating Thermal Expansion of Bridge Superstructure

Cyclic tests in Task 2 are conducted using the same machine as in Task 1. Figure 6a displays the photo of the actual test setup and the configuration of specimens inside the test chamber. Depending on the desired configuration, EPS is placed over either a rigid (non-yielding) specimen holder or compacted aggregate (Figure 6b).

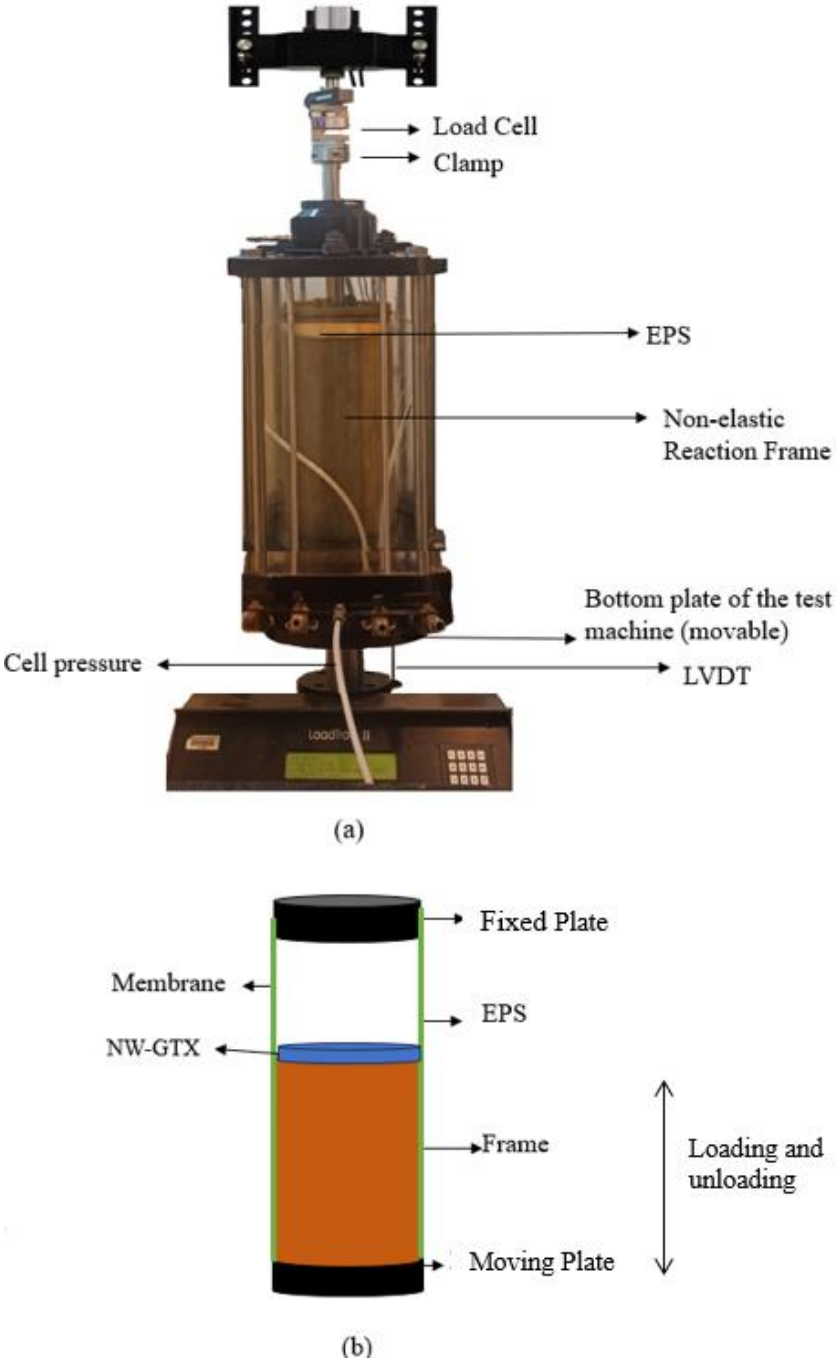

Figure 6. (a) Cyclic Test Equipment Used in this Study; (b) Configuration of EPS inside the Testing Chamber. EPS = expanded polystyrene. LVDT = Linear Variable Differential Transformer. NW-GTX = nonwoven separation geotextile.

EPS specimens used in cyclic tests were cylindrical in shape and were 2 inches in height and 6 inches in diameter (resulting in an aspect ratio of 1:3 (H:D)). Based on evaluating the VDOT database of construction projects, this aspect ratio represents VDOT field applications more accurately than other alternatives.

Cyclic movements during EPS-only tests were controlled by the desired strain rate. The magnitude of the applied loads was recorded by the load cell on top of the chamber housing the EPS specimen. Displacements associated with loading and unloading were recorded by a Linear Variable Differential Transformer attached to the bottom plate that moved during cyclic motions. In Task 2 tests, strains were applied from the bottom, and the top plate remained fixed. A nonwoven geotextile was placed between the EPS and the rigid specimen holder or aggregate (Figure 6) to simulate its presence in field applications between aggregate and EPS. All measurements were automatically recorded by the software and converted into corresponding stress and strains, which could be monitored in real time during the test.

The ASTM D1621 (2016) standard is based on applying a strain rate of 10% strain per minute for compressive loads. This strain rate is significantly faster than the strain rates caused in the field due to the expansion and contraction of bridge girders based on seasonal temperature differences. However, it is not practical to apply the actual strain rates that occur in the field during a laboratory testing program because that would result in each loading cycle taking 1 year (6 months to load and 6 months to unload) for only one cycle. Therefore, there was a need to define a strain rate that is faster than the actual field conditions but is slow enough that the compressive resistance observed from the laboratory test can still be related to the expected behavior in the field. To identify such a strain rate, researchers conducted a series of monotonic tests to define what is referred to in the literature as the "quasi-static range." Quasi-static condition means that after a certain threshold, changes in strain rate will not affect the compressive resistance behavior of the material—minimizing the influence of strain rate on the material's compressive behavior (Jones, 1995; Li et al., 2019; Malik et al., 2018). In this study, quasi-static condition is defined as the strain rate that corresponds to no changes in unconfined compressive resistance, where compressive resistance is defined based on the criteria outlined in ASTM D1621 (2016) (i.e., stress magnitude corresponding to the 10% strain condition on EPS). Once the appropriate strain rate was determined, all cyclic load tests in Task 2 were conducted with the strain rate that satisfied the quasi-static condition.

Cyclic tests were conducted with a 2 psi confining pressure. The magnitude of this pressure was determined based on the typical overburden pressure acting on EPS in abutment applications. According to documents and discussions with VDOT, the distance between the ground surface and the top of EPS is typically 18 inches. When calculating overburden stress, the asphalt layer thickness was assumed to be 2 inches, and the aggregate thickness 16 inches. The unit weight of the asphalt layer was selected as 0.085 pci, and the unit weight of the aggregate as 0.0839 pci (Chapter 17 of VDOT's (2023) *Manual of the Structure and Bridge Division, Part 2—Design Guidelines*).

Figure 7 shows that EPS is exposed to cyclic strain horizontally because of the bridge girder's movements. Because of limitations in the testing apparatus, cyclic loading on EPS specimens could only occur vertically. This phenomenon necessitated the orientation shown in Figure 7a for EPS-only tests and Figure 7b for EPS-aggregate tests. These configurations resulted in horizontal pressures representing the overburden load, maintained by a constant 2 psi confining pressure.

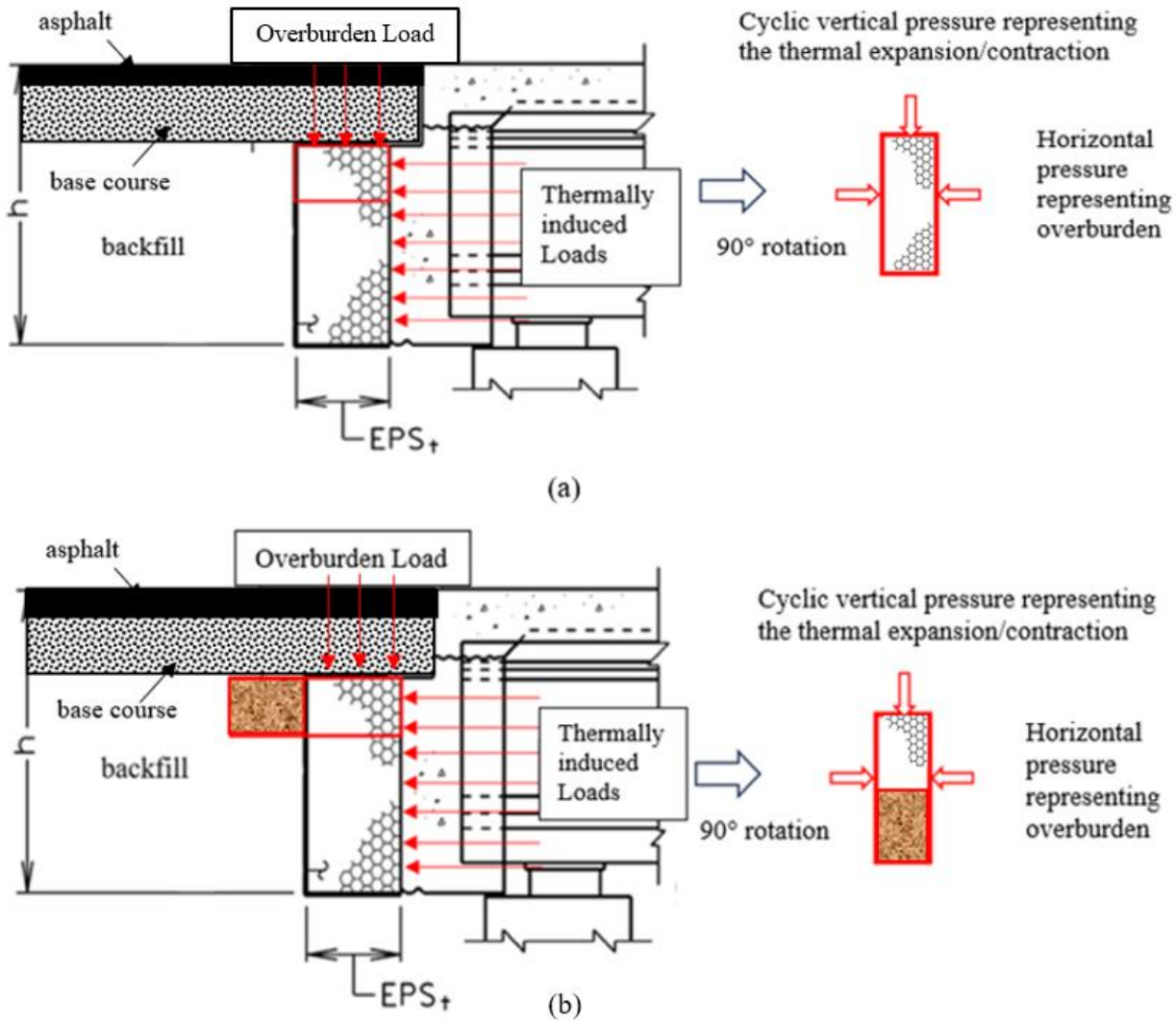

Figure 7. Configuration of EPS Specimen Testing Directions: (a) EPS-only; (b) Combined Tests (EPS plus Aggregate). EPS = expanded polystyrene.

The data VDOT shared with GMU showed that 65 constructed integral bridges are in Virginia with EPS inclusion. The average cyclic strain on EPS, calculated from VDOT data, is 5.6%. Therefore, GMU initiated tests with scenarios maintaining a net 5.6% strain on EPS. For instance, with a minimum applied strain of 1%, the maximum applied strain would be 6.6%. Similarly, if the minimum applied strain is 2%, the maximum applied strain would be 7.6%, ensuring a consistent net applied strain of 5.6% on EPS in both scenarios. Throughout Task 2 evaluation, these values (minimum, maximum, and range of net applied strains) were iteratively adjusted based on test results. Unfavorable outcomes prompted revisions until researchers achieved acceptable results.

The testing machine applied cycles of minimum and maximum loads in a pattern similar to that observed during field measurements by VDOT's instruments (Figure 8).

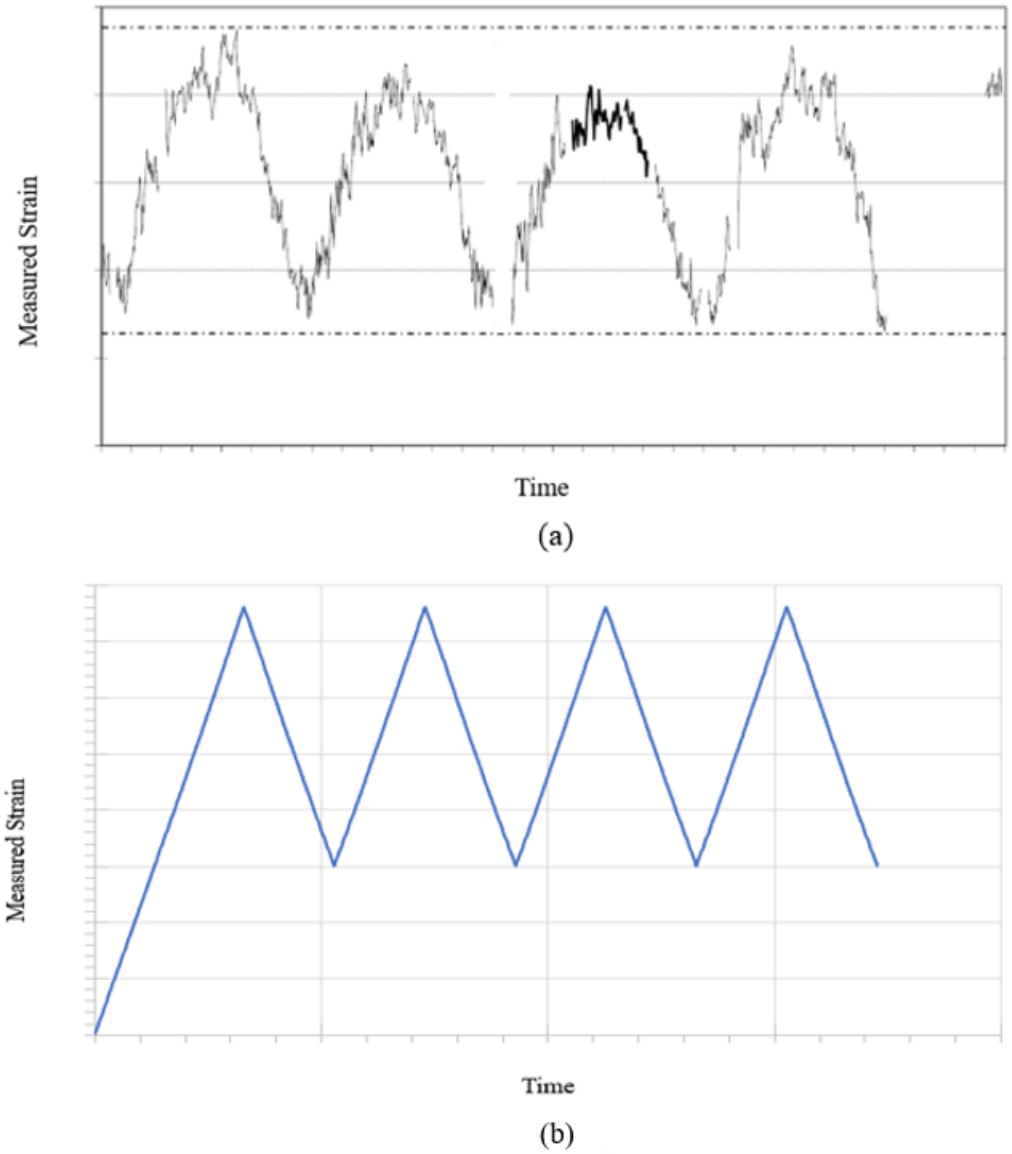

Figure 8. (a) Average Measured Compressive Strain of Elastic Expanded Polystyrene from VDOT Bridge over Route 18; (b) Applied Strain Patterns in the George Mason University Laboratory Testing

The minimum strain applied during the tests represents the compaction-induced strain. In previous VDOT reports, it is stated that immediately after compaction, EPS strain measured 11% because of lateral pressure from backfill on the bridge over Route 60 (Hoppe, 2005). In addition, Hoppe and Eichental (2012) reported a 1.7% EPS strain in the bridge over Route 18 due to compaction. Based on these reported strains and verbal communications with VDOT, the initial test was conducted with 3% strain. This value was changed iteratively based on test outcomes.

Cyclic tests were conducted with three different configurations: (1) EPS placed over a rigid specimen holder (EPS-only), (2) aggregate-only, and (3) EPS placed over the aggregate (EPS-aggregate). Aggregate-only tests evaluated how the aggregate behaves under stress conditions simulating bridge girder expansion. EPS-aggregate combined tests were conducted to confirm that the aggregate is able to provide enough support to EPS for elastic performance

under the intended cyclic conditions. To be conservative in these evaluations, based on communications with VDOT's Technical Review Panel (TRP), aggregate was compacted to 90% relative compaction (below VDOT's target) and at optimum moisture content (Figure 9). Aggregate-only and EPS-aggregate combined tests were also conducted with the same confining pressure at 2 psi, as in the EPS-only tests. However, the aggregate-only test was stress-controlled because in such tests, the testing machine keeps adjusting the loads to impose the intended strain on a given specimen. However, the magnitude of the load depends on the rigidity of the specimen. To align conditions with EPS tests, stress levels corresponding to specific EPS strains were determined and applied. The minimum and maximum stress values for aggregate and combined EPS-aggregate tests were derived from previously completed EPS-only tests. For this comparison, a test conducted with S-EPS was selected as the basis to determine stress conditions. The tests with 75 cycles corresponded to minimum and maximum strain ranges of 3 to 7.6%, respectively. The minimum stress value at 3% strain was 0 psi, and the maximum stress value at 7.6% strain was 7.8 psi. Based on the testing configuration, these measurements are the stresses applied during the aggregate and combined EPS-aggregate tests (Figure 10).

As a result of all cyclic tests, researchers analyzed graphs displaying deviator stress (the difference between applied vertical stress and 2 psi confining pressure) versus strain. The height of all EPS specimens tested in this study was measured before and after each test. All tests used new, previously untested EPS specimens.

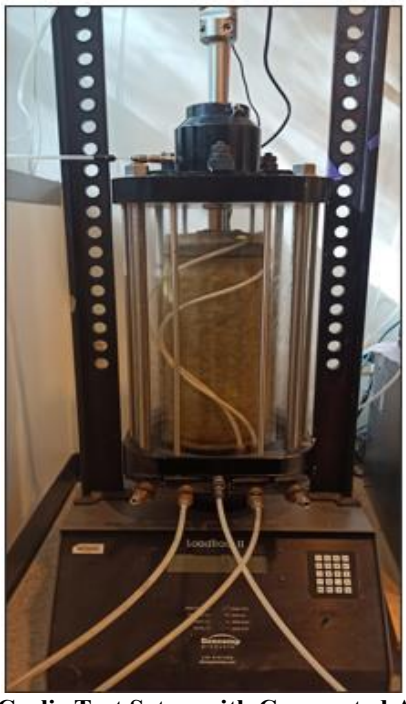

Figure 9. Cyclic Test Setup with Compacted Aggregate.

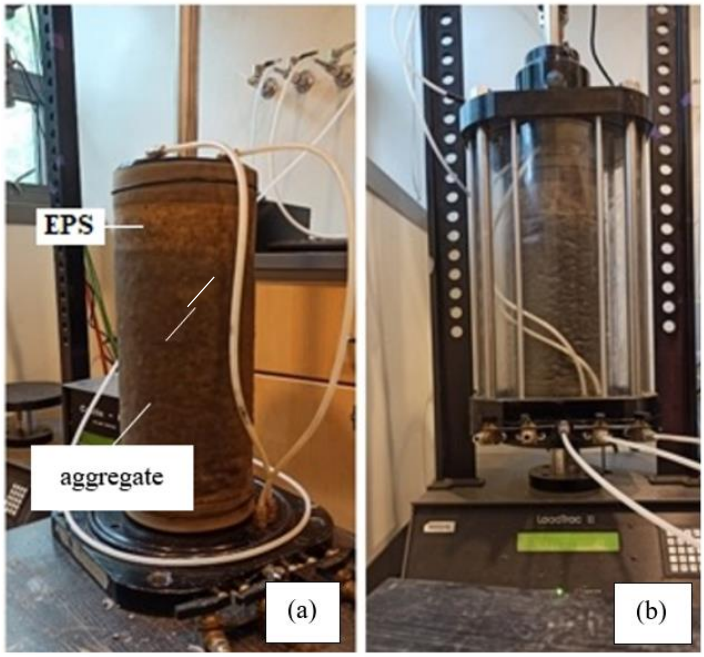

Figure 10. Combined Test Setup Preparation: (a) Appearance of Test Setup Before Placement; (b) Final Appearance of the Combined Test Setup. EPS = expanded polystyrene.

Interpretation of the results was conducted based on the graphs obtained and the physical determination of the permanent strains on EPS at the end of each test (through physical measurements). Results were used to confirm the elastic behavior of EPS under simulated testing conditions. In conventional material science, "elastic behavior" is defined as the ability of a material to deform when subjected to an external force and then return to its original shape and size once the force is removed (Dowling, 1993; Hosford, 2005). Therefore, the same definition has been applied to evaluate the behavior in cyclic load tests conducted in this study.

As Figure 6b shows, the load in these tests was applied from the bottom of the setup, and the magnitude was measured at the top where the load cell is mounted. Any permanent deformation in the EPS specimen resulted in a gap between the top plate and the specimen (Figure 11). When the observed EPS behavior was not elastic, permanent deformations (plastic strains) were noted. It was concluded that the implemented strains were not suitable for EPS to behave elastically. During the test cycles, direct measurements of permanent deformations could not be made because tests were conducted with the test chamber under pressure , therefore specimens were out of reach. However, indications of permanent deformations could be evaluated by observing the gap between the top plate and the tested specimens. Figure 12 presents the typical outcomes of test results that may be considered non-elastic and elastic behaviors. Test data of specimens with non-elastic behavior exhibited deviator stress values reducing to zero before the strain cycle is completed (Figure 12a, circled area along the x-axis). Test data of specimens with elastic behavior exhibited zero deviator stress when the strain cycle also reaches the desired minimum strain values (Figure 12b, circled area along the x-axis).

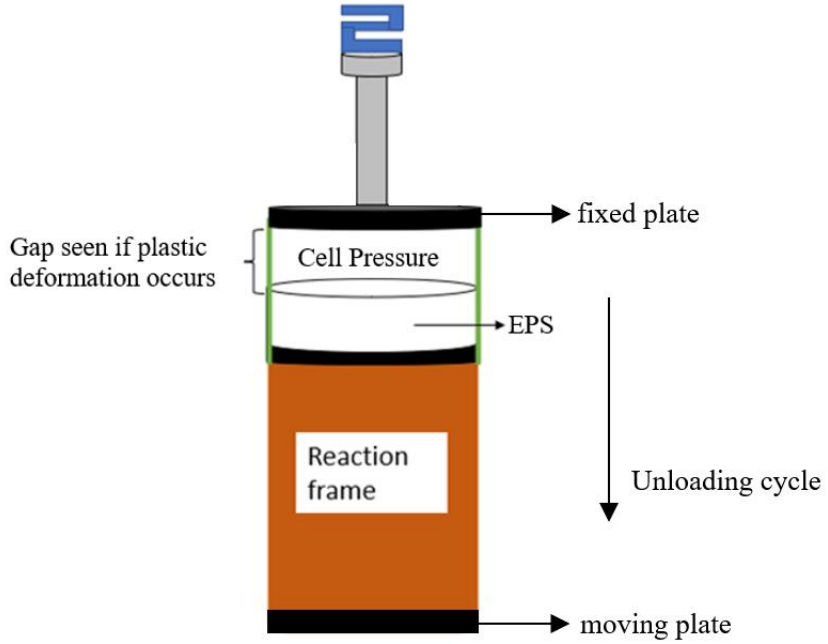

Figure 11. Observed Gap During Cyclic Tests. EPS = expanded polystyrene.

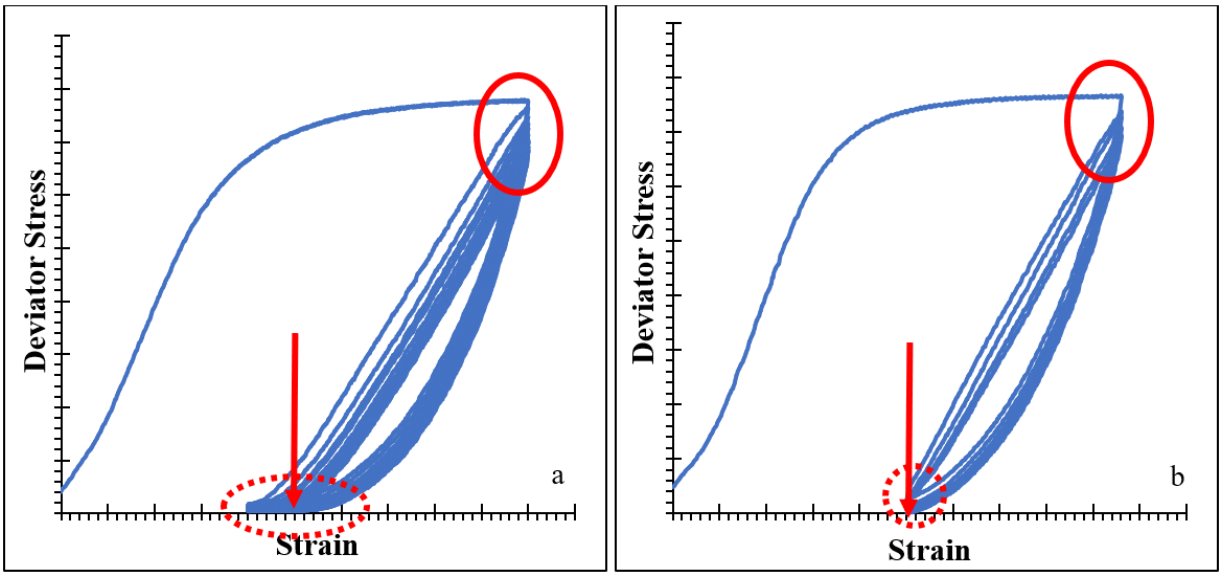

Figure 12. Interpretation of Cyclic Test Results of Expanded Polystyrene: (a) Non-Elastic Behavior Example; (b) Elastic Behavior Example

At the end of each cyclic test, the height of the exhumed EPS specimens is physically measured with a caliper to calculate the strains. This data is then compared with data obtained on the graphs by depicting this information obtained from the test. Figure 12 presents an example of this finding with red arrows. The beginning of the cyclic data along the x-axis shows the minimum strains applied during that particular test. Elastic behavior is obtained if the measured strain after the test is equal to or close to the minimum applied strain (as seen in Figure 12b where the red arrow matches the minimum strain applied). Figure 12a indicates that during the test, a gap occurred, and then EPS has recovered but not returned to its original height. This

interpretation is based on comparing the location of the arrow and the minimum strain magnitude circled along the x-axis in Figure 12a.

Figure 12 illustrates that with cyclic motions, even if EPS remains elastic, the maximum stress measured under repeated loads decreases (depicted as a solid red circle atop the stress-strain curves). This reduction may be attributed to the softening of EPS under repeating loads. However, the decline in peak stress at the applied maximum strain should not be interpreted as undesired behavior of EPS. Considering that the integral bridge girder's results in displacement leading to strain in EPS, the load transferred to the EPS and backfill decreases with increasing load cycles. Such behavior is favorable. Because EPS transfers less stress after each cycle, the corresponding passive earth pressures on the backfill decrease.

Even though a decrease in applied stress conditions occurs, when the changes in deviator stress for each cycle of loading are closely evaluated, as Figure 13 shows, such behavior is observed within the first five cycles and then starts to level off. Similarly, for the minimum applied stresses, such a decrease stabilizes around the 15th cycle and then stays more or less the same for each cycle. Therefore, to maximize the number of evaluations, some cyclic tests were conducted with 5 to 20 load cycles (for quicker evaluations). Long-term behavior was characterized by 75 load cycles.

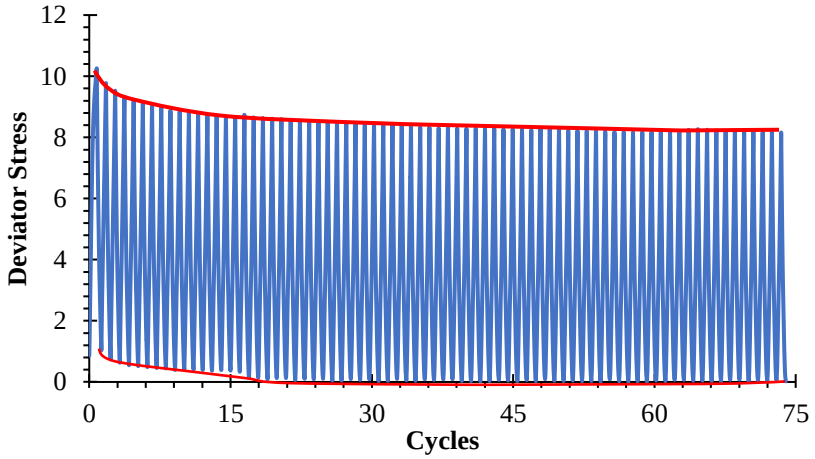

Figure 13. Example of Decrease in Stress by Increase in Number of Cycles

Methods Implemented to Address Task 3: Cyclic Load Testing Simulating Traffic Loading

EPS will be exposed to traffic loadings during its service life. To simulate field loading conditions, E-EPS is loaded in the y-direction, the non-elasticized direction. S-EPS is also loaded in the y-direction. Figure 14 illustrates the stresses applied to EPS during traffic loading tests. In these tests, confining pressure represents the horizontal pressures acting on EPS because of the thermally induced bridge movements.

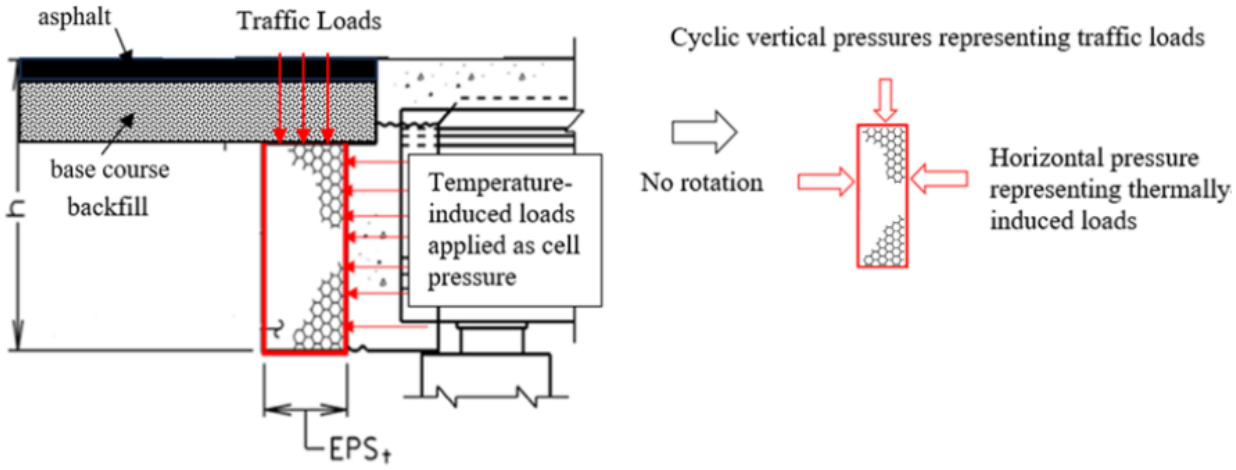

Figure 14. Explanation of Testing Directions of EPS Specimens under Traffic Loadings without Approach Slab. EPS = expanded polystyrene.

Traditionally, resilient modulus testing protocols are used to simulate traffic loading conditions on aggregates. In this study, the focus was to evaluate whether EPS behaves elastically under traffic loadings. Therefore, the testing protocol has been adopted to simulate similar traffic loading conditions as in resilient modulus testing (10,000 load cycles and Haversine load application), but the test was conducted under only one confining pressure to simulate horizontal pressure. The haversine load application was achieved based on 0.1 seconds of loading time and 0.9 seconds of resting time (Dave and Dasaka, 2018; Tanyu et al., 2013). During the resting time, the EPS specimen was exposed to a constant 2 psi vertical pressure representing overburden stress on EPS (Figure 15). The test results were extrapolated based on a logarithmic model to evaluate strains after 100,000 cycles (Bennert et al., 2000). This approach confirms that asymptotic behavior is observed, indicating that EPS does not deform under additional load cycles (desired outcome).

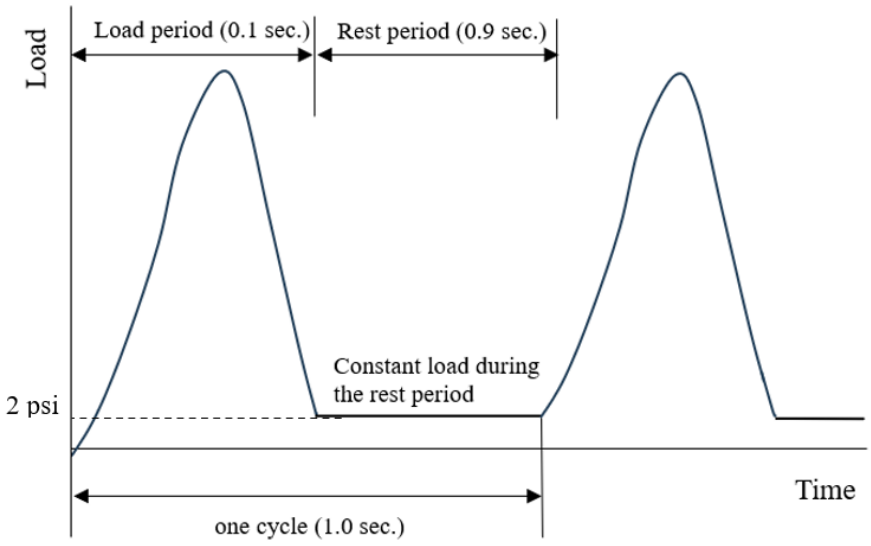

Figure 15. Applied Haversine Configuration on Expanded Polystyrene Specimens during Traffic Loading Tests

The magnitude of traffic loads on the asphalt surface is assumed to be 100 psi, representing the maximum tire pressure of passing wheels (Deacon et al., 2002; Fernandes et al., 2006; Tanyu et al., 2004). The traffic loads applied on the asphalt surface will reduce by the time they reach the top of EPS because of the presence of pavement layers. Figure 16 shows the typical integral abutment cross section with elastic inclusion and pavement layers modeled in KENPAVE analysis to determine this reduced load on EPS. The analysis was conducted based on a tire diameter of 5.31 inches at the asphalt surface (Tanyu et al., 2004). The layer below the base course, shown in Figure 16, is modeled as an EPS layer. It is not possible to model a layer with limited width in KENPAVE. Therefore, as Figure 16b depicts, the EPS layer has been modeled as continuous in the horizontal direction. The layer beneath EPS is modeled as a base course (typical field conditions). The reduced stress is determined right at the top of the EPS layer. Through discussions with VDOT, the distance between the top surface of EPS and the road surface was determined to be 18 inches, which consist of two layers: a 2-inch asphalt layer and a 16-inch base course. This approach is considered conservative in terms of asphalt thickness (thicker asphalt layers would result in a higher reduced load on top of EPS). This study did not focus on the potential effects of the wheel load if an elevation difference is between the bridge approach and bridge deck (bump at the end of the bridge).

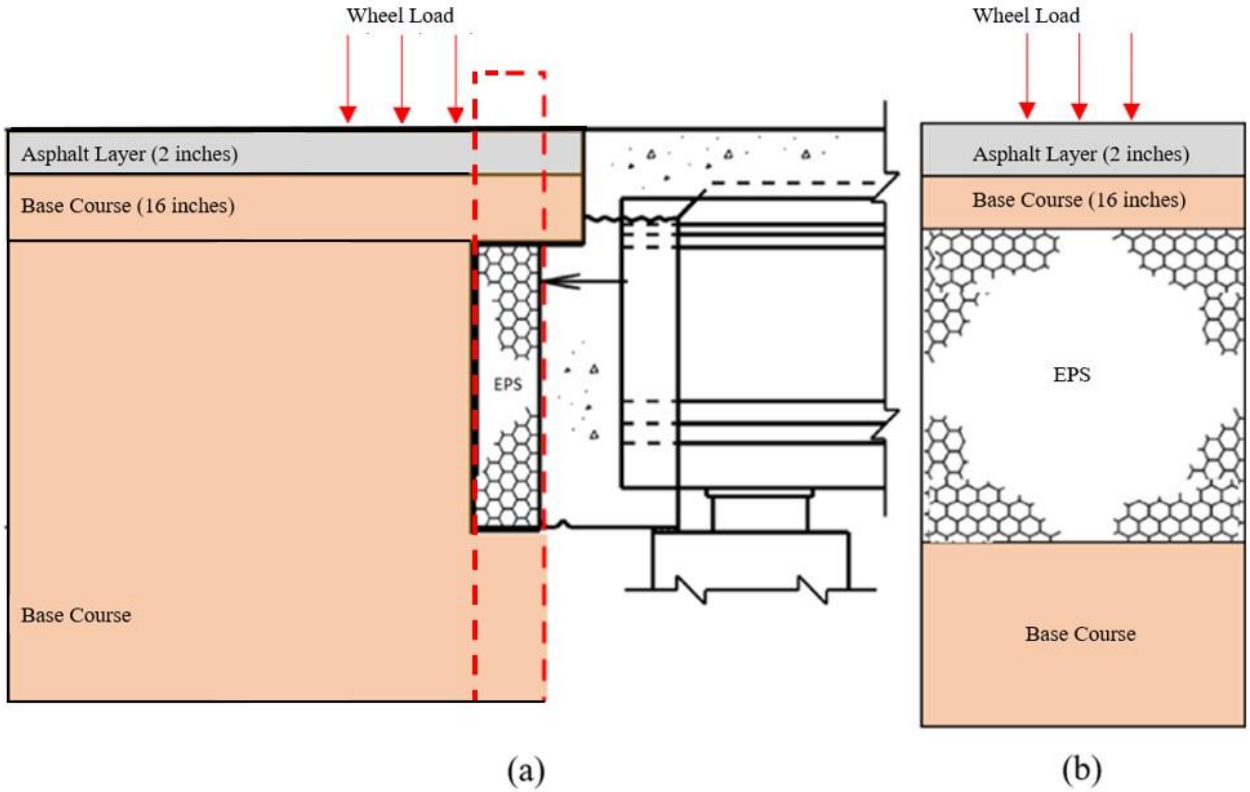

Figure 16. (a) Typical Integral Abutment Construction with EPS Inclusion; (b) Modeled Road Layer Cross Section Representing the Red-dotted Frame in (a). EPS = expanded polystyrene.

Table 3 displays four different KENPAVE model approaches for the analyses, and Table 4 outlines the input parameters. In this study, the elastic modulus of EPS was determined through

a monotonic loading test conducted at the strain rate closest to traffic loading, specifically 50% per minute (the highest achievable strain rate in the GMU laboratory).

Table 3. Summary of Different KENPAVE Model Approaches to Calculate Traffic Loading on Expanded Polystyrene

Analysis No.	Asphalt Layer	Base Course Layer
1	Linear	Linear
2	Linear	Nonlinear
3	Viscoelastic	Linear
4	Viscoelastic	Nonlinear

Table 4. Parameters Used in KENPAVE Analyses to Calculate the Stress Magnitude on Top of the EPS Surface

Layer	Parameter	Used Value	References
Asphalt	Time-temperature shift factor	0.113	Huang (2004)
	Temperature	70 °F	Huang (2004)
	Creep compliance	-	Diogo et al. (2012); Huang (2004); Software-defined values
	Density, γ	145 pcf	Huang (2004)
	Elastic modulus, E	400,000 psi	Huang (2004)
	Poisson's ratio, υ	0.35	Huang (2004)
Base Course	Internal friction angle, ϕ	38°	Defined value in VDOT (2020b) design specifications
	Density, γ	145 pcf	Defined value in VDOT (2020b) design specifications
	Nonlinear parameter, k_1	845	Tanyu et al. (2021)
	Nonlinear parameter, k_2	0.695	Tanyu et al. (2021)
	At-rest earth pressure coefficient, k_0	0.61	$k_0 = 1-\sin\phi$
	Elastic modulus, E	25,000 psi	Tanyu et al. (2021)
	Poisson's ratio, υ	0.35	Tanyu et al. (2021)
EPS	Poisson's ratio, υ	0.15	Elragi et al. (2000)
	Thickness, in	variable	Integral abutment heights constructed by VDOT with EPS
	Elastic modulus	250 psi	Results of this study from S-EPS tested under 50% per min strain rate
	Density, pcf	0.9	Density of S-EPS used in this study

EPS = expanded polystyrene. S-EPS = standard expanded polystyrene.

Laboratory tests were conducted by applying maximum vertical loads determined from KENPAVE analyses' output, simulating confining pressure to match allowed total strains on EPS. Figure 17 illustrates the test setup. A limitation is the dual action of confining pressure horizontally and vertically, possibly inducing negative Poisson's ratio behavior on EPS. Consequently, tests were conducted without confining pressure.

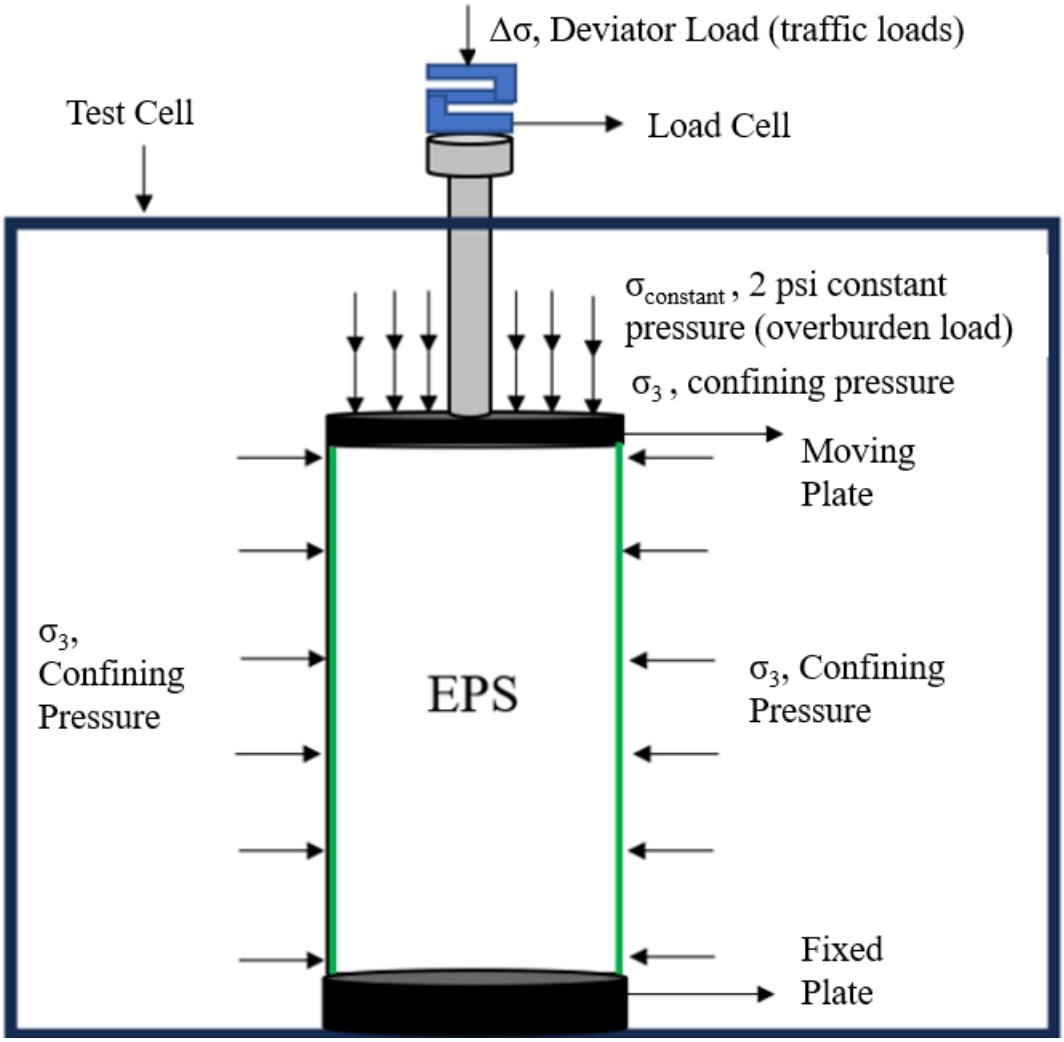

Figure 17. Details of the Testing Apparatus Setup and Applied Loads Simulating Traffic Conditions. EPS = expanded polystyrene.

Literature states that the specimen size and aspect ratio may affect test results. During Task 2, laboratory tests were conducted with EPS specimens having a 0.33:1 (H:D) aspect ratio. In Task 3, this configuration would require the specimen to have a 3:1 (H:D) aspect ratio. EPS specimens procured from the vendor were precut in 6-inch diameter cylindrical shapes. Such a configuration would require the specimen to be 18 inches in height. However, the equipment used in this study can only test up to 12 inches in height. Therefore, two different tests were conducted to evaluate the effect of specimen aspect ratio and size. The first specimen size used was 12 inches in height and 6 inches in diameter (2:1). Although this size does not satisfy the 3:1 (H:D) aspect ratio, it provides insights into the sensitivity of the aspect ratio on EPS under traffic loading conditions. A second specimen, 12 inches in height and 4 inches in diameter, was tested; it satisfied the 3:1 (H:D) aspect ratio.

RESULTS

The following presents the results obtained from each of the laboratory testing tasks.

Results of Task 1: Characterization of Materials

Aggregate Characteristics

The grain size distributions were obtained from three repeated sieve analyses, and the results are presented in Figure 18. According to Section 207 of the VDOT (2020b) *Road and Bridge Specifications*, this aggregate is classified as VDOT 21B base course material. The lower and upper limits of VDOT 21B aggregate are also depicted in Figure 18.

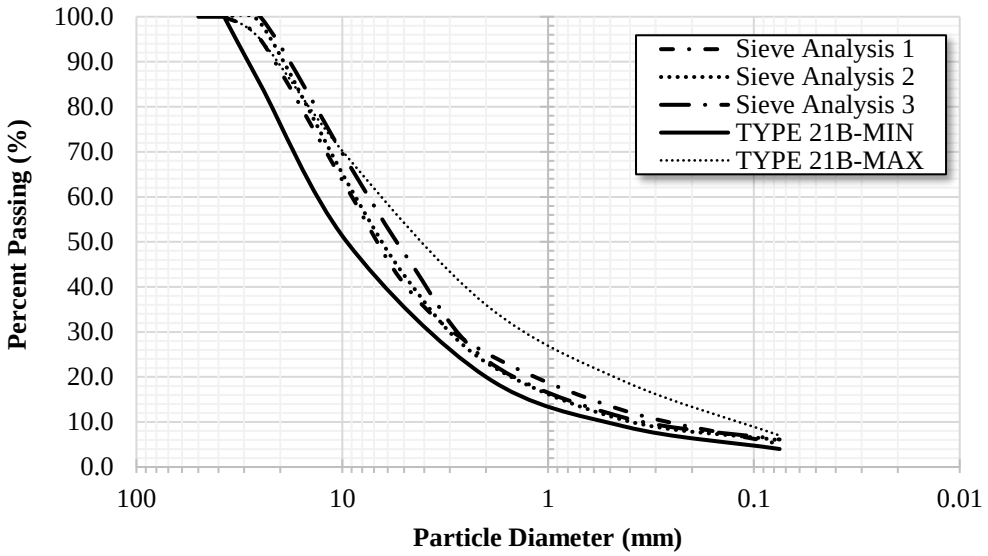

Figure 18. Grain Size Distribution of the Aggregate Sample Used in this Study

Based on American Association of State Highway Transportation Officials (AASHTO) soil classification, the aggregate is classified as A-1-a, which indicates stone fragments, gravel, and sand. The soil tested consists of approximately 7% fine particles (silt- and clay-sized), approximately 38% sand-sized particles, and approximately 55% gravel-sized particles.

The compaction curve and the zero-air void line for the 21B aggregate used in this study are presented in Figure 19. VTM 1 dictates a correction if the amount of material retained on the No. 4 sieve is greater than or equal to 10%. Therefore, for the aggregate used in this study, a correction is required. After calculations based on equations 1 and 2 in VTM 1, the corrected optimum moisture content and maximum dry density are determined as 5.7% and 158.7 pcf, respectively.

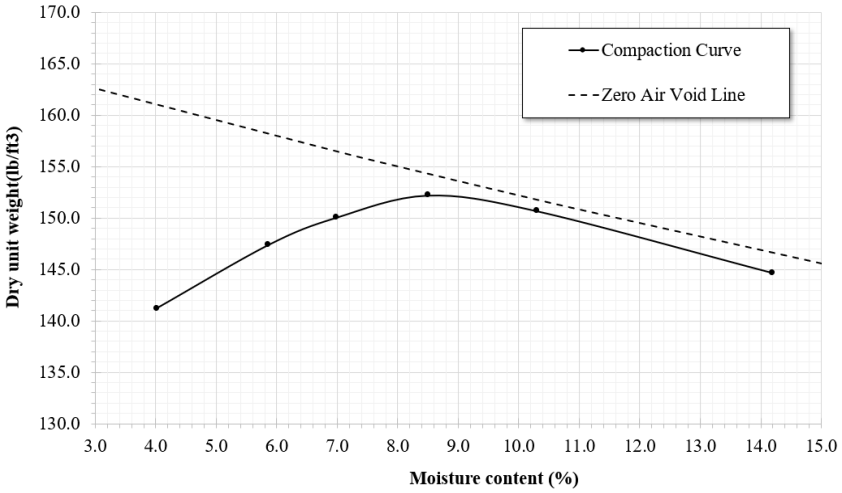

Figure 19. Compaction Curve of the Aggregate Tested in this Study

EPS Characterization

The stress-strain curve of procured EPS specimens closely aligns with the manufacturer's data available on their website (https://www.cellofoam.com/products/building-products/geostructural-foam/elastic-inclusion-eps), as Figure 20 depicts. Moreover, the manufacturer also provided five compressive resistance values at 10% strain for these EPS specimens. These results were obtained by an independent laboratory (stress-strain curve data were not provided). For comparison, the average compressive resistance of these five UC tests is calculated as 5.2 psi. In addition to the manufacturer's data, GMU also conducted tests with these specimens. Figure 20 compares all these results. The results indicate that compressive resistance values meet VDOT (2020a) requirements (5±0.4 psi based on Special Provision 404-000130-00).

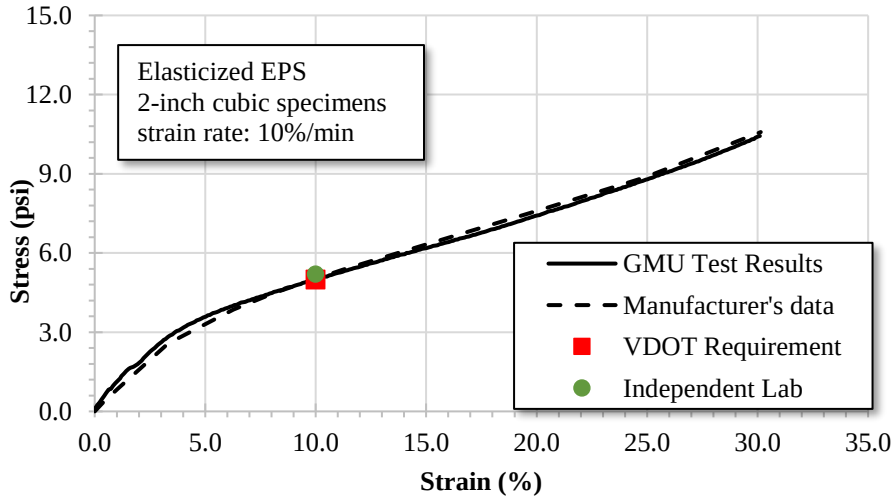

Figure 20. Comparison of GMU Test Results with Manufacturer's Data and VDOT Requirement. EPS = expanded polystyrene. GMU = George Mason University.

The size and shape of the EPS specimens tested in Task 1 of the study are tabulated in Table 5.

Table 5. EPS Specimens Used in Unconfined Compression Tests to Investigate Given Parameters

Investigated Parameters*	EPS Specimens				
	Cube	Cylindrical			
	2 in H 2 in L 2 in W	2 in H 2 in D	2 in H 6 in D	6 in H 6 in D	12 in H 6 in D
Direction of Loading	✓				
Specimen Shape	✓	✓			
Specimen Size		✓		✓	
Aspect Ratio of Specimen			✓	✓	✓
Strain Rate	✓				

D = diameter; EPS = expanded polystyrene. H = height; L = length; w = width.
* Each parameter is investigated for both standard and elasticized EPS.

The density of EPS used in this study has been reported by the manufacturer. However, considering the fact that tests were conducted with different shapes and sizes, the density of each tested specimen has also been independently determined. Table 6 presents the range of the density values that were determined.

Table 6. Densities of EPS Specimens

EPS Type	Manufacturer Reported Density (pcf)	Range of Measured Density (pcf)*
Standard	0.9	0.86±0.02
Elasticized	1.0	1.01 ±0.02

EPS = expanded polystyrene.
*The range indicates the results obtained from 33 of the specimens used in Task 1.

ASTM D6817 (2021) is used to classify S-EPS material based on density and minimum compressive resistance at 10% strain. The compressive resistance of S-EPS was noted to be 10.2 psi. Based on the information in Table 6 and the compressive resistance values, S-EPS has classified as EPS15 in accordance with ASTM D6817 (2021) and Type I based on ASTM C578 (2022). On the other hand, E-EPS did not satisfy the ASTM D6817 (2021) and ASTM C578 (2022) requirements.

Repeatability of the Tests of Unconfined Compression Tests

Each compressive resistance test is conducted at least three times. The results of all three tests for each EPS type are presented in Figure 21. As seen, stress-strain curves of the EPS specimens in all repeat tests are nearly identical. Therefore, one can conclude that the repeatability of the tests in this study was satisfactory. For the remaining test results in this report, only the average results of the repeat tests were plotted.

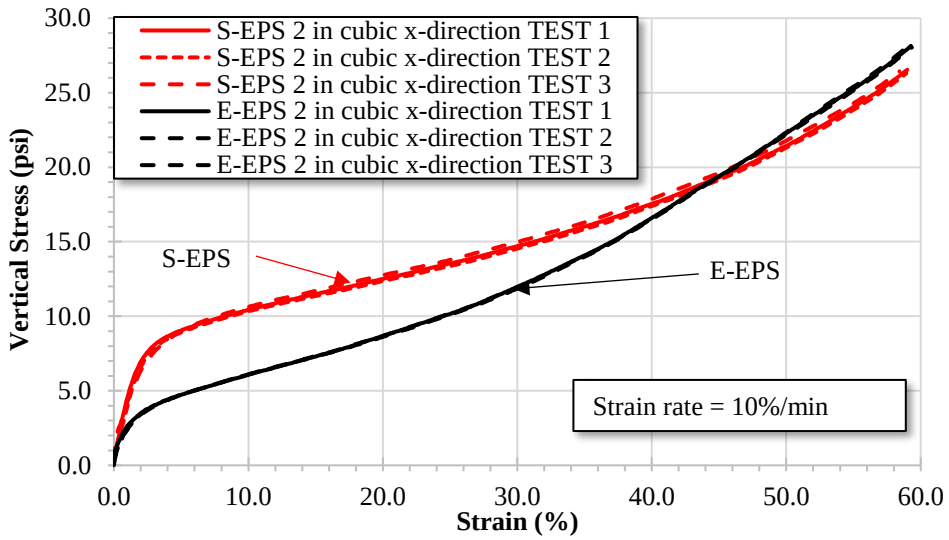

Figure 21. Repeatability of the Unconfined Compression Tests for Standard EPS (S-EPS) and Elaticized EPS (E-EPS). EPS = expanded polystyrene.

Effect of EPS Type and Loading Direction

As Table 5 presents, the effect of the direction of loading on EPS was investigated with cube specimens. Figure 22 shows the coordinate system used to evaluate the effects of direction of loading. For E-EPS, the term x-direction is used to depict the direction of the elasticization on EPS.

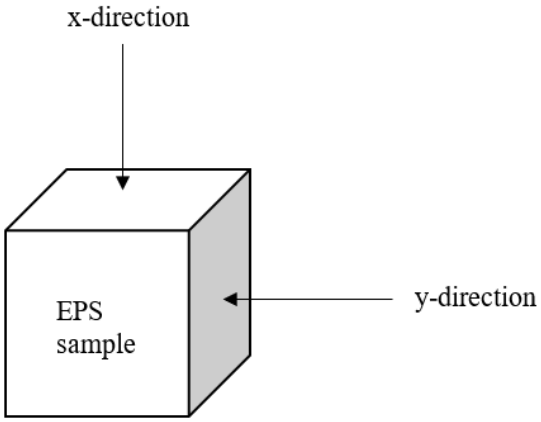

Figure 22. Direction of Loading on EPS Specimens: X-direction Indicates Elasticized Direction for Elasticized EPS. EPS = expanded polystyrene.

Figure 23 presents the results obtained from this evaluation for both types of EPS. The results show that when both types of EPS are loaded in the same x-direction, a difference between the stress-strain curves exists. The difference in stress-strain behavior between the two EPS types could possibly be attributed to the shape of the beads within the EPS material. For S-EPS, the beads within the material appear to be quite spherical prior to testing, but for E-EPS, the beads appear in an ellipsoidal shape (Figure 24). This difference is most likely the reason for the two EPS types to exhibit different behavior when loaded in the x-direction. Such a difference in stress-strain behavior also results in differences in the unconfined compressive resistances, as

defined by ASTM D1621 (2016). At 10% strain, the compressive resistance of E-EPS is 6.1 psi and 10.5 psi for S-EPS. These results indicate that E-EPS is a weaker material compared with S-EPS. However, this finding may not be negative because the load is imposed on EPS based on strain-controlled conditions in the case of integral bridge applications. Another way to evaluate the results shown in Figure 23 is that for a given strain condition, E-EPS results in smaller stresses. This phenomenon could be an advantage in the field, which is why this study evaluated the performance of both E-EPS and S-EPS.

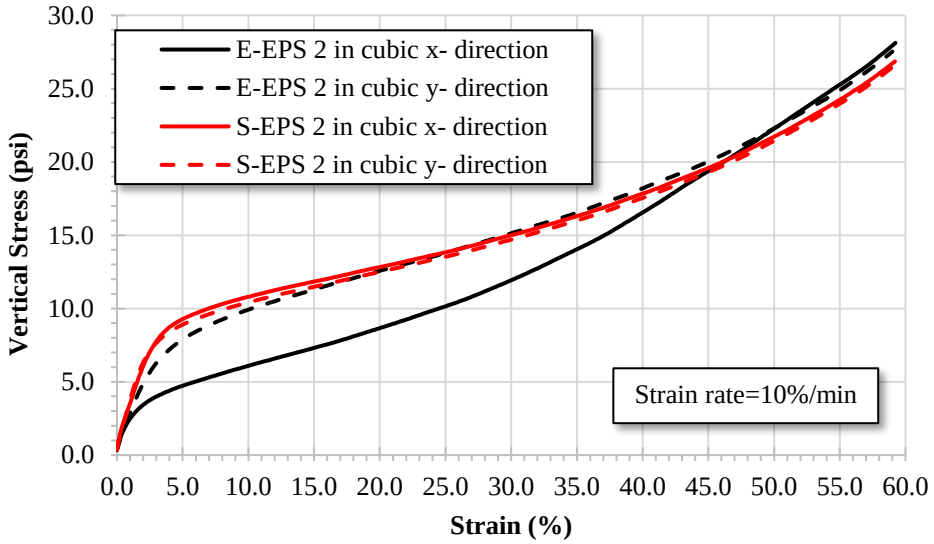

Figure 23. Effect of Loading Direction on EPS. EPS = expanded polystyrene; E-EPS = elasticized EPS; S-EPS = standard EPS.

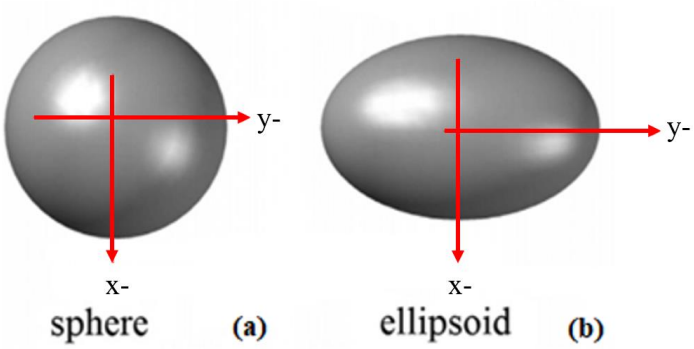

Figure 24. Typical Shape of EPS Beads: (a) Standard EPS; (b) Elasticized EPS. EPS = expanded polystyrene.

Data in Figure 23 also show that when EPS is loaded in the y-direction, the stress-strain behavior of both types of EPS is the same. This may be explained by the shape of the beads. S-EPS has spherical-shaped beads, resulting in isotropic behavior. For E-EPS, the long axis of the ellipsoid beads (y-direction) provides similar performance to spherical-shaped beads. This is because, when the ellipsoid beads are loaded in the y-direction, they gradually turn into spheres.

Effect of Specimen Shape and Size

As presented in Table 5, the effect of specimen shape was investigated using both cubic and cylindrical EPS specimens, each with identical 2-inch dimensions. Figure 25 displays the results of unconfined compressive tests conducted with a 10% per minute strain rate in the x-direction. The results indicate no significant difference in testing cubic and cylindrical specimens at these dimensions for both types of EPS. However, the compressive resistance of cubic specimens is slightly higher for both EPS types. For instance, the compressive resistance at 10% strain for S-EPS and E-EPS, cubic and cylindrical specimens, is 10.9 and 10.1 psi, 6.3 and 6.0 psi, respectively.

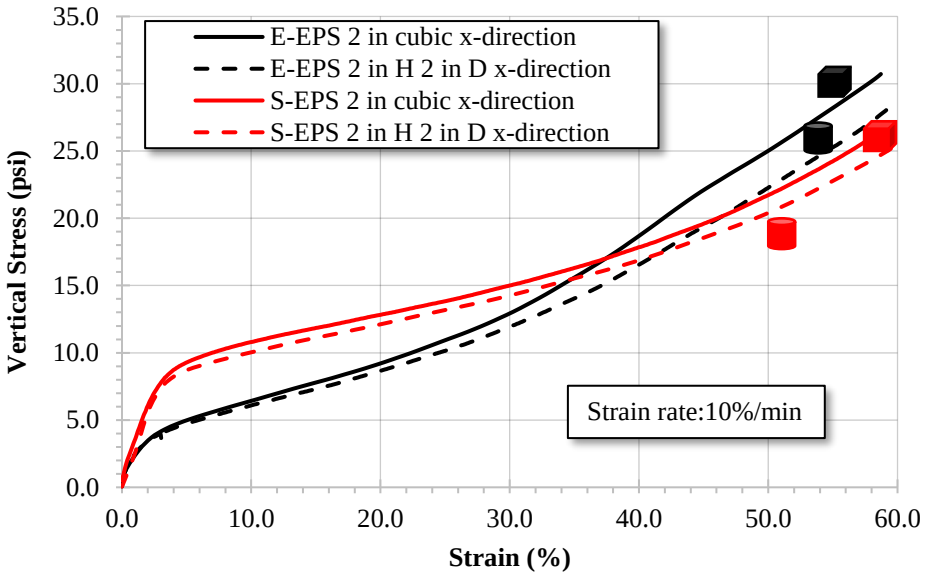

Figure 25. Results of Monotonic Compression Tests with Cubic and Cylindrical Standard and Elasticized EPS Specimens. EPS = expanded polystyrene.

Figure 25 shows that the behavior of the 2-inch cube and 2-inch cylindrical specimens is not significantly different from each other. Because of the abundance of precut specimens by the vendor, cylindrical samples were used in remaining tests, except for those evaluating the effect of strain rate. Specimens were prepared at two different sizes: 2 inches height, 2 inches diameter, and 6 inches height, 6 inches diameter, both resulting in a 1:1 height-to-diameter aspect ratio. Figure 26 presents the results of the unconfined compressive resistance tests conducted with these EPS specimens in the x-direction at a 10% per minute strain rate. These results are used to evaluate the effect of specimen size.

Tests were conducted until the strain limits of the GMU test setup were reached, as shown in Figure 26. In the case of S-EPS, the stress-strain behavior of both sizes of specimens was consistent. However, for the E-EPS specimens, not only was the stress-strain behavior different, but the compressive resistance at 10% strains, as defined by ASTM D1621 (2016), also varied.

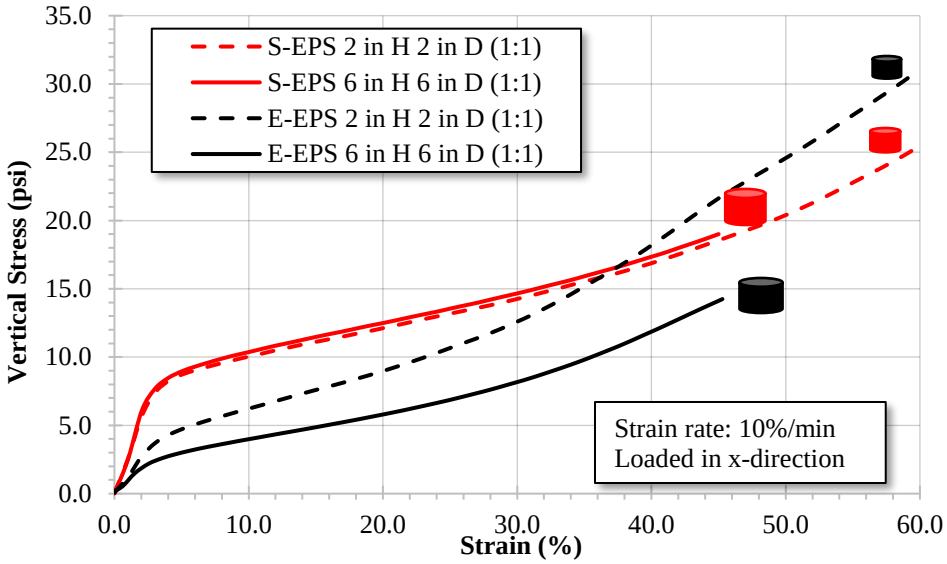

Figure 26. Results of Monotonic Compression Tests with Cylindrical Standard and Elasticized EPS Specimens at Different Size. EPS = expanded polystyrene.

Effect of Aspect Ratio

Previous literature studies suggest that increasing the aspect ratio of the EPS specimen enhances the tangent elastic modulus (Atmatzidis et al., 2001; Hazarika, 2006). However, the effect of aspect ratio on the stress-strain behavior of E-EPS is not well documented. This study evaluates both EPS types with three aspect ratios (1:3, 1:1, and 2:1). Table 5 presents the shapes and dimensions of the specimens used for evaluation.

Figure 27 presents the results obtained from monotonic UC tests conducted at a 10% per minute strain rate. Findings indicate that changes in aspect ratio affect the compressive resistance of E-EPS (Figure 27a) but not S-EPS (Figure 27b). At 10% strain, E-EPS specimens with 2:1 and 1:3 aspect ratios exhibited 2.6 and 5.2 psi compressive resistance, respectively. This comparison reveals that in case of E-EPS, the compressive resistance increases as the aspect ratio decreases.

When examining the aspect ratio in terms of the initial elastic modulus (as defined in Figure 5), no significant difference is observed for E-EPS specimens (ranging from 10.5 to 10.8 psi). In contrast, an increase in the aspect ratio appears to correlate with an increase in elastic modulus for S-EPS. For S-EPS specimens, the elastic moduli are 30.9, 37.5, and 52.3 psi for aspect ratios of 1:3, 1:1, and 2:1, respectively. These S-EPS results align with those presented in the literature.

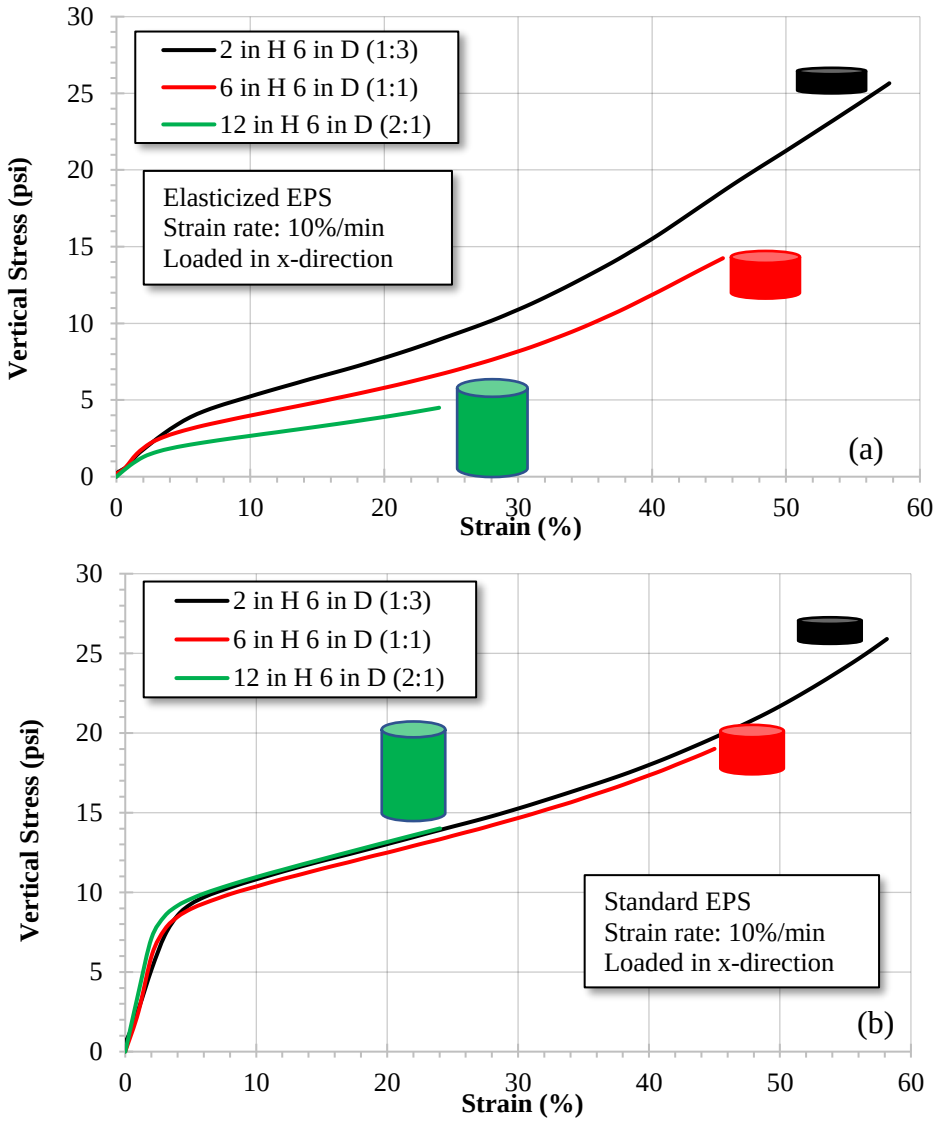

Figure 27. Effect of Aspect Ratio on Cylindrical (a) Elasticized EPS (b) Standard EPS Specimens. EPS = expanded polystyrene.

Effect of Strain Rate

In the literature, studies on S-EPS have shown that the strain rate significantly affects stress-strain behavior (Athanasopoulos et al., 1999; Duškov, 1997; Khalaj et al., 2020; Ossa and Romo, 2009). These studies report that increasing strain rate raises compressive resistance (at 10% strain). However, the response of E-EPS to changes in strain rates has yet to be investigated. Therefore, this study investigates the effect of strain rate on both EPS types when specimens are tested in UC and in the x-direction. The effects of six different strain rates (i.e., 50, 10, 5, 1, 0.5, and 0.1% per minute) were evaluated. Considering that most commercial laboratories test EPS specimens with cube specimens at 10% per minute to facilitate comparison (Figure 20), all tests in Task 1 were conducted with cube specimens, as Table 5 depicts. Figure 28 presents the results of these tests.

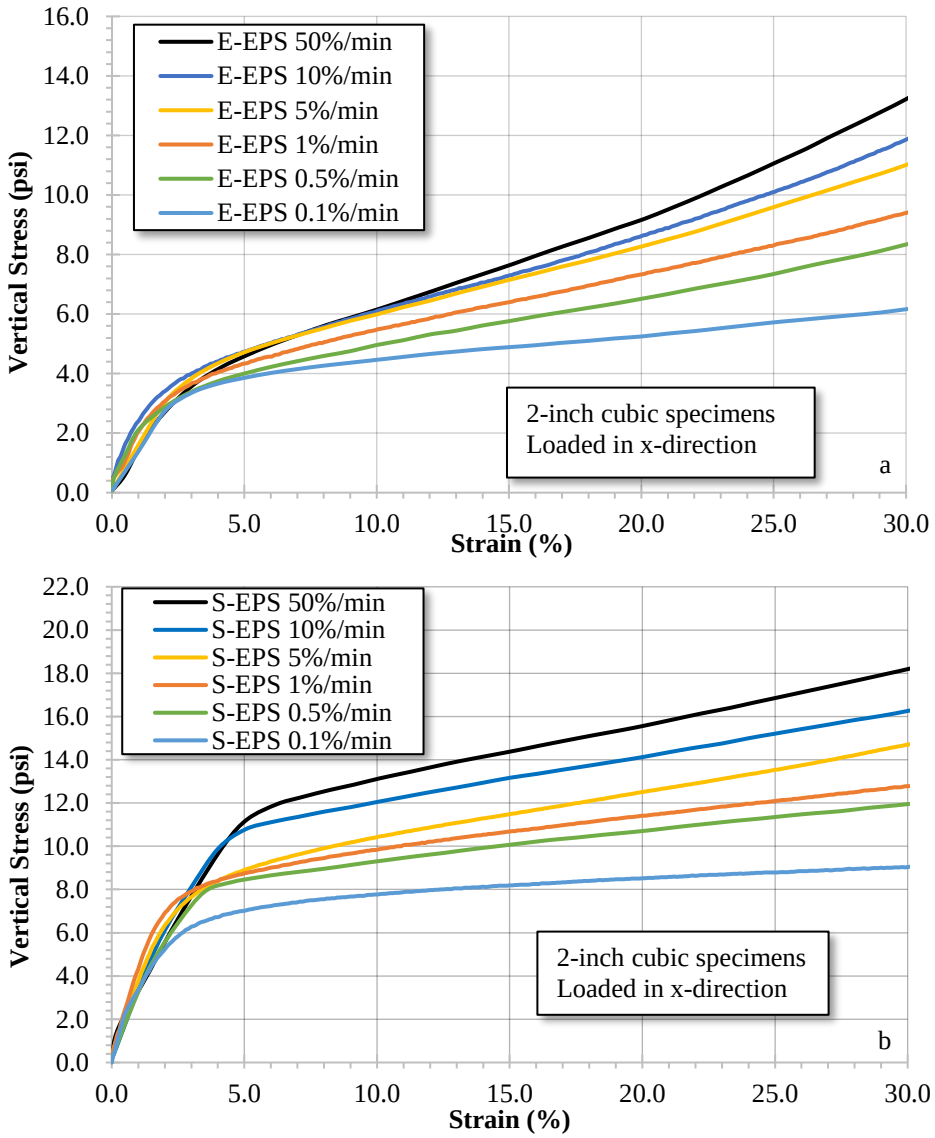

Figure 28. Effect of Strain Rate on Specimens: (a) Elasticized EPS; (b) Standard EPS. EPS = expanded polystyrene.

As shown in Figure 28, the compressive resistance of both EPS types is affected by the strain rate under which the materials are compressed. Increasing the speed (strain rate) results in a stronger material response. Although less apparent for S-EPS (Figure 28b), increasing the strain rate also extends the zone where the material exhibits elastic behavior. At 0.1% per minute, S-EPS appears elastic up to 2% strain; then, from 0.5 to 2% per minute, the elastic range increases to 3%, and at 50% per minute, the elastic range extends to 4% strain.

Results of Task 2: Cyclic Load Testing Simulating Movement of Bridge Superstructure

The results determined in Task 1 of this study clearly show that the speed at which EPS is loaded and unloaded has an effect on the stress-strain behavior of both types of EPS. Because thermally induced bridge movements occur at a very slow rate in field applications, it is

impractical to test the long-term behavior of EPS in the laboratory at the exact rate as in the field. However, if the test is conducted at a slow enough rate—one in which strain-rate changes do not affect the compressive resistance of EPS—it is possible to correlate the results to the most likely field conditions. This concept is referred to as the "quasi-static" condition.

Considering the results from Task 1, it was important to determine a specific EPS specimen shape and size (with a specific aspect ratio) for quasi-static evaluation and the remainder of the Task 2 tests. The results from Task 1 (Figure 25) led researchers to choose the cylindrical shape of the specimens for the Task 2 tests. This shape also provided advantages for the Task 2 tests requiring the specimen to be confined with air pressure (uniform distribution along the specimen). The selection of the aspect ratio for the specimens was more complex and required evaluating both the results obtained from Task 1 (Figure 27) and the detailed evaluation of the VDOT database of the constructed integral bridges. Increasing the EPS thickness for a fixed abutment height in field constructions will change the aspect ratio (ratio of the EPS inclusion thickness to abutment height). It is not practical to capture all different aspect ratios within the time limits of a given study, but the evaluation of the VDOT database showed that in general, a 1:3 aspect ratio in the laboratory represented the field-installed conditions fairly. The results in Figure 27 also indicated that for a given strain, E-EPS would transfer higher stress at a 1:3 aspect ratio compared with other aspect ratios. Such a condition also resulted in the highest compressive resistance at 10% strain. Consider this relationship, the higher the compressive resistance, the higher the lateral earth pressure that would be exerted. The selection of the 1:3 aspect ratio is also considered as adding conservatism to the evaluations in Task 2. The largest specimens that could be tested with a 1:3 aspect ratio within GMU's SGI testing apparatus were 2 inches in height and 6 inches in diameter. Considering that the conventional tests (ASTM D1621 (2016)) are already based on 2 inches in height, this condition has been determined to be favorable.

Figure 29 illustrates the stress-strain behavior of tests conducted at various strain rates to determine a quasi-static condition for EPS. The results in Figure 29 were then used to determine the unconfined compressive resistance at 10% strain (as per ASTM D1621 (2016) definition). The corresponding values for each strain rate are plotted in Figure 30. The data trendline indicates that the unconfined compressive resistance levels out around a 0.1% per minute strain rate, and the difference becomes negligible starting at a 0.02% per minute strain rate (Figure 30). The slight differences observed in compressive resistances result from the specimens' slightly different densities. For practical purposes and to complete tests within reasonable time limits, a 0.02% per minute strain rate is determined to satisfy the quasi-static definition. Although these tests used E-EPS, a prior study by Al-qarawi et al. (2020) with S-EPS (density = 1.25 pcf) also claimed a quasi-static conditions at 0.02% per minute. Therefore, it is concluded that a 0.02% per minute strain rate is suitable for achieving quasi-static conditions for both types of EPS.

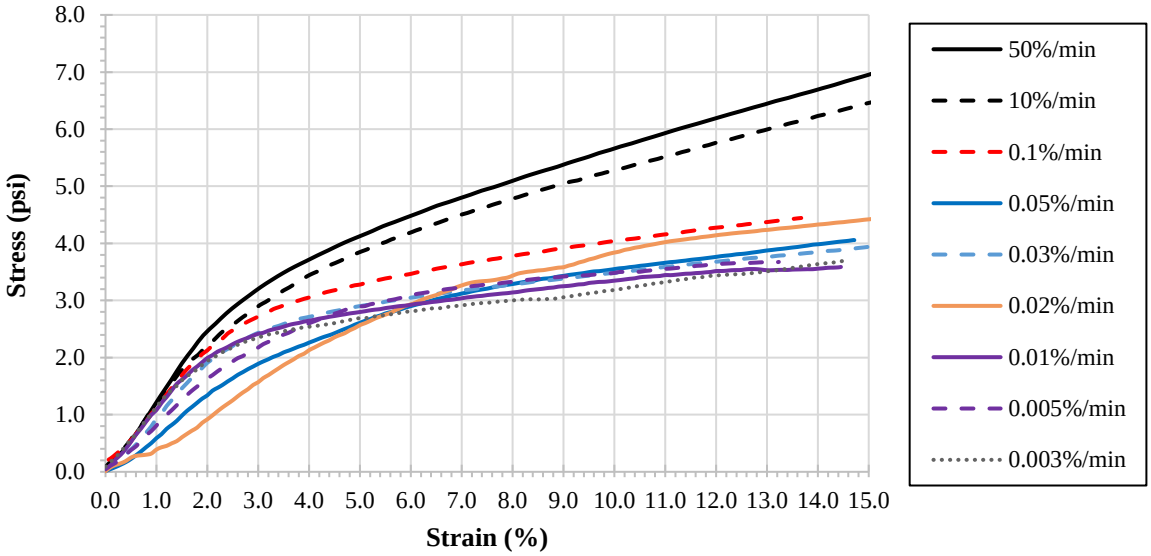

Figure 29. Unconfined Compression Tests to Determine the Quasi-Static Strain Rate

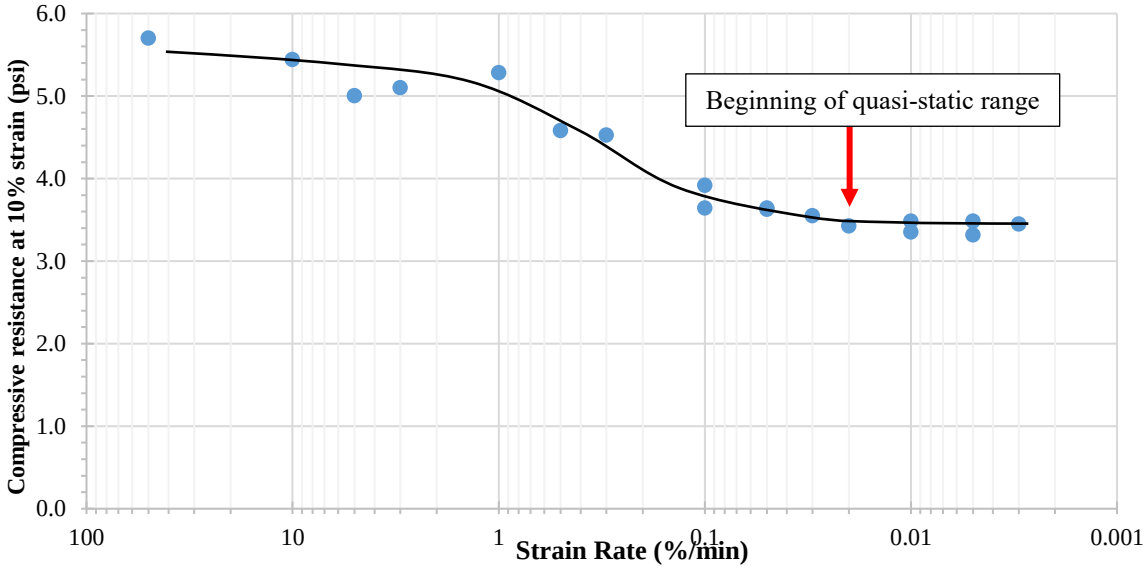

Figure 30. Determining the Quasi-Static Range of Expanded Polystyrene Specimens Based on Compressive Resistances at 10% Strain

Quasi-Static Cyclic Tests Simulating Bridge Expansion and Contraction

Repeatability of the EPS Tests

The repeatability of the monotonic unconfined compressive resistance tests was confirmed in Task 1. Tests in Task 2 evaluated EPS behavior under cyclic loads applied at a 0.02% per minute rate and with a 2 psi confinement. To confirm repeatability for this configuration, some tests were repeated. Figure 31 shows example data of a repeated test result. The comparison of the repeat test results shows that, except for the initial loading, no significant difference was observed between the two tests. It is believed that the difference in the initial

loading was due to minor density differences between the EPS specimens (see Table 6). The example data in Figure 31 were gathered from S-EPS testing. Repeat tests were also conducted with E-EPS, and the results were similar to the example shown in Figure 31 (results not shown here).

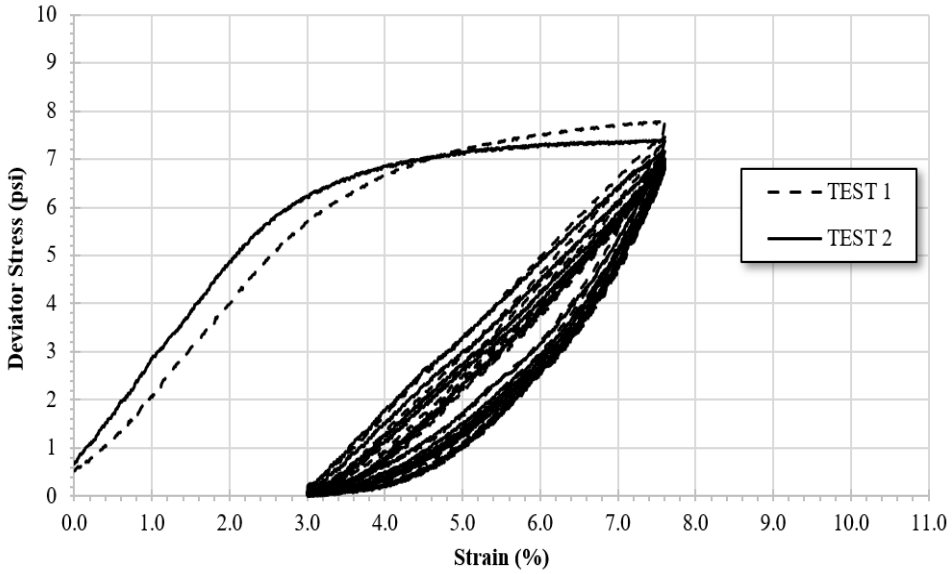

Figure 31. Example Data to Evaluate Repeatability of the Quasi-Static Cyclic Tests

Results of the Tests Conducted Only with EPS

Table 7 presents the results of cyclic loading tests conducted with S-EPS. The table was created based on iteratively conducted tests, where the range of minimum and maximum applied strains was revised to identify conditions deemed satisfactory. The criterion for a test to be labeled "satisfactory" was determined based on conditions where the EPS specimen exhibited only permanent strains equal to or less than the minimum applied strain (meaning, EPS could compensate any additional strain that was applied during the cyclic loading based on the elastic behavior). Due to time constraints and the iterative process, initial tests involved 5 cycles. Subsequent conditions were extended to 20 and 50 cycles based on outcomes. The final test that was determined to be the "satisfactory" condition was then tested at 75 cycles.

Tests considered unsatisfactory are listed in Table 7 as "yes" for the gap between the load plate and the EPS specimen. The gap, illustrated in Figure 12, is confirmed by test data (Figure 12a) and the measured EPS strain recorded on dismounted specimens after the test. In other words, if the calculated strain from the specimens after cyclic loading exceeded the minimum applied strain during the test, results were deemed unsatisfactory. For tests with only 5 cycles, evaluation relied primarily on the test data's shape. In some cases, the EPS strain at the end of the test end was only 0.1% higher than the minimum applied strain. Although it is a small difference, if results exhibited cyclic behavior similar to Figure 12a, it was determined from previous tests that such a condition in the long-term would result in problematic behavior. Therefore, in the interest of time, those tests were terminated as opposed to continuing to 75 cycles. Figure 32 shows an example of an unsatisfactory test result.

Table 7. Cyclic Loading Tests Conducted with S-EPS

EPS Type	Min. Applied Strain (%)	Max. Applied Strain (%)	Difference Between Min. and Max. Applied Strains (%)	Number of Load Cycles	Applied Strain Rate (%/min)	Measured Strains on EPS After Tests (%)	Gap Occurred Between EPS and Load Plate? *
Standard	1.0	5.6	4.6	5	0.02	1.6	YES
Standard	2.0	6.6	4.6	5	0.02	2.2	YES
Standard	4.0	7.6	3.6	5	0.02	3.7	NO
Standard	5.0	9.6	4.6	5	0.02	3.7	NO
Standard	4.0	8.6	4.6	20	0.02	4.0	NO
Standard	4.0	10.0	6.0	20	0.02	5.5	YES
Standard	3.0	8.6	5.6	50	0.02	4.3	YES
Standard	3.0	7.6	4.6	75	0.02	3.1	NO
Standard	10.0	14.6	4.6	20	0.02	9.8	NO

EPS = expanded polystyrene.
*For the five-cycle test, the occurrence of gap has been interpreted. For all other tests, actual gap has been observed.
Note: Gray-shaded conditions confirm that standard EPS demonstrated elastic behavior under the quasistatic test condition.

In the test result shown in Figure 32, S-EPS was loaded and unloaded for 50 cycles between 3.0 and 8.6% strains. At the end of the 50th cycle, the load drops to zero at 4.6% strain, contrary to the intended 3%. As Figure 12a presents, this typical behavior is observed when a gap between EPS and the load plate occurs (Figure 11). In addition, after the test, when EPS was removed from the chamber and its height measured, the permanent strain was determined to be 4.3%—significantly exceeding the minimum applied 3% strain.

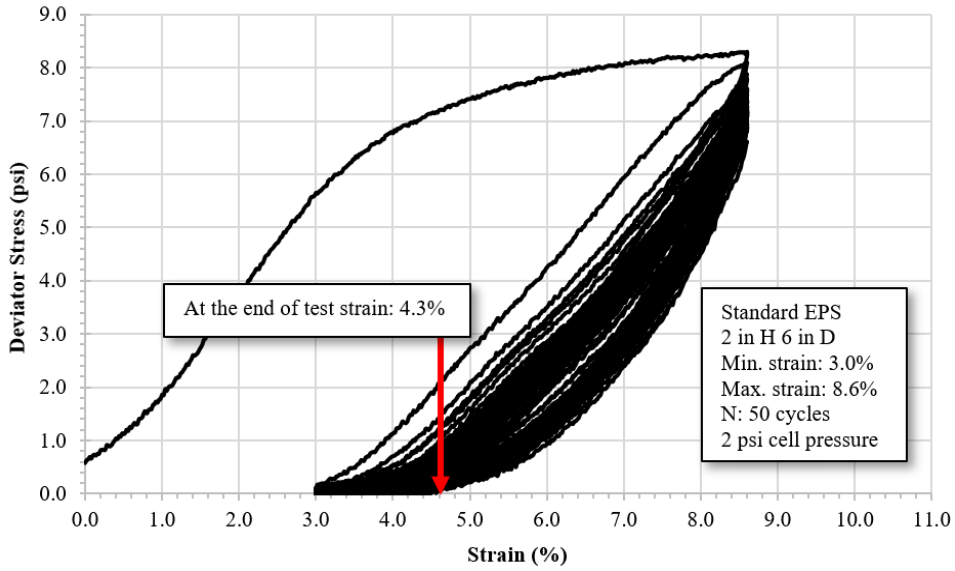

Figure 32. Example Unsatisfactory Test Result from Standard EPS (50 Cycles). EPS = expanded polystyrene.

Figure 33 illustrates a dataset representing a satisfactory result. The test depicted in this figure was performed on S-EPS with strain levels ranging from 5.0 to 9.6%. As observed in Figure 33, the load cycles never reach a zero load (as depicted in Figure 12b), indicating elastic behavior. In this specific example, the measured S-EPS strain at the test's conclusion was 3.7% (considerably less than the minimum applied 5%), thus confirming the elastic behavior.

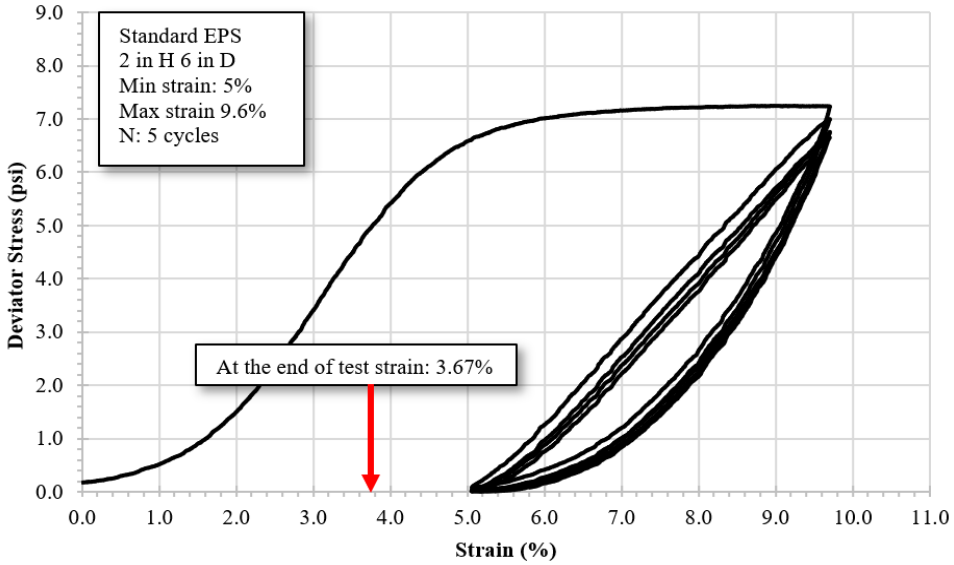

Figure 33. Example of Satisfactory Standard EPS Test Result (Five Cycles). EPS = expanded polystyrene.

When evaluating the results from both Figures 32 and 33, it can be observed that in both tests, the deviator stress values decrease with an increase in the number of cycles. This behavior is consistent across all test results, indicating that even if EPS remains elastic, it begins to soften with an increased number of cycles.

Based on similar observations from different tests shown in Table 7, only the following conditions are determined to produce satisfactory results:

- The difference between the maximum and minimum applied strains should not exceed 4.6%. This threshold is determined as the maximum allowed strains that EPS could withstand due to thermally induced movement of the integral bridge.
- The minimum applied strain on EPS, which corresponds to compaction-induced strain during the field installation, must be 3%.

All tests shown in Table 7 were conducted with the initial movement on EPS being in compression. However, if the bridge moves away from EPS immediately after the EPS installation, the minimum applied 3% strain on EPS may not be enough to result in a satisfactory condition. Such bridge movements may occur in installations during colder seasons when the bridge girders contract. In these types of cases, EPS should be subjected to larger initial induced strains during the compaction of backfill aggregate adjacent to EPS. Based on the findings in this study, the following conditions are determined to produce satisfactory results:

- The minimum applied strain on S-EPS should be 3% if the bridge movement right after installation is expected to be in compression; additional strains will be imposed on EPS.
- The minimum applied strain on S-EPS should be 7.6% if the bridge movement right after installation is expected to be in the direction away from EPS; strains will be reduced on EPS.
- In all conditions, the maximum allowed thermally induced strains on S-EPS should be limited to 4.6%.

If the previous conditions are satisfied, as evidenced by the outcome of the 75 cycles test in Table 7, S-EPS appears to remain elastic.

The last test in Table 7 was conducted to determine the maximum induced strains that EPS may experience before showing signs of negative Poisson's ratio behavior. This condition could be met by maintaining the minimum applied strain at no more than 10% and the maximum cyclic strains at no more than 4.6%. Exceeding this threshold would necessitate not only additional laboratory testing but also rigorous field observation and data collection.

A similar iterative testing process was conducted for E-EPS. Table 8 displays a summary of the test results, with satisfactory outcomes shaded in gray. Figures 34 and 35 illustrate examples of unsatisfactory and satisfactory test results, respectively.

Table 8. Quasi-Static Cyclic Loading Tests Conducted with Elasticized EPS

EPS Type	Min. Applied Strain (%)	Max. Applied Strain (%)	Difference Between Min. and Max. Applied Strains (%)	Number of Load Cycles	Applied Strain Rate (%/min)	Measured Strains on EPS after Tests (%)	Gap Occurred Between EPS and Load Plate? *
Elasticized	2.0	6.6	4.6	5	0.02	2.1	YES
Elasticized	5.0	9.6	4.6	20	0.02	3.7	NO
Elasticized	3.0	8.6	5.6	50	0.02	4.3	YES
Elasticized	3.0	7.6	4.6	75	0.02	3.1	NO
Elasticized	10.0	14.6	4.6	20	0.02	8.9	NO

EPS = expanded polystyrene.

*For the five-cycle test, the occurrence of gap has been interpreted. For all other tests, actual gap has been observed.

Note: Gray-shaded conditions confirm that elasticized EPS demonstrated elastic behavior under the quasistatic test condition.

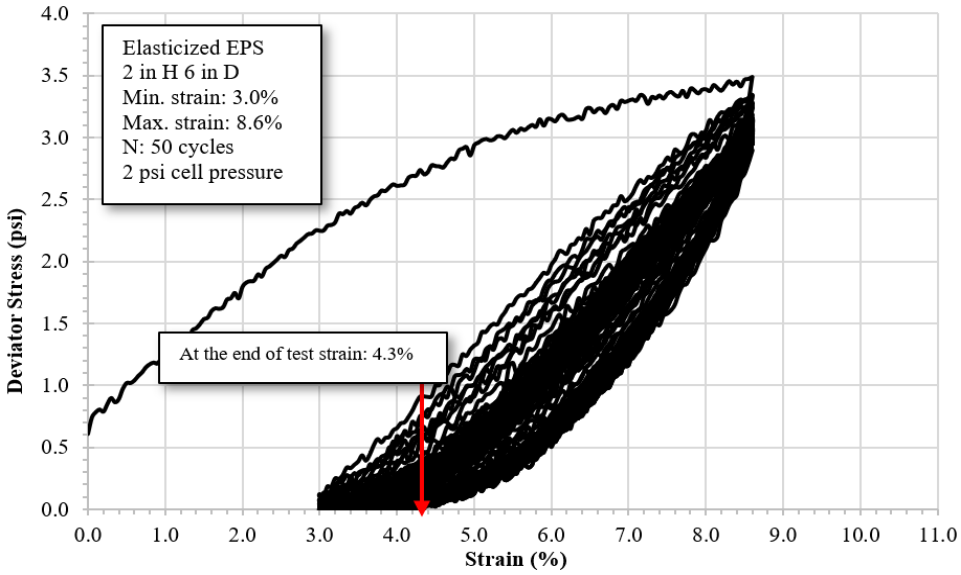

Figure 34. Example Unsatisfactory Test Result for Elasticized EPS (50 Cycles). EPS = expanded polystyrene.

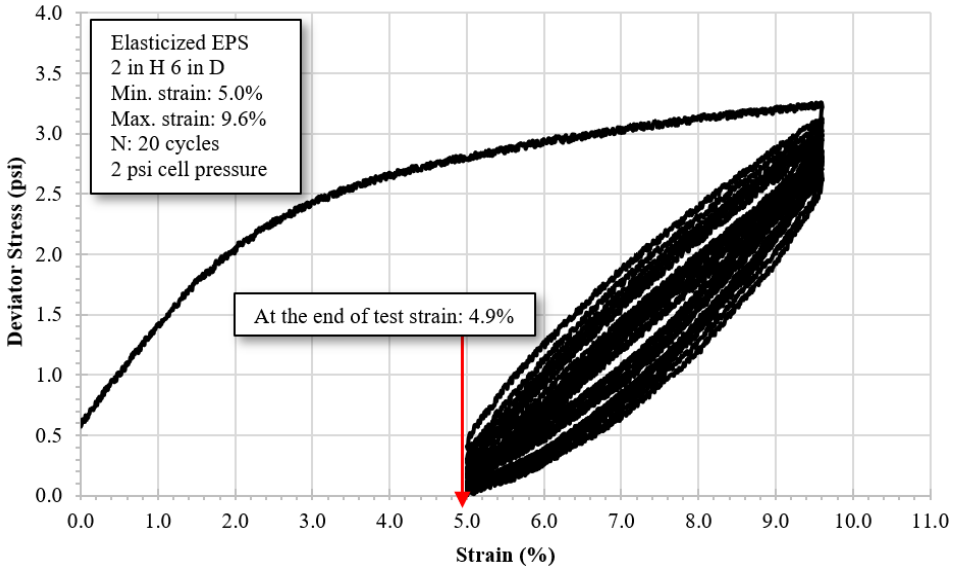

Figure 35. Example of Satisfactory Test Result for Elasticized EPS (20 Cycles). EPS = expanded polystyrene.

During the S-EPS tests, the unsatisfactory result revealed that the measured strain on E-EPS was higher than the minimum applied strain (i.e., 4.3% compared with 3%; Figure 34). The satisfactory result indicated a very close match between the measured strain on E-EPS and the minimum applied strain (i.e., 4.9 and 5%; Figure 35). In addition, in S-EPS, all E-EPS specimens exhibited a consistent behavior where, with increased load cycles, the deviator stress decreased.

The results in Table 8 indicate that the range of strain conditions for E-EPS to exhibit elasticity is similar to S-EPS, implying that, like S-EPS, E-EPS requires the following for elastic behavior under cyclic load tests:

- The minimum applied strain on E-EPS should be kept at 3% if the bridge movement is expected to be in compression right after installation, meaning additional strains will be imposed onto EPS.
- The minimum applied strain on E-EPS should be raised to 7.6% if the bridge movement right after installation is expected to be away from EPS, meaning the initial strains imposed on EPS during construction will be reduced by the bridge movement.
- In all conditions, the maximum allowed thermally induced strains on E-EPS should be limited to 4.6%.

The results obtained from the test conditions described in the last row of Table 8 show that E-EPS exhibited only 8.9% permanent strains after 20 load cycles, opposed to the 9.8% observed for S-EPS (last row in Table 7). This finding may suggest that E-EPS could remain elastic even with a slightly higher minimum applied strain than 10%. However, to determine the precise threshold, additional laboratory tests and field confirmation are needed. Therefore, it is conservative to treat both S-EPS and E-EPS based on the same strain condition requirements.

Results of the Test Conducted Only with Compacted Aggregate

After installation, with bridge movement, EPS experiences cyclic loading and unloading conditions. In compression mode, EPS bears some bridge-imposed load while transferring some load onto compacted adjacent aggregate as backfill. Therefore, in field applications, the behavior of both EPS and adjacent aggregate is crucial. The most appropriate condition is to test both aggregate and EPS together under the same cyclic conditions that are deemed satisfactory when EPS is tested alone. However, before evaluating the complex behavior of this multilayer system, it is important to quantify the behavior of the aggregate, which ensures a more reliable interpretation of the combined tests involving multilayers (aggregate and EPS).

EPS-only tests were conducted as strain controlled because bridge movement imposes strains on EPS. Aggregate tests were conducted as stress-controlled so that the stresses corresponding to strains from satisfactory EPS tests. As determined in Task 1, S-EPS is stronger than E-EPS, transferring larger stresses to the aggregate for a given strain. To ensure conservatism, the satisfactory S-EPS result (Figure 33, result with 0.02% per minute) was used to determine the maximum and minimum stresses to be used on the aggregate-only test. It was determined that when S-EPS reached a strain of 7.6%, the stress reached 7.8 psi. Similarly, at a strain value of 3.0%, the stress was approximately 0 psi. Thus, a 6-inch diameter and 12-inch height aggregate sample was cyclically loaded between 0 and 8.5 psi for 75 cycles. The test was conducted at the same speed (0.02% per minute) as used for the EPS-only tests (quasi-static condition). The aggregate was compacted to 90% relative compaction, providing a more conservative scenario. Figure 36 shows the result of this experiment.

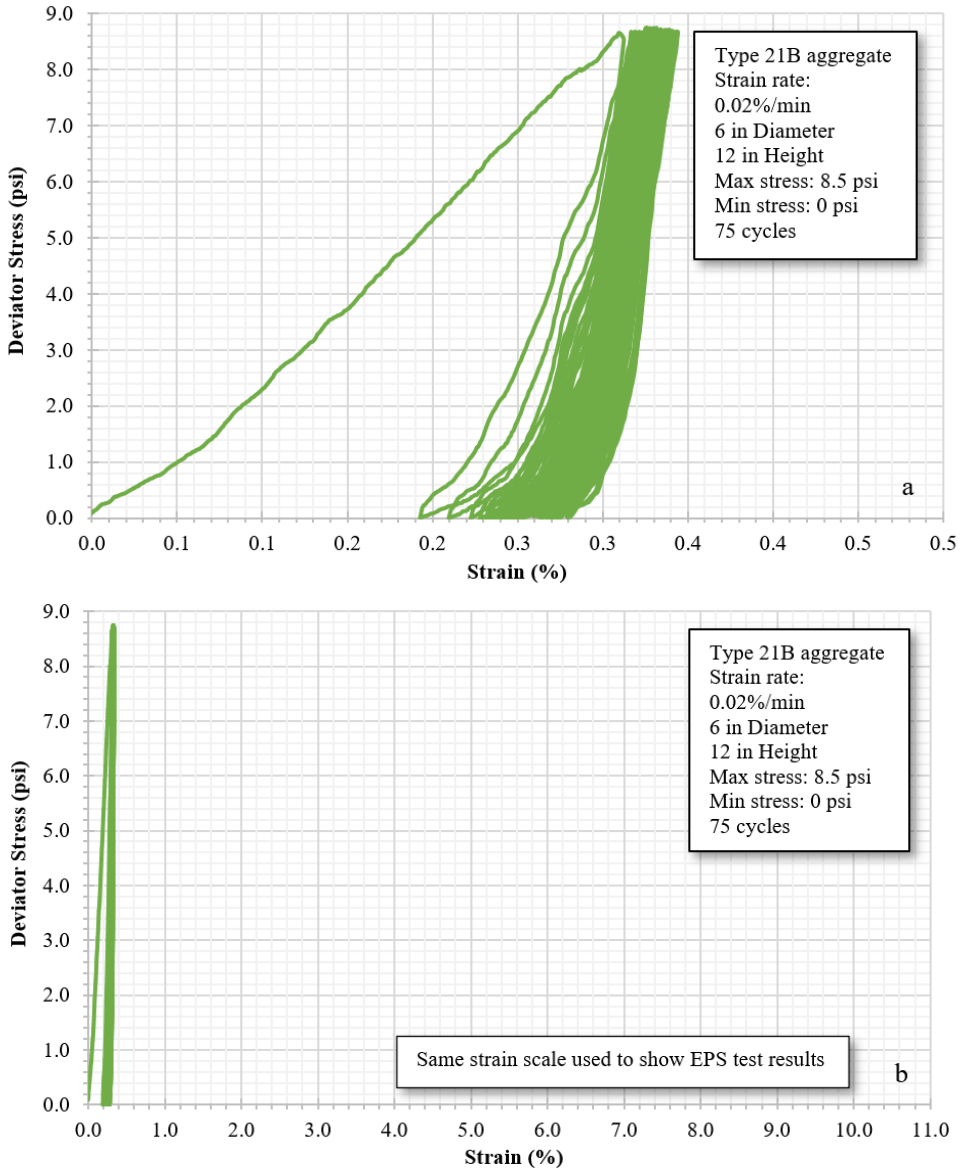

Figure 36. Quasi-Static Cyclic Loading on Compacted Aggregate Test Results: (a) Smaller (b) Larger Scale of Horizontal Axis. EPS = expanded polystyrene.

As Figure 36 shows, the backfill aggregate experienced approximately 0.27% plastic deformation after undergoing 75 loading and unloading cycles. This plastic strain is compared with the strain measured on S-EPS after a satisfactory test with 75 cycles. The measured strain on S-EPS at the end of this test was 3.1%. When compared, the measured 0.27% strain on the aggregate is interpreted as relatively small and can be considered negligible. This outcome means that, under the same loading conditions, EPS observes most of the strain. Although this comparison is suitable for determining that EPS is experiencing most of the strains, this result should not be interpreted as confirmation that aggregate compacted to a relative compaction of 90% would be satisfactory to achieve the minimum compaction-induced strains on EPS for field applications.

Results of the Combined Tests

The aggregate-only test was useful for evaluating the behavior of the aggregate alone under stress conditions relevant to the EPS application. However, combined tests were needed to assess the system's behavior (Aggregate and EPS working together). In these tests, 2 inches of EPS (in a cylindrical shape) were placed over the 10 inches of aggregate, separated by geotextile (creating a 12-inch height with a 6-inch diameter cylinder). The entire specimen (EPS and aggregate) was subjected to 75 cyclic loads, representing the expansion and contraction of bridge girders. These tests were conducted as strain-controlled between range of 3.0 to 7.6%. At the end of the tests, the strain of the dismounted EPS was measured.

Figure 37 presents the results of the combined test conducted with S-EPS. The results showed a satisfactory outcome based on parameters that were discussed for EPS-only tests. In addition, the measured strain on S-EPS at the end of the test was very close to the minimum applied strain (2.9 versus 3.0%), further confirming the elastic behavior.

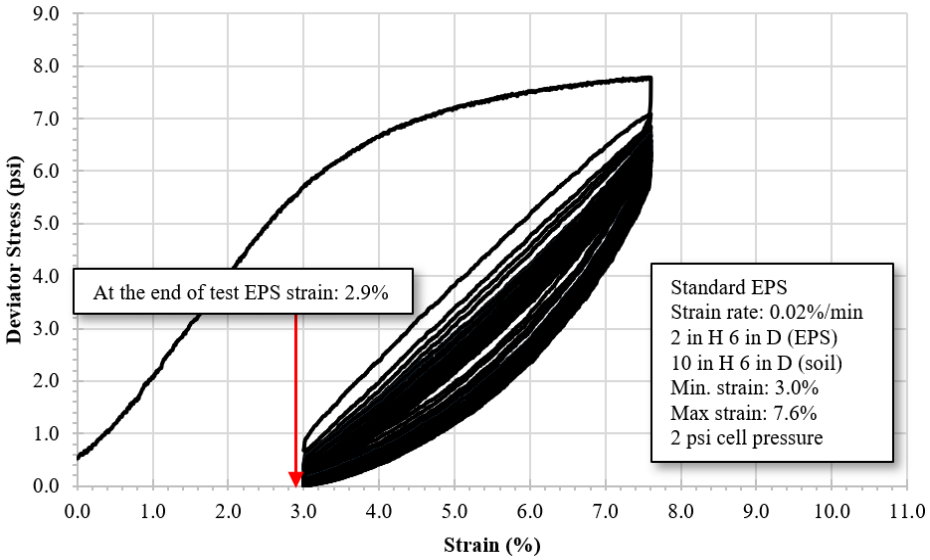

Figure 37. Combined Test Results for Standard EPS plus Aggregate. EPS = expanded polystyrene.

Figure 38 illustrates the results of the combined test conducted with E-EPS. As observed from the S-EPS tests, E-EPS also exhibited elastic behavior under the combined test conditions. The combined tests showed that the conditions satisfying the elastic EPS elastic behavior also result in satisfactory conditions when EPS is placed adjacent to aggregate.

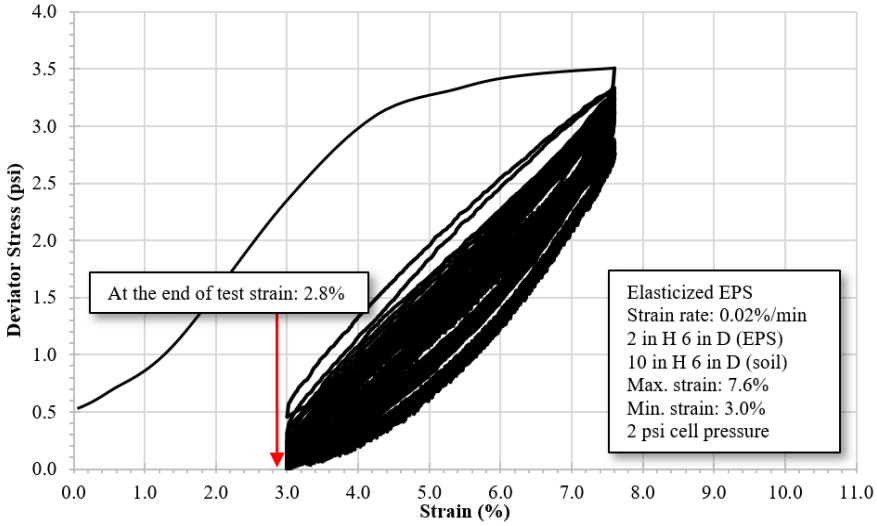

Figure 38. Combined Test Result of Elasticized EPS plus Aggregate. EPS = expanded polystyrene.

Results of Task 3: Cyclic Load Testing Simulating Traffic Loadings

The cyclic traffic loading tests were conducted to examine the performance of EPS installed behind the integral abutment under the applied traffic load. Based on the four modeling types mentioned in the methods section, the stress on the top surface of EPS is determined via KENPAVE analysis. The height of EPS also plays a role in the calculated stress due to traffic loads. Therefore, in the KENPAVE analyses, stress on the top of the EPS surface is determined for different EPS heights. In these analyses, the asphalt layer was modeled as linear, and the base course layer was modeled as nonlinear to represent the worst-case scenario (Figure 39). As a result of these analyses, stress at 18 inches below the road surface did not significantly change after 37 inches of EPS height, which is also the minimum EPS height installed by VDOT (as reported). Because a greater EPS height would result in less transferred traffic stress on top of EPS, for conservatism, the height of the EPS layer is determined as 37 inches in the KENPAVE analyses based on Figure 39.

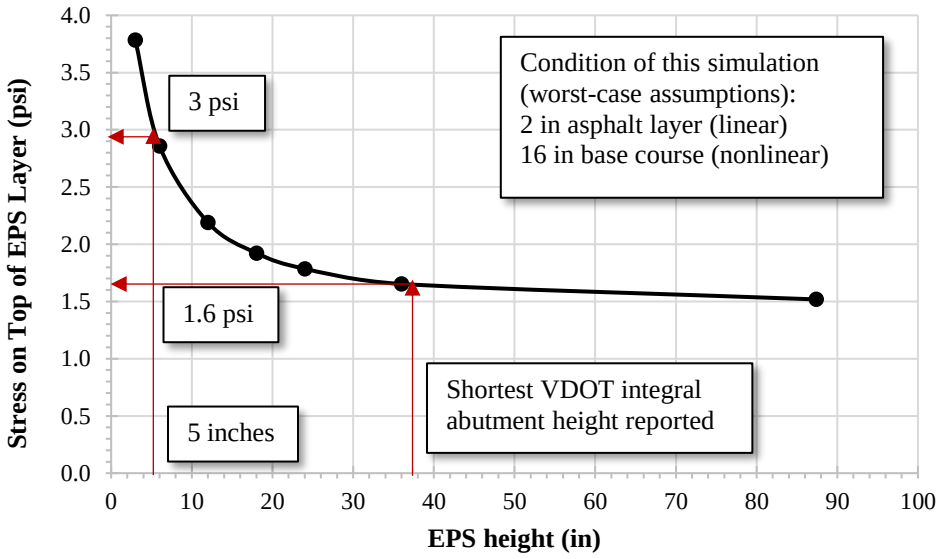

Figure 39. Vertical Stress at 18 Inches below the Surface for Different EPS Heights. EPS = expanded polystyrene.

Table 9 presented the KENPAVE analysis results. The results show that different models affect the determination of the magnitude of vertical stress on top of EPS. The maximum vertical stress calculated on the surface of EPS corresponds to 1.6 psi. To be conservative, the magnitude of the cyclic loads applied during the laboratory tests to simulate traffic loading was selected as 3 psi. This condition resulted in a total applied stress on the EPS specimens equal to 5 psi, which was obtained based on 2 psi constant stress followed by 3 psi cyclic stress. The results of the laboratory test conducted with both EPS types are presented in Figures 40 and 41.

Table 9. Summary of KENPAVE Analysis to Determine Applied Stress on Top of 37 Inches High EPS

Analysis No.	Asphalt Layer (2-inch thickness)	Base Course Layer (16-inch thickness)	Overburden Stress over EPS (Contact Stress)	Reduced Traffic Loads on Top of EPS (Results from KENPAVE Analyses)	Total Stress at Top of EPS (Overburden + Reduced Traffic Loads)
1	Linear	Linear	2.0 psi (See figure 15)	0.8 psi	2.8 psi
2	Linear	Nonlinear		1.6 psi (See Figure 39)	3.6 psi
3	Viscoelastic	Linear		0.2 psi	2.2 psi
4	Viscoelastic	Nonlinear		0.5 psi	2.5 psi

EPS = expanded polystyrene.

As observed in Figures 40 and 41, the aspect ratio of the tested S-EPS and E-EPS specimens has a slight effect on the final strain under traffic loads. Results showed that specimens with higher aspect ratios exhibited slightly greater final strains under traffic loading. In addition, S-EPS specimens experienced slightly higher final strains than the E-EPS specimens under traffic loads, although both are non-elasticized in the vertical direction. For specimens with a 3:1 height-to-diameter ratio, final strains were 0.8 and 0.9% for E-EPS and S-EPS, respectively.

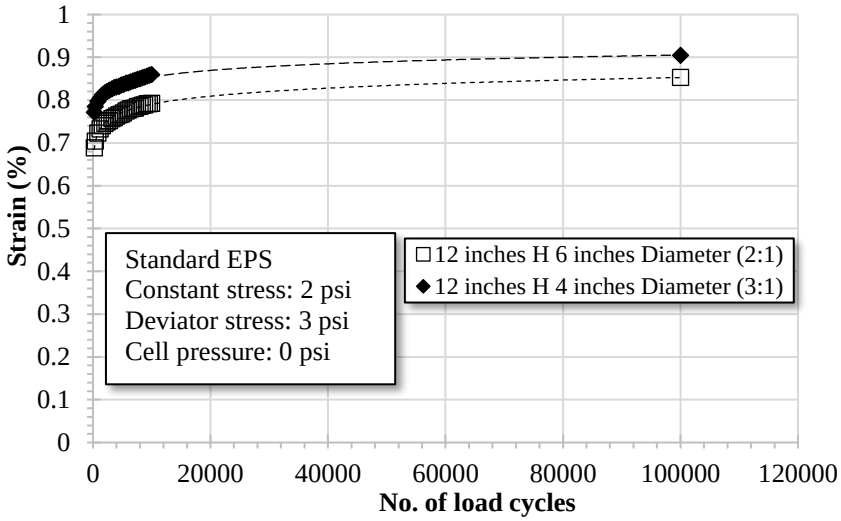

Figure 40. Traffic Loading Test Results Conducted with Standard EPS. EPS = expanded polystyrene.

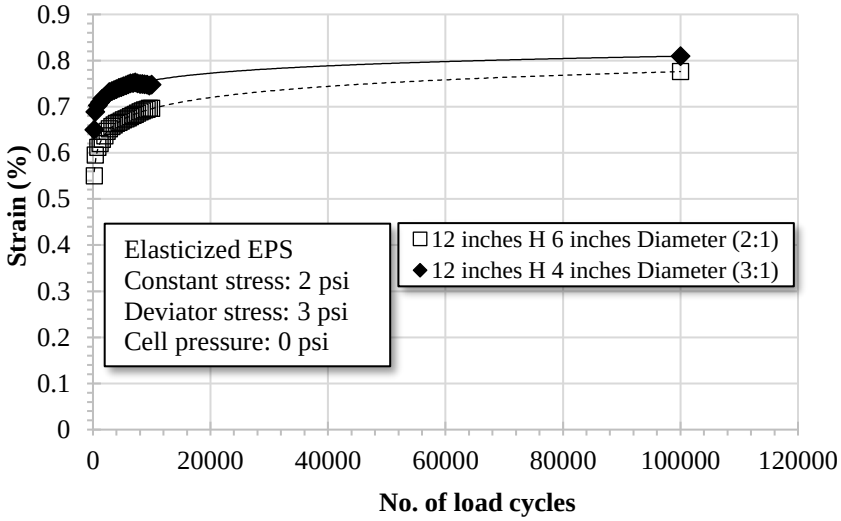

Figure 41. Traffic Loading Test Results Conducted with Elasticized EPS. EPS = expanded polystyrene.

DISCUSSION

Characterization of Materials

Tests conducted in Task 1 revealed that S-EPS and E-EPS exhibit distinct stress-strain behavior when E-EPS is loaded in the direction of the material's elasticization, indicating that the installation direction of E-EPS is crucial. In the case of S-EPS, no apparent favorable direction exists, as the material displays more isotropic behavior. E-EPS appears to be a more complex material, and the aspect ratio of the tested specimens (which also implies the aspect ratio of the installed material in the field) also affects the material's behavior. One significant observation in Task 1 of this study is that, despite differences in stress-strain behavior and unconfined compressive resistances between S-EPS and E-EPS, their elastic ranges were similar—ranging from 2 to 3% depending on specimen size, aspect ratio, and test speed. The elastic range noted in Task 1 of this study is significantly different from what VDOT assumes characterizes E-EPS. Prior to this study, VDOT assumed E-EPS to be elastic with up to 10% strains, with the stress-strain curve being linear in this range. Based on Task 1 findings, VDOT specifications regarding elastic inclusion should be revised. The most notable difference between S-EPS and E-EPS is their stress values at the same strain condition. The compressive resistance of S-EPS at 10% strain is approximately twice that of E-EPS. Consequently, the load transferred to the compacted aggregate used as backfill adjacent to EPS will also be twice as much when comparing S-EPS with E-EPS. As a result, the lateral soil pressures affecting the bridge will be higher for S-EPS. The calculations of lateral earth pressure coefficients are discussed in detail in subsequent sections of this report.

Vendors characterize EPS based on unconfined compressive resistance tests conducted in accordance with ASTM D1621 (2016). This standard requires testing EPS at a 10% per minute strain rate. However, this rate is much faster than that which the stress rate EPS inclusion is exposed to under field conditions. Thermally induced bridge movements occur daily and annually. Results of this study (and previous studies in the literature) show that the strain rate affects the stress-strain behavior of both E-EPS and S-EPS. Therefore, unless the experiments are conducted in the quasi-static strain range, relating EPS behavior to what one may expect during field applications may not be the best approach. In this study, for the tested EPS materials, the onset of the quasi-static range is determined as 0.02% per minute. This speed aligns with literature findings (Al-qarawi et al., 2020). ASTM D1621 (2016) has additional limitations when it comes to relating the behavior to the integral bridge applications. Tests conducted with ASTM D1621 (2016) are monotonic and unconfined, yet EPS undergoes cyclic loadings with confinement in the field. Therefore, for appropriate evaluations of EPS behavior, custom-designed cyclic loading tests simulating the conditions resulting from thermal bridge movement and traffic are needed. For this reason, Task 1 has been named as material characterization, and Tasks 2 and 3 are conducted to evaluate EPS performance.

Cyclic Load Testing Simulating Thermal Expansion of Bridge Superstructure

Based on Task 1 results, researchers decided that the aspect ratio of the EPS specimens tested in Task 2 should be 1:3 (H:D). Observations indicating that aspect ratio affects the compressive resistance of E-EPS influenced this decision. As Task 1 test results noted, an aspect

ratio of 1:3 for E-EPS specimens resulted in the highest compressive resistance at 10% strain. In field applications, higher compressive resistance is expected to result in increased lateral earth pressures. In addition, considering practical limitations in laboratory apparatus for specimen sizes, selecting an aspect ratio of 1:3 for both EPS types was deemed the most conservative approach.

The effect of the overburden layer in the field on confining EPS has been simulated in quasi-static tests in the horizontal direction. According to VDOT drawings for full integral and semi-integral bridge details, the typical pavement layers above EPS are expected to be approximately 18 inches. Based on Virginia Transportation Research Council (VTRC) TRP communications, researchers decided to calculate the overburden pressure on EPS using this thickness. The calculation yielded a 2 psi stress, which is applied to EPS as cell pressure in Task 2 tests. Because of time constraints in the study, this research did not focus on how changes in cell pressure might affect overall results. It is worth noting that the literature indicates EPS's behavior sensitivity to applied confining pressures. Wong and Leo (2006) demonstrated that increasing confining pressure from 0 psi to 8.7 psi reduced compressive resistance from 16 psi to 14 psi for S-EPS with 1.25 pcf density. Thus, changes in pavement profile thickness (i.e., increasing from 18 to 30 inches for pavement layers) in field applications may slightly affect EPS behavior because of alterations in overburden pressure.

Task 2 test results revealed that when EPS is exposed to load conditions resulting in more than 2 to 3% strains, the material shows plastic strains. However, under constant strain conditions (i.e., minimum applied strain in this study) up to a certain threshold, the material exhibits elastic behavior. Task 2 tests determined this threshold to be within the range of 3 to 10% constant strains. Within this range, both EPS types show elastic behavior, as long as the magnitude of cyclic strains remains within 4.6%. These observations restrict the maximum applied strain on EPS to 14.6% (constant 10% strain + 4.6% cyclic strain). This limitation is established based on two different considerations:

- One of these considerations is associated with the negative Poisson's ratio of EPS, as described in the literature (Atmatzidis et al., 2001; Elragi et al., 2000; Zou, 2001). The negative Poisson's ratio of EPS is explained by the material collapsing inward under specific horizontal and vertical stress conditions. Determining a threshold for EPS which results in the negative Poisson's ratio is complex. Limiting the target maximum compaction-induced strain to 10% is considered a viable precaution to avoid the excessive negative Poisson's ratio effect.
- The other consideration is associated with the VDOT-reported field data. Hoppe (2005) and Hoppe and Eichental (2012) reported field measurements of compaction-induced strains on EPS installed in integral bridge abutments from two different sites. The field observations indicated that in one of these sites, the compaction of the backfill resulted in 11% strains on EPS right after construction. However, within 2 weeks, the measured strains on EPS stabilized at 8% (Hoppe, 2005). Considering the limited field information regarding the effects of compaction and the maximum-induced strains on EPS, limiting the target for the maximum compaction-induced strains to 10% in this study has been adopted until additional field measurements become available.

The results of the experiments have shown two conditions: (1) Not only is it important to apply constant strains on EPS (simulated as compaction-induced strain in field applications), but also, (2) depending on the installation time of EPS, the magnitude of compaction-induced strains is crucial. If EPS is installed when the bridge movement imposes additional strains on it, then test results indicate that a minimum of 3% compaction-induced strains is required for EPS to rebound (exhibiting elastic behavior). If EPS is installed during a period when the bridge movement is anticipated to reduce strains on EPS, then a minimum 7.6% compaction-induced strain is required for EPS to exhibit elastic behavior. In cases where the expected bridge movement (contraction versus expansion) right after EPS installation is unknown, the conservative approach would be to target a minimum compaction-induced strain of 7.6%. For all conditions, the cyclic strain range (simulated in field applications as thermally induced strains) must not exceed 4.6%.

The previous comments are valid for both S-EPS and E-EPS. However, VDOT currently specifies only E-EPS for elastic inclusion. The results indicate that properly strained S-EPS procedures may also provide adequate substitution. The commercial availability of S-EPS is significantly broader than that of E-EPS.

To visualize the disturbance on the EPS surface, a three-dimensional model of the tested EPS is created. The procedure involves first capturing a photo of the unused EPS and then capturing a second photo of the exhumed EPS from the combined EPS-aggregate laboratory test. Creating this model requires at least 40 photographs from various angles. The MagiScan application was used to compile these photographs and generate the three-dimensional model. This model is transferred to AutoCAD 2022 software to quantify displacements. Figure 42 shows an example of AutoCAD 2022 output. Figure 42a displays the exhumed EPS surface post-test, and Figure 42b illustrates the projection of the unused EPS surface (red) onto the modeled exhumed EPS surface (white). Based on the model shown in Figure 42b, the entire surface of the exhumed EPS shows signs of aggregate penetration from the geotextile. This finding suggests that the geotextile used by VDOT may not sufficiently serve as protection for EPS. In field applications, the aggregate penetration could potentially be more severe due to installation procedures. The maximum indentation of the aggregate from the geotextile surface onto EPS in this example was determined to be 0.13 inches. Considering that EPS behavior is sensitive to loads on uneven surfaces, such observations may require further investigation.

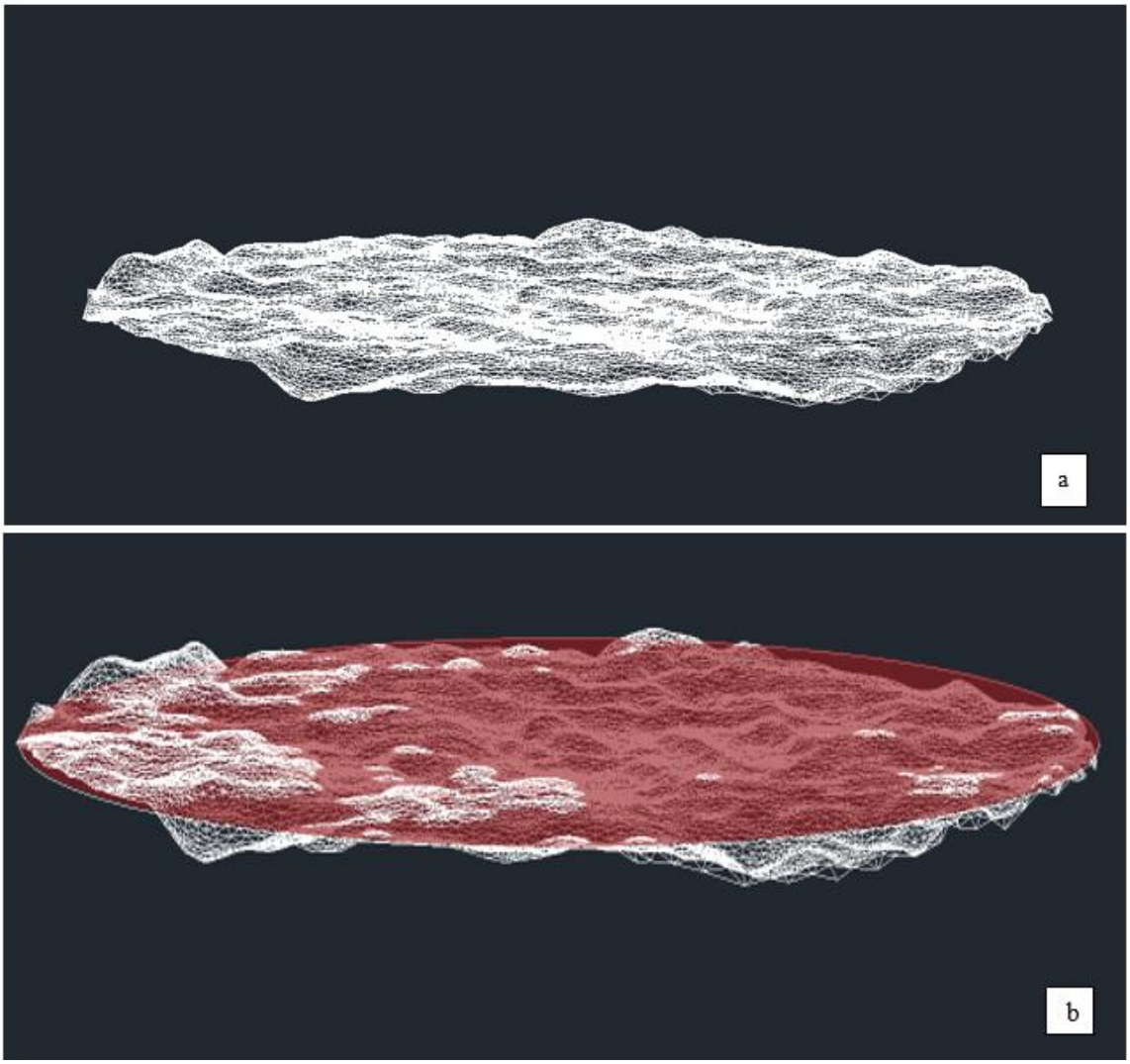

Figure 42. (a) Three-Dimensional Model of the Surface of Exhumed Expanded Polystyrene (EPS) Specimen from Combined Tests; (b) Comparison of the Exhumed and Unused EPS Surfaces

Cyclic Load Testing Simulating Traffic Loadings

EPS, installed as an elastic inclusion, is exposed to vertical loads in addition to the lateral loads generated by thermally induced bridge movements. The goal is for EPS to display elastic behavior under both types of loads. Traffic loading tests were conducted to assess its performance under vertical loads.

The findings from the test results indicate similar strain values for both S-EPS and E-EPS. This finding is an expected outcome because in traffic loading conditions, both EPS materials are loaded in a non-elasticized direction. The magnitude of the strain values at 100,000 load cycles for both S-EPS and E-EPS was less than 1%. This observation is interpreted as the materials behaving elastically because the total strains were significantly less than 3% (remaining in the elastic zone).

Laboratory testing conditions are insufficient to accurately simulate EPS behavior under field traffic loads. One limitation is simulating simultaneous horizontal and vertical stress conditions (Figure 17). In the worst-case scenario, study findings suggest limiting maximum total strains on EPS to 14.6%. This condition for S-EPS results in approximately a 9 psi load. As Figure 17 depicts, horizontal pressure should be applied for tests simulating traffic conditions. However, because of limitations in the test setup, this horizontal pressure is also exerted on the EPS specimen vertically. This condition causes premature EPS failure and does not accurately reflect actual field conditions. As outlined in Table 9, the maximum expected vertical wheel load on EPS is 1.6 psi (even though for the laboratory test to be conservative, it is assumed as 3 psi). A proper way to test traffic conditions would require subjecting the specimen to 9 psi horizontal pressure (representing maximum allowable strain on EPS), 2 psi constant vertical pressure (representing overburden pressure), and 3 psi cyclic vertical pressure (representing traffic loading). As seen in Figure 17, simulating this condition in the laboratory setup is impractical due to lateral stresses being higher than vertical stresses.

The second limitation of the laboratory setup to simulate the behavior of EPS under traffic loads in the field is associated with accounting for the effect of EPS thickness. Figure 43 demonstrates the potential effects of EPS thickness. In the KENPAVE analysis, the assumption is that all layers are continuous horizontally. However, in the field, EPS is placed with a certain thickness. When EPS bears traffic loads in the field, it is possible for stress to distribute to the adjacent bridge abutment and the backfill aggregate. These features possess greater strength than EPS (i.e., a higher elastic modulus), allowing them to withstand higher stresses. This phenomenon is attributed to potential arching behavior within the layers above EPS. Consequently, smaller stresses may occur on top of EPS compared with results from KENPAVE analyses (Table 9). EPS's thickness heavily influences the effect of this behavior. The combination of the mentioned laboratory test setup limitations and the combined effects of these two constraints necessitates further investigation, including a field study.

In addition to the limitations described previously, the conditions to which EPS may be exposed during the construction of the base course and the asphalt layer above require complex evaluation that cannot be replicated in a laboratory environment because the thickness of EPS and the procedures to construct the base course will have significant effects on the outcome. Evaluation of these conditions is better suited when field observations are combined with numerical studies.

Based on the literature and observations noted during the study, certain conditions may cause EPS to exhibit signs of a negative Poisson's ratio. This behavior is explained by the negative Poisson's ratio of EPS, where the material tends to collapse inward under specific horizontal and vertical stress conditions. Determining a threshold for the stress conditions that result in a negative Poisson's ratio is complex. As a result of these observations, findings from this study indicate that for smaller EPS thicknesses, traffic loading will not be detrimental. However, it cannot be concluded that the system will function as desired for all EPS thicknesses. This study's findings indicate that a thicker EPS is preferred for horizontal loads, whereas a thinner EPS is preferred for vertical loads. These two concepts create a complex problem requiring further evaluation. Therefore, it is not possible at this point to determine the maximum EPS thickness which does not require a steel plate (or approach) slab.

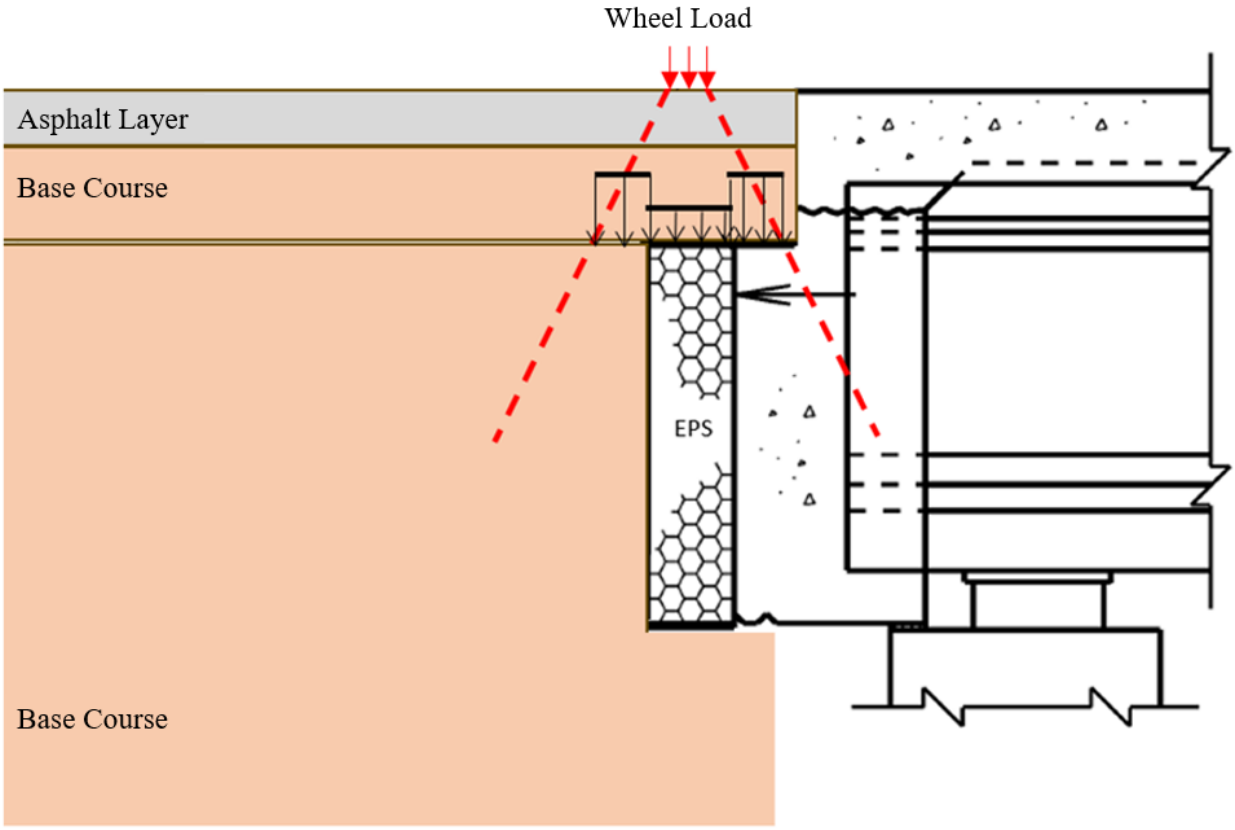

Figure 43. Possible Stress Distribution on Top of the Expanded Polystyrene within the Integral Abutment under Traffic Loadings

Discussions for VDOT Special Provision

VDOT (2020a) published a special provision for elastic inclusions on October 13, 2020 (SP404-000130-00). The provision includes sections on description, materials, procedures, testing, measurement, and payment. Based on results observed in monotonic, cyclic, and traffic loading tests, it is recommended that VDOT revise current specifications. Suggested revisions to Special Provision 404-000130-00 are presented in Item C of the supplemental materials with tracked changes. Note that only sections related to this study's findings were revised. Insect resistance, water absorption, adhesives, and potential concerns from chemical intrusions (oil spills, de-icing compounds, etc.) were not investigated, so no comments related to these topics were added to the suggested revisions.

Proposed EPS Thickness Equation and Installation

VDOT uses an equation to calculate thickness of E-EPS inclusion that will be used in the integral bridge abutments (Equation 1). Based on the results of this study, the current VDOT EPS thickness equation has been revised and is presented in Figure 44 as a flowchart that is applicable to both S-EPS and E-EPS.

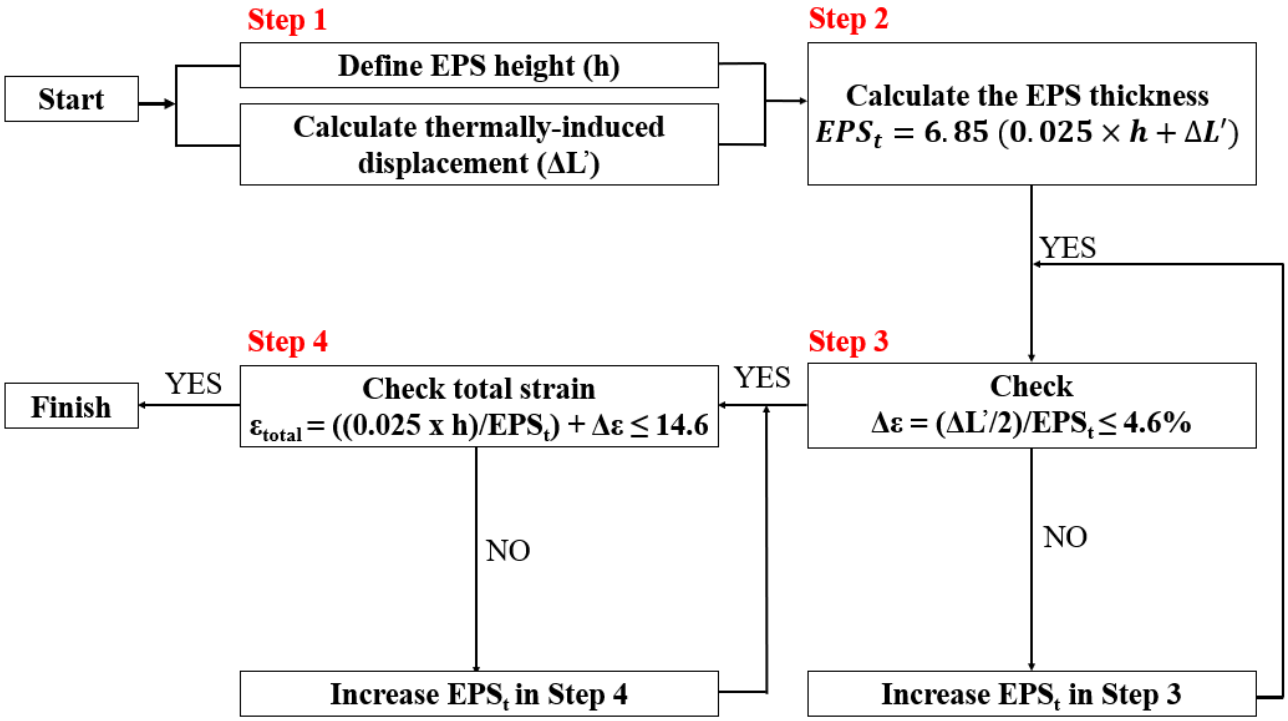

Figure 44. Flowchart to Calculate the EPS Inclusion Thickness. EPS = expanded polystyrene.

Based on the flowchart presented in Figure 44, the first step is to determine the height of EPS (h) and thermally induced displacement of the bridge (ΔL'). VDOT suggests determining ΔL' as 0.67 times the maximum theoretical thermally induced bridge movement (ΔL), which can be determined based on Equation 2. After the h and ΔL' are determined in Step 1, the EPS thickness should be determined based on the following equation, which is proposed as a result of this study (Equation 3).

$$EPS_t = 6.85\ (0.025 \times h + \Delta L') \qquad \text{Equation 3}$$

Where—

EPS_t = thickness of EPS inclusion (inches).
h = height of zone where EPS is installed (inches).
$\Delta L'$ = 0.67 x ΔL (inches).

Note that in Equation 3, coefficient of 6.85 is determined based on the ratio of 100/14.6, where 14.6 represents the maximum total strains that should be limited to applied on EPS. Also, the coefficient of 0.025 in Equation 3 is the result of 0.33 multiplied by 0.076. The 0.33 is the aspect ratio of the EPS samples used in this study (H:D). The value of 0.076 was selected based on the test results shown in Tables 7 and 8. The selected value was the minimum of the maximum applied strains during laboratory testing that resulted in satisfactory conditions (did not create a gap) for both S-EPS and E-EPS (Tables 7 and 8).

Even though EPS thickness is calculated in Step 2, the proposed EPS thickness equation (Equation 3) requires additional steps as described in Figure 44. Results of this study revealed

that thermally induced EPS strain (Δε) should be less than or equal to 4.6%. This outcome should be checked in Step 3 as provided in Equation 6. If the Δε on EPS is higher than 4.6%, EPS thickness should be increased until the criterion is met.

$$\Delta\varepsilon = \frac{\Delta L'/2}{EPS_t} \leq 4.6\% \qquad \text{Equation 4}$$

Where—

$\Delta L'$ = thermally induced displacement of the bridge.
EPS_t = calculated EPS thickness based on the Equation 3 (inches).
$\Delta\varepsilon$ = annual thermally induced EPS strains (%).

In addition to the check in Step 3, another parameter needs to be checked in Step 4. This check requires the maximum strain applied on EPS to be less than or equal to 14.6%. The total strain of EPS (ε_{total}) in Step 4 can be calculated per Equation 5.

$$\varepsilon_{total} = \frac{0.025 \times h}{EPS_t} + \Delta\varepsilon \leq 14.6 \qquad \text{Equation 5}$$

If the ε_{total} is greater than 14.6%, EPS thickness should be increased until the criterion is met. Restricting the total strain to 14.6% is based on concerns associated with the elastic behavior limits and the potential negative Poisson's ratio of EPS.

Figure 44 and associated equations are presented to calculate the EPS thickness. Regardless of the thickness of EPS, for EPS to behave elastically, VDOT must implement proper compaction-induced strains on EPS during construction. If EPS is installed in warmer seasons, the compaction-induced strain on EPS should be between 7.6 and 10.0%. For construction in colder weather, the compaction-induced strain on EPS should be between 3.0 and 10.0%. A detailed explanation of the season-based minimum and maximum compaction-induced requirements are provided in Item D of the supplemental materials.

Review of VDOT Integral Bridges with EPS Inclusion

VDOT has provided information regarding the EPS thicknesses that were installed on its integral bridges. In addition, the data included the EPS thicknesses calculated for these bridges based on VDOT's existing design equation (Equation 1). As part of this study, researchers conducted analyses comparing the EPS thicknesses—calculated based on the proposed procedures presented in this study (Figure 44)—with the information provided in the VDOT's database. This database contains information on 65 constructed bridges. In addition to the installed EPS thickness information, data also include abutment type (full- or semi-integral), girder type (concrete or steel), span information (single or multi), presence of approach slab, abutment height, and bridge length for a given location.

Preliminary examination of the provided data indicated that of the 65 constructed bridges, 60% are semi-integral abutments and 40% are full-integral abutments. In terms of girder type, 52% of the bridges have concrete girders and 48% have steel girders. In addition, 34% of the

bridges are single-span and 66% are multi-span. More than one-half of the bridges were also constructed with approach slabs (54%).

Based on the VDOT-provided data, the following calculations could be made to determine the magnitudes of:

- Maximum theoretical thermally induced movement of the constructed bridges based on Equation 2.
- EPS thickness that would be determined during the design of the constructed bridges based on Equation 1 (current VDOT procedure).
- A comparison between the VDOT-installed EPS thickness and the thickness of EPS determined based on VDOT's current equation.
- EPS thickness that would be required if the design was conducted based on proposed procedures in this study (Figure 44).

The maximum theoretical thermally induced movement (ΔL) of the constructed bridges were between 0.33 and 2.35 inches (average 0.96 inches). The EPS thickness of the 65 bridges that would have been required during the design of the installed EPS was calculated based on VDOT's current design approach. Based on discussions with VTRC TRP, bridges with and without approach slabs were evaluated separately. VDOT's current practice is to install 10 inches of E-EPS within the top 3 feet of the backwall for the bridges without approach slab regardless of the calculated EPS thickness. Data evaluations showed that this procedure was implemented in 18 out of 30 bridges without approach slab. In 5 out of 30 bridges, the installed EPS thickness was more than 10 inches but less than the EPS thickness calculated based on Equation 1 (typically 3 to 4 inches difference). In 3 out of 30 bridges, the installed EPS thicknesses were also more than 10 inches and more than the calculated EPS thickness based on Equation 1 (typically 4 to 7 inches difference). In one of the bridges, the installed EPS thickness was 6 inches (significantly less than 10 inches) and less than the EPS thickness calculated based on Equation 1 (11 inches difference). The data evaluations also showed that in 21 out of 35 bridges with approach slab, the installed EPS thicknesses were less than the calculated EPS thickness based on Equation 1 (some of the differences were as high as 9 inches). These comparisons indicate that some of the installed EPS thicknesses were not in conformance with the VDOT's current EPS thickness design approaches (Equation 1 and 10 inches target).

For comparison purposes, the required EPS thicknesses of the 65 bridges that would have been obtained during design stage were also calculated based on the newly proposed procedures in this study (Figure 44). By following the flowchart and the referred equations in Figure 44, the following findings were obtained:

- Average $\Delta\varepsilon$ would be determined as 2.1 % (minimum 0.6%, maximum 4.6%).
- Average ε_{total} would be calculated as 9.7% (minimum 8.3%, maximum 12.2%).
- The average difference between the EPS thicknesses based on VDOT's current design procedure and the EPS thicknesses based on the newly proposed procedure in this study is determined as 1.0 inches (minimum –4.2 inches and maximum 6.1 inches).
- Average difference between the reported installed EPS thicknesses and the EPS thicknesses based on the newly proposed procedure is determined as 2.8 inches (minimum –14.8 inches and maximum 24.5 inches).

Note that the negative values listed previously indicate that the required EPS thicknesses based on the newly proposed procedure in this study would be less than the compared values. For example, if the EPS thickness calculated based on Figure 44 is 21 inches and the installed EPS thickness is reported as 27.2 inches, the difference between these two values would be calculated as –6.2 inches. The comparisons showed that if the EPS thickness was determined based on the newly proposed procedure, the maximum difference compared with the installed EPS is determined as 24.5 inches. The reason for this larger difference is associated with VDOT's current practice of installing 10 inches of EPS for the bridges with no approach slab regardless of the EPS thickness calculation. Similarly, if the EPS thickness was determined based on VDOT's current procedure, the maximum difference compared with the thickness calculated based on the newly proposed procedure was determined as 6.1 inches. This information indicates that if VDOT chose to implement the newly proposed approach, it should be acknowledged that, in some instances, the outcome may produce results differing from current VDOT calculations. However, when compared with the data from the 65 bridges, the 6.1-inch variance does not appear greater than what is already observed in VDOT's current practices. Although the resulting design thicknesses may not be very different between the two equations, the components of the VDOT- and GMU-proposed equations are different.

Although VDOT's current practice is to limit the EPS thickness to 10 inches for the conditions with no approach slab, the findings from this study indicate that it may result in the EPS layer that is insufficient for elastic behavior. However, as shown in Figure 43, as the thickness of the EPS increases, the arching effect will decrease, potentially exerting additional vertical loads on the EPS. Therefore, placement of a steel plate or approach slab over the EPS layer is a viable option to consider.

EPS may be designed based on the current equation or the newly proposed procedure. However, for field installation, compaction-induced and thermally induced strains of EPS become substantial parameters. These parameters are calculated for the 65 constructed bridges.

In Equation 1 (VDOT's current design equation), the compaction-induced movements on installed EPS are estimated as a function of abutment height (0.01×h) as discussed by Hoppe and Eichental (2012). In this study, Equation 6 was created to check the theoretical compaction-induced strains. With this equation, the compaction-induced movements are converted to compaction-induced strains based on the installed EPS thicknesses reported in the VDOT database. Therefore, theoretical compaction-induced EPS strains could be estimated as follows:

$$\varepsilon_{compaction} = \frac{0.01 \times h}{EPS_{installed}} \times 100\ (\%) \qquad \text{Equation 6}$$

Where—

$\varepsilon_{compaction}$ = compaction-induced EPS strain (%).
h = abutment height (inches).
$EPS_{installed}$ = installed EPS thickness (inches).

Based on the evaluation of 65 bridges, minimum and maximum $\varepsilon_{compaction}$ on installed EPS range between 1.8 and 13.3%, respectively. A detailed explanation of the season-based minimum and maximum compaction-induced requirements is provided in Item D of the

supplemental materials. Based on that information, the theoretical $\varepsilon_{compaction}$ figures calculated were satisfactory within 53 of the 65 bridges for the installations in colder seasons. In 12 of the 65 bridges, the theoretical $\varepsilon_{compaction}$ figures calculated were more than 7.6% and less than 10%. These conditions satisfy the requirements for the installations in warmer seasons. These comparisons indicate that for EPS that may be constructed during the warmer seasons, most of the installed EPS thicknesses did not satisfy the proposed requirements based on the findings of this study (Item E of the supplemental materials, Figure B-5).

The calculated thermally induced strains (as calculated based on Equation 4) on the installed EPS ($\Delta\varepsilon_{installed\text{-}EPS}$) within the constructed bridges were determined to be in the range of 0.8 and 11.2%. Based on procedures proposed in this study, the maximum thermally induced strains on EPS are suggested to be 4.6%. The data from the constructed bridges indicate that 56 of the 65 bridges satisfy the proposed maximum thermally induced strain condition. For the remaining 9 bridges, based on the findings of this study, the installed EPS thicknesses should have been thicker than the reported values.

After calculating the $\varepsilon_{compaction}$ and $\Delta\varepsilon_{installed\text{-}EPS}$, the ε_{total} on each installed EPS has been calculated by summing these two values. The results indicate that the maximum, minimum, and average ε_{total} on the installed EPS are 20.3, 3.7, and 9.5%, respectively. Of the 65 bridges, 58 bridges satisfy the requirements set forth based on the newly proposed procedures in this study (i.e., $\varepsilon_{total} \leq 14.6\%$), which means that for the 7 bridges, the installed EPS thicknesses should have been wider.

Lateral Earth Pressure Coefficient Calculations for Bridges where EPS Is Installed

The lateral earth pressure coefficient, Kp, for bridges with EPS installation was calculated using data from this study and bridge configurations from the VDOT database. VDOT Design Specifications mandate a target Kp value of 12 for backfill behind bridges without EPS. Using this required Kp value and knowing the vertical stress distribution along the backside of the abutment, researchers back calculated the horizontal forces acting on each of the 65 bridge abutments. This calculation initially assumed a condition without EPS installed. The total horizontal force for this condition acting on the abutment was calculated based on a triangular distribution, shown in Figure 44a. The unit weight of the backfill soil for these calculations was assumed to be 145 pcf, as specified in the VDOT (2023) Manual of the Structure and Bridge Division, Chapter 17.

For conditions where EPS is present, horizontal stresses above the zone where EPS is installed were also calculated based on Kp value being 12 (Figure 44b). The distance between the road surface and the top of EPS was 18 inches in these calculations. For the EPS-installed zone, data from 65 bridge configurations were used to calculate total strain on EPS. This information was then incorporated into this study's test results to convert total strain values into horizontal stresses transferring from the abutment to the backfill. For example, based on the quasi-static strain rate test results, an 11% total strain on E-EPS would correspond to a 4 psi stress on the backfill. A rectangular distribution of horizontal stresses is assumed behind the abutment for the area which has EPS (red area in Figure 44b). To determine Kp values for bridges with installed EPS, total horizontal resultant forces for the no-EPS and EPS cases were

compared. This comparison revealed that bridges with installed EPS had smaller total resultant horizontal forces compared with the same bridge configuration with no EPS. It was assumed that the decrease in the total horizontal force would result in a decreased Kp value. Based on this assumption, a relationship was developed to estimate the Kp value for the condition with EPS. For example, for one of the bridges, the total horizontal resultant force without EPS was calculated as 107,193 lb/f (corresponding to Kp = 12). For the same bridge configuration with S-EPS, the total horizontal resultant force was calculated as 17,010 lb/f. The Kp value for this bridge was calculated as $\frac{17010}{107193} \times 12 = 1.9$.

Kp values were calculated for all 65 VDOT bridges, and the minimum and maximum values for both S-EPS and E-EPS conditions were determined. Table 10 presents data based on abutment and girder type, whereas Table 11 presents data based on abutment type and the presence of an approach slab. Kp values were calculated for both reported and newly proposed EPS thicknesses in this study (Figure 45).

Table 10. Comparison of Calculated Minimum and Maximum Lateral Earth Pressure Coefficients Based on Abutment and Girder Type

Abutment Type	Girder Type	Minimum and Maximum Kp Values			
		For Standard EPS Based on		For Elasticized EPS Based on	
		Installed Thickness*	Calculated Thickness**	Installed Thickness	Calculated Thickness*
Full Integral	Concrete	1.44–2.20	0.95–1.47	0.88–1.40	0.64–1.02
	Steel	1.45–3.44	1.23–3.71	0.90–2.33	0.65–2.50
Semi-Integral	Concrete	1.95–3.55	1.64–3.14	1.18–2.29	1.02–2.10
	Steel	2.01–3.81	1.56–3.54	1.24–2.62	0.94–2.51

EPS = expanded polystyrene.
*Calculations were made based on provided thicknesses of installed EPS.
**Calculations were made based on steps outlined in Figure 45.

Table 11. Comparison of Calculated Minimum and Maximum Lateral Earth Pressure Coefficients Based on Abutment Type and Presence of Approach Slab

Abutment Type	Is There an Approach Slab?	Kp Values			
		For Standard EPS Based on		For Elasticized EPS Based on	
		Installed Thickness	Calculated Thickness*	Installed Thickness	Calculated Thickness*
Full Integral	YES	1.57–3.44	0.95–3.71	0.88–2.33	0.64–2.50
	NO	1.69–2.20	1.04–1.70	1.05–1.40	0.87–1.02
Semi-Integral	YES	1.95–3.32	1.64–2.96	1.18–2.25	1.02–1.86
	NO	2.01–3.55	1.56–3.54	1.29–2.62	0.94–2.51

EPS = expanded polystyrene
*Calculations were made based on steps outlined in Figure 45.

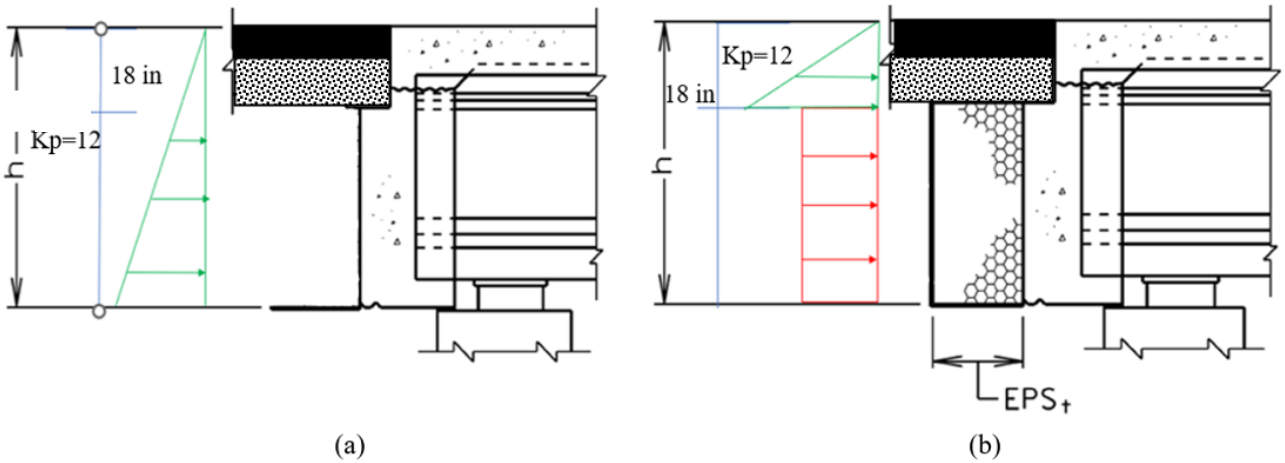

Figure 45. Theoretical Earth Pressure Distributions Acting on Abutments: (a) without EPS; (b) with EPS. EPS = expanded polystyrene.

It is worth noting that the calculated Kp values for both EPS types do not appear to exceed VDOT's target of 4, except for one bridge in the case of S-EPS, which is very close to 4 (3.81). This finding can be attributed to the relatively shorter abutment height of that bridge (3.09 feet), which increased the Kp value. However, it should be emphasized that if E-EPS were used in that bridge instead of S-EPS, the Kp value could have been significantly reduced (from 3.81 to 2.62). Therefore, for low integral backwalls (< 3.5 feet), E-EPS is preferred to meet the Kp requirement. This tendency is because, in shorter abutments, the earth pressure within the zone above EPS becomes dominant.

As Tables 10 and 11 show, Kp values are lower for E-EPS compared with S-EPS. This outcome occurs because S-EPS transfers higher loads to the backfill at the same strain value, yielding higher Kp values. On average, utilizing E-EPS reduces Kp by approximately 35%.

Decision to Choose EPS Type for Elastic Inclusion

In this study, both types of EPS were tested under monotonic, cyclic, and traffic loadings. The test results provide detailed differences in behavior between S-EPS and E-EPS. However, the decision for the EPS type for elastic inclusion design ultimately rests with VDOT. The following summarizes findings to aid VDOT in determining the EPS type for a given bridge project:

- S-EPS and E-EPS can both be used in elastic inclusion applications because they exhibit similar stress-strain behavior. E-EPS has no advantages over S-EPS, because both types of EPS appear to have the same elastic range (2 to 3%).
- E-EPS most likely will transfer lower loads to the abutment than S-EPS. Therefore, lower Kp values may be obtained when E-EPS is installed.
- For short abutments (< 3.5 feet), E-EPS could be beneficial to satisfy VDOT's Kp criterion for bridges with elastic inclusions (≤ 4.0).
- Based on monotonic test results, the elastic modulus of E-EPS appears to be significantly lower than that of S-EPS. The difference in elastic modulus implies that E-EPS is a more

compressible material. Thus, achieving compaction-induced strains may require less effort in the field when E-EPS is used, as Figure 23 shows.

CONCLUSIONS

- *The use of elastic inclusion at integral abutments can be considered a viable approach for reducing the Kp value and addressing soil-structure interaction issues at integral bridges, as long as appropriate materials are used for the elastic inclusion and installed based on proper thicknesses, protection, and compaction procedures.*

- *Both standard and elasticized EPS may function effectively at integral abutments when properly dimensioned and installed.*

- *Under the same thickness conditions, elasticized EPS results in smaller Kp values than standard EPS.*

- *Neither of the EPS materials will experience appreciable plastic vertical deformation under the simulated 3 psi traffic-induced load.*

- *The results of this study indicate that the assumption currently adopted by VDOT's Structure and Bridge Division overestimates the elastic strain range as 10% for elasticized EPS material.* The findings, based on unconfined monotonic loading tests, suggest that the elastic range of standard EPS and elasticized EPS is approximately the same and is no more than 3%.

- *Based on the findings of the study, EPS strains due to compaction should never exceed 10% for both EPS types regardless of the thermal expansion or contraction phases.*

- *The thermally induced strain on EPS should be limited to 4.6% for both EPS types.* Such conditions can be achieved by choosing the appropriate EPS thickness, as outlined in the newly proposed procedure to determine EPS thickness.

- *The total strain on standard EPS and elasticized EPS should not exceed 14.6% (compaction-induced strain (maximum 10.0%) + thermally induced strain (maximum 4.6%).* Exceeding this condition indicates that standard EPS may exhibit a negative Poisson's ratio effect. For elasticized EPS, the upper limit concerning negative Poisson's ratio behavior was not observed in the laboratory. However, as a conservative approach, a total strain limitation of 14.6% is suggested.

- *The quasi-static strain-controlled test conducted with both aggregate and EPS (combined tests) indicates that VDOT's selected geotextile may be insufficient to prevent particle intrusion.*

RECOMMENDATIONS

1. VDOT's Structure and Bridge Division should consider allowing the use of standard EPS in addition to elasticized EPS as elastic inclusion at integral abutments.
2. VDOT's Structure and Bridge Division should consider adopting the proposed modifications to the existing special provision for EPS, thickness determination, and installation practices, as presented in Items C and D of the supplemental *materials.*
3. *VTRC should consider developing guidelines for the following concerns that were identified as part of this research but were not addressed. These concerns need additional research that was not part of the scope of this study:*
    - Compaction of the aggregate adjoining EPS plays a major role in inducing the necessary (constant) strains that dictate the elastic behavior of EPS. Inappropriate compaction (too little or too much) may jeopardize the intended functionality. Initial compaction-induced strains on EPS may not reflect the long-term conditions it may experience. VDOT already has existing target compaction criteria for the aggregate; however, procedures should be confirmed to ensure the aggregate is compacted to achieve the required constant EPS strains under various conditions (warmer versus colder construction). Alternatively, a specific procedure may be established to induce compaction strains on EPS satisfying both warmer and colder construction conditions. A follow up study is recommended.
    - Laboratory testing conditions are insufficient to accurately simulate EPS behavior under field traffic loads. One of the limitations is associated with simulating appropriate horizontal and vertical stress conditions at the same time. The second limitation is associated with simulating the effect of EPS thickness under traffic conditions. In addition, the conditions to which EPS may be exposed during the construction of the base course and the asphalt layer above it require complex evaluation that cannot be replicated in a laboratory environment. Follow up field and numerical studies are recommended to assess these conditions and determine if a steel plate or approach slab is needed in all applications. Determining or quantifying the effects of potential arching that could eliminate the need for a steel plate or approach slab could be a key factor in this evaluation.
    - Geotextile plays a role in protecting EPS from particle intrusion. A follow up study is recommended to select the appropriate geotextile for protection.
    - The interaction of the pavement section with integral abutment is not well defined in VDOT's current practice. Field evaluations indicate soil-structure interaction problems causing roadway distress and settlement at the bridge approach. Whether these problems are directly associated with EPS is not well understood. A detailed study is recommended to investigate proper approaches for analyzing soil-structure interaction on bridges with elastic inclusions.

IMPLEMENTATION AND BENEFITS

Researchers and the Technical Review Panel (TRP) for the study (listed in the Acknowledgments) collaborated to craft a plan to implement the study recommendation and to determine the benefits of doing so. This is to ensure that the implementation plan is developed and approved with the participation and support of those involved with VDOT operations. The implementation plan and the accompanying benefits are provided here.

Implementation

With regard to Recommendations 1 and 2, VDOT's Structure and Bridge Division will consider making the proposed revisions to Chapter 17 of the VDOT (2023) *Manual of the Structure and Bridge Division* and VDOT (2020a) Special Provision 404-000130-00. Implementation is expected to begin within 12 months of the report's publication.

Successful implementation of Recommendation 3 will require field experimentation and associated monitoring. VTRC personnel will meet with VDOT's Materials Division, and VDOT's Structure and Bridge Division to determine the appropriate steps and resources needed to implement field trials at selected bridge sites. Implementation is expected to begin within 12 months of the report publication and conclude in the following 24 months.

Benefits

The recommendations proposed in this study will: (1) enable the use of standard EPS as an alternative to elasticized EPS, (2) allow VDOT to implement revised EPS design thickness equation, and (3) allow revising VDOT special provision to properly characterize the selected EPS material properties.

It is estimated that the regular EPS is approximately 35% the cost of the elasticized EPS (Les Rush, Universal Foam, personal communication). Currently, the only elasticized EPS available on the North American market is produced in Canada. The option of allowing standard EPS, available through several U.S. manufacturers, will result in a more competitive procurement process.

ACKNOWLEDGMENTS

The study presented in this report was funded by the Virginia Transportation Research Council, the research arm of VDOT. This research need was championed by Dr. Junyi Meng, Assistant State Structure and Bridge Engineer. In addition, Technical Review Panel (TRP) members included Park Thompson, Bruce Shepard, Dr. Soundar Balakumaran, Dr. Wansoo Kim, and Lewis Lloyd. The authors greatly appreciate the contributions and feedback of all TRP members. Special thanks also go to Thomas Miller of VDOT, Marvin Cook of Oracle Group Inc., Les Rush of Universal Foam Products, and Dr. Harry Karasopoulos of Cellofoam North America Inc. for their interaction and feedback. Arthur Apostolov of Geocomp Inc. and Aamir Ahmad and Emre Akmaz of GMU's Sustainable Geotransportation/Geoenvironmental

Infrastructure (SGI) Research Group provided contributions to the success of laboratory testing. Dr. Edward Hoppe's communications with Prof. Dr. Steven Barlett from the University of Utah are also appreciated.

REFERENCES

Abdelrahman, G.E., Kawabe, S., Tatsuoka, F., and Tsukamoto, Y. 2008. "Rate Effects on the Stress-strain Behavior of EPS Geofoam," *Soils and Foundations* 48(4): 479–494.

Alqarawi, A., Leo, C., Liyanapathirana, D., and Ekanayake, S. 2016. "A Study on the Effects of Abutment Cyclic Movements on the Approach of Integral Abutment Bridges," *Australian Geomechanics* 51(2): 1–3.

Al-qarawi, A., Leo, C., and Liyanapathirana, D.S. 2020. "Effects of Wall Movements on Performance of Integral Abutment Bridges," *International Journal of Geomechanics* 20(2): 04019157.

ASTM International. 2016. *ASTM D1621: Standard Test Method for Compressive Properties of Rigid Cellular Plastics.* West Conshohocken, PA: ASTM International.

ASTM International. 2021. *ASTM D6817: Standard Specification for Rigid Cellular Polystyrene Geofoam.* ASTM D6817. West Conshohocken, PA: ASTM International.

ASTM International. 2022. *ASTM C578: Standard Specification for Rigid, Cellular Polystyrene Thermal Insulation.* West Conshohocken, PA: ASTM International.

Arizona Department of Transportation. 2021. "Section 16: Bridge Construction." Bridge Design Guidelines. Phoenix, AZ.

Athanasopoulos, G.A., Pelekis, P.C., and Xenaki, V.C. 1999. "Dynamic Properties of EPS Geofoam: An Experimental Investigation," *Geosynthetics International* 6(3): 171–194.

Atmatzidis, D.K., Missirlis, E.G., and Theodorakopoulos, E.B. 2001. "Shear Resistance on EPS Geofoam Block Surfaces." In *Proceedings of the 3rd Annual International Conference on EPS Geofoam.*

Ahmed Awol, T. 2012. "A Parametric Study of Creep on EPS Geofoam Embankments." Master's thesis, Institutt for bygg, anlegg og transport.

Beinbrech, G., and Hillmann, R. 1997. "EPS in Road Construction—Current Situation in Germany," *Geotextiles and Geomembranes* 15(1–3): 39–57.

Beinbrech, G., and Hohwiller, F. 2000. "Cushion Foundations: Rigid Expanded Polystyrene Foam as a Deforming and Cushioning Layer," *Proceedings of the Institution of Civil Engineers-Ground Improvement* 4(1): 3–12.

Beju, Y.Z., and Mandal, J.N. 2016. "Compression Creep Test on Expanded Polystyrene (EPS) Geofoam," *International Journal of Geotechnical Engineering* 10(4): 401–408.

Bennert, T., Papp Jr, W.J., Maher, A., and Gucunski, N. 2000. "Utilization of Construction and Demolition Debris Under Traffic-type Loading in Base and Subbase Applications," *Transportation Research Record* 1714(1): 33–39.

California Department of Transportation. 2018. *Bridge Design Practice.* Sacramento, CA.

Dave, T.N., and Dasaka, S.M. 2018. "Experimental Model Study on Traffic Loading-induced Earth Pressure Reduction Using EPS Geofoam." In *Physical Modelling in Geotechnics, Volume 1: Proceedings of the 9th International Conference on Physical Modelling in Geotechnics (ICPMG 2018),* July 17–20. London: CRC Press: 169.

Deacon, J.A., Harvey, J.T., Guada, I., Popescu, L., and Monismith, C.L. 2002. "Analytically Based Approach to Rutting Prediction," *Transportation Research Record* 1806 (1): 9–18.

Diogo, J.F.R., Shubber, A.A. M., Enhui, Y., and Yang, L. 2012. "The Effect of Visco-Elastoplastic Behavior of Asphalt on Thin Asphalt Pavement." In *Logistics: The Emerging Frontiers of Transportation and Development in China*. Reston, VA: American Society of Civil Engineers: 2258–2265.

Dowling, E.N. 1993. *Mechanical Behavior of Materials.* Englewood Cliffs, NJ: Pearson Prentice Hall.

Duškov, M. 1997. "Materials Research on EPS20 and EPS15 Under Representative Conditions in Pavement Structures," *Geotextiles and Geomembranes* 15(1–3): 147–181.

Elragi, A.F. 2000. *Selected Engineering Properties and Applications of EPS Geofoam*. Syracuse, NY: State University of New York College of Environmental Science and Forestry.

Fernandes Jr., J.L., Pais, J.C., and Pereira, P.A. 2006. "Effects of Traffic Loading on Portuguese and Brazilian Pavements Performance." *Proceedings of the 85th Annual Meeting of the Transportation Research Board.* Washington, DC: Federal Highway Administration.

Florida Department of Transportation. 2022. *Structures Manual.* Tallahassee, FL.

Hazarika, H. 2006. "Stress–strain Modeling of EPS Geofoam for Large-strain Applications," *Geotextiles and Geomembranes* 24(2): 79–90.

Hawaii Department of Transportation. 2013. Bridge Inspection Manual. Honolulu, HI.

Hoppe, E.J. 2005. *Field Study of Integral Backwall with Elastic Inclusion*. No. FHWA/VTRC 05-R28. Charlottesville, VA: Virginia Transportation Research Council.

Hoppe, E.J., and Eichenthal, S.L. 2012. *Thermal Response of a Highly Skewed Integral Bridge.* No. FHWA/VCTIR 12-R10. Charlottesville, VA: Virginia Center for Transportation Innovation and Research.

Horvath, J.S. 1995. "Geoinclusion: A New, Multifunctional Geocomposite," *Geotechnical Fabrics Report* 13(2).

Horvath, J.S. 2000. *Integral-abutment Bridges: Problems and Innovative Solutions Using EPS Geofoam and Other Geosynthetics*. No. CE/GE-00-2. Bronx, NY: Manhattan College.

Horvath, J.S., and VanWagoner, J.D. 1992. "Geoinclusion Method and Composite." U.S. Patent No. 5,102,260, issued April 7.

Hosford, F.W. 2005. *Mechanical Behavior of Materials.* United Kingdom: Cambridge University Press.

Huang, Y.H. 2004. *Pavement Analysis and Design*, Vol. 2. Upper Saddle River, NJ: Pearson Prentice Hall: 401–409.

Jones, N. 1995. “Quasi-Static Analysis of Structural Impact Damage,” *Journal of Constructional Steel Research* 33(3): 151–177.

Indiana Department of Transportation. 2022. *Indiana Design Manual.* Indianapolis, IN.

Iowa Department of Transportation. 2017. Bridge Design Manual. Ames, IA.

Kannan, P., Biernacki, J.J., and Visco Jr, D.P. 2007. “A Review of Physical and Kinetic Models of Thermal Degradation of Expanded Polystyrene Foam and Their Application to the Lost Foam Casting Process,” *Journal of Analytical and Applied Pyrolysis* 78(1): 162–171.

Kansas Department of Transportation. 2015. *Bridge Construction Manual.* Topeka, KS.

Khalaj, O., Siabil, S.M.A.G., Tafreshi, S.N.M., Kepka, M., Kavalir, T., Křížek, M., and Jeníček, Š. 2020. “The Experimental Investigation of Behavior of Expanded Polystyrene (EPS),” *IOP Conference Series: Materials Science and Engineering* 723(1): 012014.

Li, K., Wang, Y., Zhao, Y., Jin, C., Tang, H., Zou, Q., and Wang, M. 2019. “High Strain Rate of Quartz Glass and Its Effects During High-speed Dicing,” *Ceramics International* 45(10): 13523–13529.

Liu, H., Han, J., and Parsons, R.L. 2021. “Mitigation of Seasonal Temperature Change-induced Problems with Integral Bridge Abutments Using EPS Foam and Geogrid,” *Geotextiles and Geomembranes* 49(5): 1380–1392.

Malai, A., Youwai, S., and Jaturabandit, N. 2017. “Stress-strain Mechanism of Expanded Polystyrene Foam Under Cyclic Loading Conditions Within and Beyond Yield States.” In *Proceedings of the International Conference on Transportation Infrastructure and Materials (ICTIM2017)*. Qingdao, China.

Malik, A., Chakraborty, T., and Rao, K.S. 2018. “Strain Rate Effect on the Mechanical Behavior of Basalt: Observations from Static and Dynamic Tests,” *Thin-Walled Structures* 126: 127–137.

Minnesota Department of Transportation. 2020. *Bridge Details Manual – Part II*. St. Paul, MN.

Mississippi Department of Transportation. 2017. *Standard Specifications for Road and Bridge Construction*. Jackson, MS.

Missouri Department of Transportation. 2021. *Missouri Standard Specifications for Highway Construction*. Jefferson City, MO.

Negussey, D. 2008. “Design Parameters for EPS Geofoam,” *Soils and Foundations* 48(6): 861–861.

New Hampshire Department of Transportation. 2016. *Bridge Design Manual*. Concord, NH.

New York State Department of Transportation. 2019. *Bridge Manual*. Albany, NY.

Ossa, A., and Romo, M.P. 2009. “Micro- and Macro-mechanical Study of Compressive Behavior of Expanded Polystyrene Geofoam,” *Geosynthetics International* 16(5): 327–338.

Ossa, A., and Romo, M.P. 2011. “Dynamic Characterization of EPS Geofoam,” *Geotextiles and Geomembranes* 29(1): 40–50.

Ouellet, S., Cronin, D., and Worswick, M. 2006. “Compressive Response of Polymeric Foams Under Quasi-Static, Medium and High Strain Rate Conditions,” *Polymer Testing* 25(6): 731–743.

Padade, A. H., and Mandal, J.N. 2012. “Behavior of Expanded Polystyrene (EPS) Geofoam Under Triaxial Loading Conditions,” *Electronic Journal of Geotechnical Engineering* 17: 2542–2553.

Preber, T., Bang, S., Chung, Y., and Cho, Y. 1994. “Behavior of Expanded Polystyrene Blocks,” *Transportation Research Record* 1462: 36–46.

Pennsylvania Department of Transportation. 2018. *Design Manual Part 4 – Structures.* Harrisburg, PA.

Ramli Sulong, N.H., Mustapa, S.A.S., and Abdul Rashid, M.K. 2019. “Application of Expanded Polystyrene (EPS) in Buildings and Constructions: A Review,” *Journal of Applied Polymer Science* 136(20): 47529.

Siabil, S. G., Tafreshi, S.M., and Dawson, A.R. 2020. “Response of Pavement Foundations Incorporating Both Geocells and Expanded Polystyrene (EPS) Geofoam,” *Geotextiles and Geomembranes* 48(1): 1–23.

Srirajan, S., Negussey, D., and Anasthas, N. 2001. “Creep Behavior of EPS Geofoam.” In *Proceedings of EPS Geofoam 3rd Annual International Conference:* 10–12.

Tanyu, B.F., Abbaspour, A., Alimohammadlou, Y., and Tecuci, G. 2021. “Landslide Susceptibility Analyses Using Random Forest, C4. 5, and C5. 0 with Balanced and Unbalanced Datasets,” *Catena* 203: 105355.

Tanyu, B.F., Aydilek, A.H., Lau, A.W., Edil, T.B., and Benson, C.H. 2013. “Laboratory Evaluation of Geocell-reinforced Gravel Subbase Over Poor Subgrades,” *Geosynthetics International* 20(2): 47–61.

Tanyu, B.F., Benson, C.H., Edil, T.B., and Kim, W.H. 2004. “Equivalency of Crushed Rock and Three Industrial By-products Used for Working Platforms During Pavement Construction,” *Transportation Research Record* 1874(1): 59–69.

Tennessee Department of Transportation. 2021. *Standard Specifications for Road and Bridge Construction*. Nashville, TN.

Texas Department of Transportation. 2004. *Bridge Design Manual – LRFD*. Austin, TX.

Trandafir, A.C., Bartlett, S.F., and Lingwall, B.N. 2010. “Behavior of EPS Geofoam in Stress-controlled Cyclic Uniaxial Tests,” *Geotextiles and Geomembranes* 28(6): 514–524.

Virginia Department of Transportation. 2023. “Chapter 17: Integral/Jointless Bridges.” In *Manual of the Structure and Bridge Division, Part 2, Design Aids and Particular Details*. Richmond, VA.

Virginia Department of Transportation. 2020a. *Special Provision for Elastic Inclusion Expanded Polystyrene (EPS)*. SP404-000130-00. Richmond, VA: VDOT, Material Division.

Virginia Department of Transportation. 2020b. *Road and Bridge Specifications*. Richmond, VA.

Washington State Department of Transportation. 2022. *Bridge Design Manual – LRFD*. Olympia, WA.

Wong, H. and Leo, C.J. 2006. “A Simple Elastoplastic Hardening Constitutive Model for EPS Geofoam,” *Geotextiles and Geomembranes* 24(5): 299–310.

Zou, Y. 2001. *Behavior of the Expanded Polystyrene (EPS) Geofoam on Soft Soil*. Sydney, Australia: University of Western Sydney.